Mechanisms of tau fragmentation, aggregation and degradation in transgenic mouse models

Inauguraldissertation
zur
Erlangung der Würde eines Doktors der Philosophie
vorgelegt der
Philosophisch-Naturwissenschaftlichen Fakultät
der Universität Basel
von

Sefika Ozcelik
aus Frankreich

Basel, 2013

Genehmigt von der Philosophisch-Naturwissenschaftlichen Fakultät
auf Antrag von

Prof. Dr. Yves Alain Barde
Dr. Dr. David Winkler
Dr. Matthias Staufenbiel

Basel den 18 Juni 2013

Prof. Dr. Jörg Schibler
Dekan

To my husband, my love Cemil

To our family

To Tim's mother

Acknowledgments

First, I would like to thank my supervisor Dr. David Winkler for giving me the opportunity to work on this challenging and exciting project. Thank you for your advice and support. I thank my dissertation committee: Prof. Yves-Alain Barde, Matthias Staufenbiel and Prof. Stephan Krähenbühl for their participation, evaluation and academic support of my thesis; and our collaborator, Dr. Michel Goedert and Dr. Graham Fraser for their expertise. I would also like to express my gratitude to Prof. Markus Tolnay for hosting and supporting my work at the Institute of Pathology, University of Basel.

From the Neuropathology lab, I thank Sabina Weingärtner, Sabine Ipsen, Bea Maurer, Myriam Vonlanthen and Markus Bänziger for their dedicated help with cutting and staining a lot, sometimes even more than a thousand of tissue sections. Without your help I would never have all those nice pictures. Special thanks also to Sabina and Markus for supporting me during my work, for helping me get through difficult time, and for the entire emotional support, entertainment, and care they provided.

I am grateful to Prof. Alphonse Probst for his intellectual input and support during my thesis as well as for proofreading the manuscript. Many thanks to Prof. Stephan Frank for his kindness and advice.

I thank the staff from Animal Facility for their advice and tremendous assistance with our transgenic lines.

I am very grateful to my colleagues in our Neuropathology group, Zhiva, Björn, Elisa, Lisa, Patricia, Elisabeth, Gabrielle, Molecular lab, Mariacarla, Sara, Alex, Rosi, Anja, Tanja and Ralph, René and Oscar for their companionship, humour and social input.

I would like to thank my French connection, here in Basel, Valérie, Fabi and Alexis thank you for everything, for being there whenever I needed help or advice.

I would like to acknowledge « our spinning team », Justyna and Piotr for motivating me to do spinning even if I was still a beginner. It was great to have you during around my stay in Basel. Justyna thank you for your support, advice and happiness and Piotr thank you for being there and baking delicious cakes. Many thanks to give me the opportunity of being your friend.

I thank Perrine for her enormous efforts in dealing with my thesis and doing so in timely manner with a great attitude. All words are not enough to tell you how much I am grateful. Thank you for being yourself, never change, you are great person and I am happy to be your friend. You are always welcome in Montreal.

I would like to thank my family and Cemil's family for being there. Most importantly, I would like to thank my husband, Cemil, for his courage, honesty and kindness. I thank him for being with me, believing in me, supporting and loving me. You are my best friend and you have been always here despite the long distance between Montreal and Basel.

Mechanisms of tau fragmentation, aggregation and degradation in transgenic mouse models

Summary

Neurodegenerative disorders with abnormal accumulation of tau protein are termed "tauopathies". These disorders, including Alzheimer's disease, are affecting more than 20 million people worldwide. Although their pathogenesis is related to the formation of tau aggregates, the exact molecular mechanisms underlying these disorders are still not well understood. The main aim of my thesis was to characterize the mechanisms of tau accumulation and removal. I therefore studied the role of truncated tau in the development of taupathies and tested whether induction of autophagy, a well-known catabolic process, may be sufficient to reverse tau accumulation and ameliorate tau-induced pathology.

In the first part of our studies, we analyzed a novel inducible transgenic mouse model (TAU62 mice), expressing a truncated form of human wild-type tau ($tau_{151-421}$, noted Δtau). TAU62 mice displayed axonal dysfunction and slowly progressive motor phenotype. Importantly, the neurotoxicity of Δtau was strongly enhanced when full-length P301S tau was co-expressed. In particular, P301SxTAU62 (abbreviated P62) double transgenic mice showed rapidly progressive, severe motor impairment, which was reversed by stopping the Δtau expression. Consistently, neuronal dysfunction and tau hyperphosphorylation were reversed in P62 mice when expression of Δtau was switched-off. These results demonstrate that Δtau exacerbates the toxicity of full-length tau and thereby induces severe but reversible neuronal dysfunction associated with structural changes. In parallel, we showed that induction of autophagy, using the mTORC1 inhibitor rapamycin, is sufficient to improve tau clearance in a transgenic mouse model of tauopathy (P301S mice). Rapamycin significantly delayed the progression of tau pathology in P301S mice, which was associated with a reduction in the accumulation of insoluble tau.

Together, these data provide novel insights into the pathogenesis of tauopathies. They pave new ways for novel therapeutic strategies, which can prevent the fragmentation of tau and/or promote the process of autophagy.

Key words: Tauopathies, autophagy, fragmentation.

Table of contents

List of Illustrations

Introduction

Discussion and Perspectives

Materials and Methods

List of Abbreviations

Aß	Beta-amyloid
AD	Alzheimer's disease
ADI	Alzheimer's disease Internationale organization
AgD	Argyrophilic grain disease
APH-1	Anterior pharynx defective
APP	Amyloid precursor protein
Asp	Aspartic acid
ATG	Autophagy-related genes
BACE	Beta-site APP cleaving enzyme 1 (Beta-secretase 1)
C-terminal	Carboxy-terminal
CAA	Cerebral amyloid angiopathy
CaM	Calmodulin kinase II
CBD	Corticobasal degeneration
Cdc2	Cell division control protein 2 homolog (Cyclin-dependent kinase 1)
Cdk5	Cyclin-dependent kinase 5
CKII	Casein kinase II
CNS	Central nervous system
CQ	Chloroquine
CTF	Carboxy-terminal fragment
DNA	Deoxyribonucleic acid
ECL	Enhanced chemiluminescence
eEF2	Eukaryotic elongation factor 2
ER	Endoplasmic reticulum
FDA	Food and drug administration
FTDP-17	Frontotemporal dementia and parkinsonism linked to chromosome 17
g	Gram
GA	Golgi apparatus
Glu	Glutamic acid
GSK3	Glycogen synthase kinase 3
h	Hour
HD	Huntington's disease
HTT	Huntingtin

JNK	Jun N-terminal kinase
kDa	Kilo daltons
LC3	Light chain 3 protein
M	Molar
MAP	Microtubule-associated protein
MAPK	Microtubule-associated protein kinase
MARK	Microtubule-affinity regulating kinase
MTBR	Microtubule binding region
MTOC	Microtubule organizing center
µm	micrometer
mtHTT	mutated huntingtin
mTOR	mammalian Target of Rapamycin
N-terminal	Amino-terminal
NFT	Neurofibrillary tangles
NT	Neuropil threads
O-GlcNaC	O-linked N-acetylglucosamine
O/N	Over/night
OXPHOS	Oxidative phosphorylation
P62	Transgenic mice resulting from the bredding of P301SxTAU62
PBS	Phosphate buffered saline
PCR	Polymerase chain reaction
PD	Parkinson's disease
PEN-2	Presenilin enhancer 2
PHF	Paired helical filaments
PI3K	Phosphoinositide 3 kinase
PiD	Pick's disease
PKA	Protein kinase A
PKC	Protein kinase C
PP	Protein phosphatases
PSP	Progressive supranuclear palsy
rDNA	Ribosomal DNA
RT	Room temperature
sec	Seconde
SMERs	Small molecule enhancers of the cytostatic effects of rapamycin

ΔTau	Truncated tau
TAU62	Transgenic mice expressing a truncated form of human wild-type tau
TCA	Tricarboxylic acid cycle
TRE	Tetracycline responder element
tTS	Tetracycline controlled transcriptional silencer element
UPS	Ubiquitin proteasome system
VAMP2	Vesicle-associated membrane protein 2

PREFACE

"Men ought to know that from nothing else but the brain come joys, delights, laughter and sports, and sorrows, griefs, despondency, and lamentations. And by the same organ we become mad and delirious, and fears and terrors assail us, some by night, and some by day, and dreams and untimely wanderings, and cares that are not suitable, and ignorance of present circumstances, desuetude, and unskillfulness. All these things we endure from the brain, when it is not healthy..." [1]

By these words, Hippocrates in 400 B.C. unequivocally identified and defined the brain as the center of mind and soul, while earlier and contemporary philosophers favored the heart and considered the brain only as an accessory organ. During the following centuries, improvement of the techniques allowed to better identify the structures of the brain, the anatomical connections between nerves and organs, as well as some pathological features within the brain [2]. New methods of staining and development of advanced microscopy, imaging, and electrochemistry, in the 20th century, lead to a precise description of the different types of neurons, their connectivity and properties, and to a better understanding of the brain functions.

The brain is the main constituent of the nervous system in all vertebrate and most invertebrate animals [3]. In vertebrates, it is composed of the cerebral hemispheres (or cerebrum), which are organized in the frontal, parietal, occipital and temporal lobes. Together with the cerebellum, they control all voluntary actions of the body. The cerebral cortex of human and some other vertebrates includes the hippocampal structure, which is involved in the acquisition of new memories, in the consolidation from short- to long-term memory, as well as in spatial memory. In the brain, one can also distinguish the thalamus and hypothalamus, which are associated with the regulation of various behaviours, such as drinking or sleeping (Figure 1A). Neurons are the basic excitating cells constituting the nervous system and are characterized by their ability to conduct the electrical signal, called nervous influx. Neurons are composed of one cellular body (or soma) with multiple dendrites and with a long axon, conducting the nervous influx (Figure 1B). Neurons are tightly linked together by an intricate network of connections established by synapses. These complex

interconnections allow for the development of various functions, such as muscle activity or secretion of hormones, which are centrally controlled by the brain, and drive a quick and coordinated reaction of the body according to the environmental signals. It is also well known that, although the general organization of the brain is genetically programmed, experience can refine the connections existing between neurons, hence allowing for the essential plasticity of the brain [4, 5].

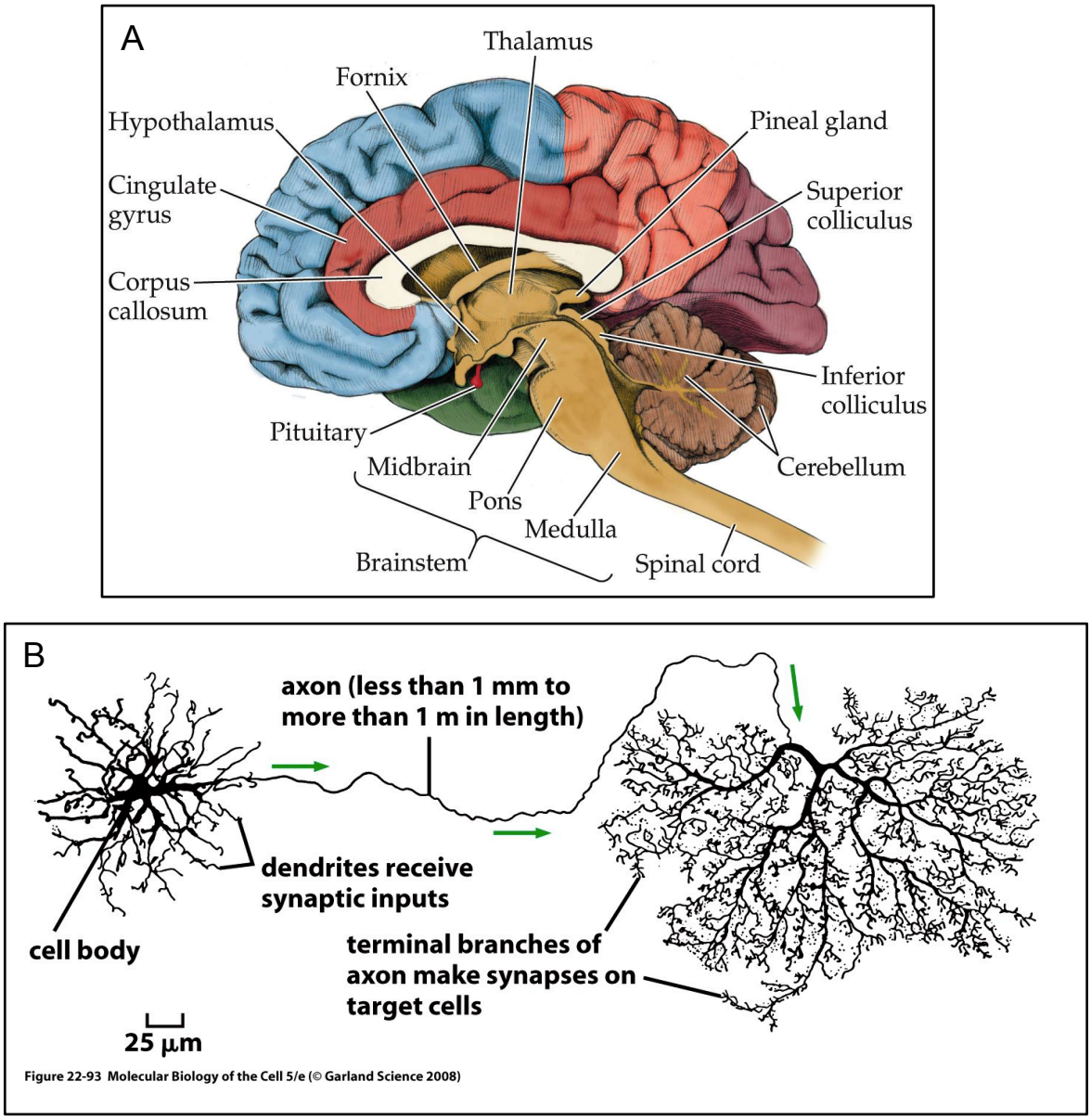

Figure 1: Organization of the nervous system

A) Simplified scheme of the main regions of the human brain (Biological Psychology 6e).
B) Neuron cells contain a soma, numerous dendrites and one prolonged axone. They are interconnected with other neurons through thousand of synaptic connections (Mol. Biology Cell 5e).

Given this central, determinant function of the brain, it is not surprising that alterations of cerebral tissues are responsible for numerous severe pathologies in human, which are characterized by an important variability of symptoms. Neurodegenerative disorders refer to diseases affecting the nervous system, leading to a loss of neurons and to the perturbation of the corresponding cerebral functions. While some of these disorders, such as Parkinson's or Huntington's diseases, preferentially affect the motility of patients and their ability to perform coordinated movements, other alter rather their memory, thinking, behaviour and ability to perform everyday activities. These latter groups of pathologies, recognized as dementia, are the main cause of heavy dependence and institutionalization. Among them, the Alzheimer's disease (AD) is the most common one, affecting more than 35 million of individuals worldwide, according to the Alzheimer's Disease International organization (ADI) [6]. ADI further estimates that this number will double in the next twenty years to reach 115 million in 2050. While recently a progress has been done in the identification and understanding of the mechanisms associated with the onset and progression of AD and associated dementia, there is no efficient and safe treatment yet.

During my doctoral work, I focused on one group of dementia, called tauopathies, which are characterized by an intracellular accumulation of tau protein. I focused on analyzing the mechanisms underlying neuronal dysfunction in these disorders, by testing the toxicity of a truncated form of tau in transgenic mouse models of tauopathy. I also investigated whether promoting autophagy can reverse tau accumulation and alleviate the pathology. For these reasons, the introduction to my thesis is divided into three parts: the first part describes the tau protein and its functions in neurons; the second part presents the neurodegenerative disorders constituting the group of tauopathies and discusses hypothesized pathomechanisms associated with their onset and progression; the third part is dedicated to autophagy and its potential use as a therapeutic target for neurodegenerative disorders. In the following, the results obtained during my studies are presented with the corresponding manuscripts, which are either in preparation (Manuscript N°1) or published (Publication N°2 and N°3). In the first manuscript, we show that truncated forms of tau exacerbate the propensity of tau protein to aggregate and likely contribute to an early onset of the pathology; in the following two publications show that induction of autophagy ameliorates tau pathology in mouse models of tauopathies. Finally, a general discussion on the generated data and the perspectives arising from them will be presented.

INTRODUCTION

PART I:

Microtubule-associated tau protein: diversity, properties and functions

PART II:

Neurodegenerative disorders and animal models

PART III:

Autophagy: an essential catabolic process

PART I

Microtubule-associated tau protein: diversity, properties and functions

The tau protein belongs to the microtubule-associated protein family (MAP) and is abundant in both central and peripheral nervous system neurons. In 1975, Weingarten et al. isolated a heat stable protein that is primordial for microtubule assembly and they called it tau due to its ability to induce tubule formation. *In vitro*, tau protein can control the polymerization of microtubules. Microtubules are a major constituent of axons and serve for the trafficking of cargoes. So far, tau protein, together with tubulin, is the only protein found to be important for the assembly of microtubules [7]. The role and the identity of tau were not defined in detail until its implication in neurodegenerative disorders such as in Alzheimer's disease (AD) has been identified [8-11]. After that, many studies have been done to better understand its structure and principal function.

1.1. Tau isoforms

The *TAU* gene, located on the chromosome 17 (locus 17q21), contains a total of 16 exons, the predominant form of the tau protein isoforms being produced from 11 of them [12]. Through alternative splicing of exons 2, 3 and 10, six isoforms of tau are generated in adult human brain [13]. The six isoforms differ by the presence or absence of either three (3R tau) or four (4R tau) microtubule-binding domains and by the number of amino terminal (N-terminal) inserts. In parallel, the alternative splicing of exons 2 and 3 results in the absence (0N) or presence of one (1N) or two (2N) insert(s) of 29 amino acids in the half N-terminal part of the tau. Thereby, splicing of exons 2, 3 and 10 allows for six combinations corresponding to isoforms containing 441 amino acids (2N4R), 410 amino acids (2N3R), 412 amino acids (1N4R), 381 amino acids (1N3R), 393 amino acids (0N4R) and, for the shortest, 352 amino acids (0N3R) (Figure 2). During development, these six isoforms are differentially expressed and each of them has particular physiological roles [14]. For example, in rodents, only the three 4R tau isoforms are expressed in adult brain, whereas the 0N3R isoform is predominantly detected during development [15].

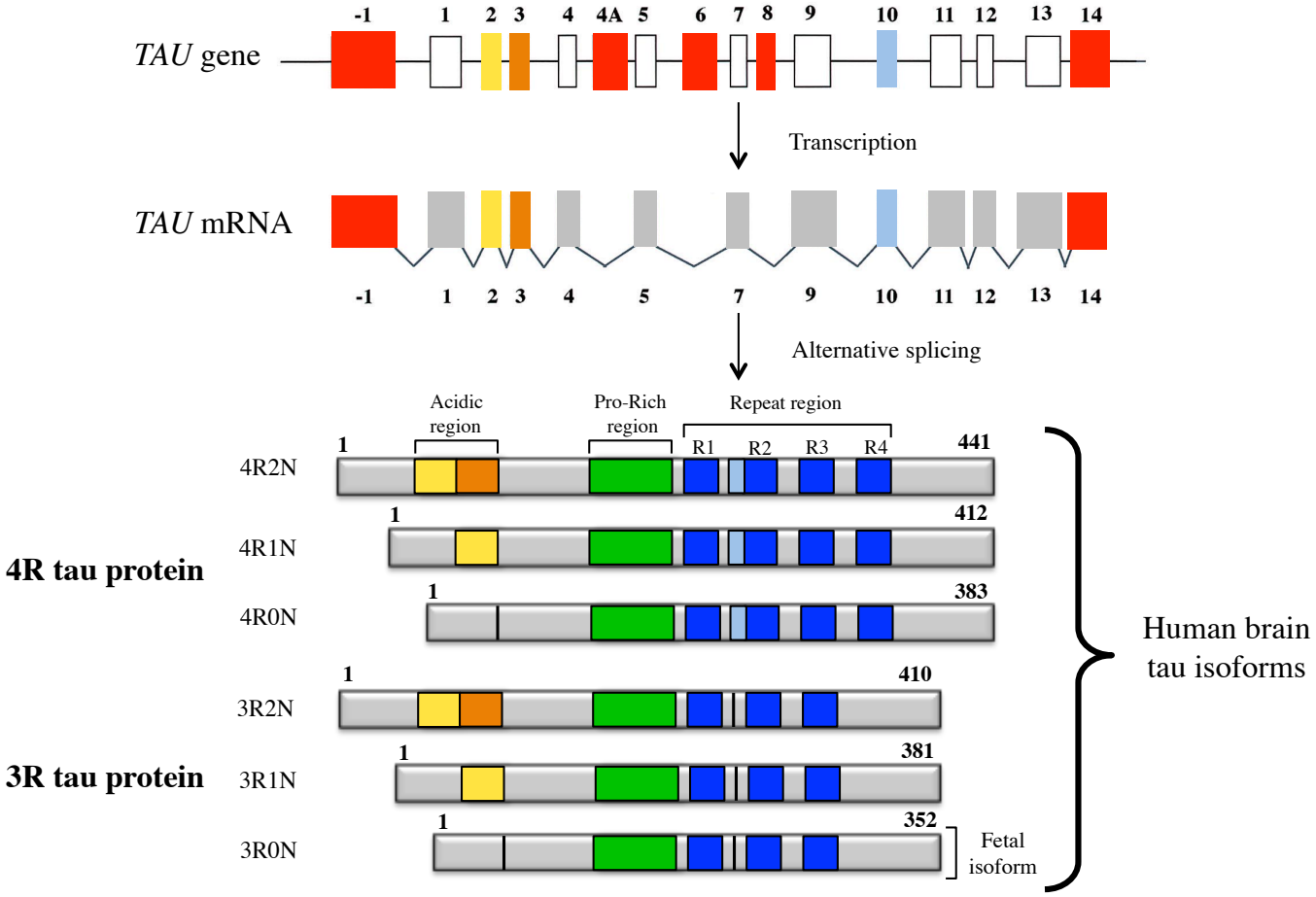

<u>Figure 2:</u> Schematic representation of the human *TAU* gene, the *TAU* primary transcript and the six tau protein isoforms

The human *TAU* gene is located on the long arm of the chromosome 17 at position 17q21 and contains 16 exons, the exon-1 being a part of the promoter. The *TAU* primary transcript contains 13 exons, since exons 4A, 6 and 8 are not transcribed in human. Through alternative messenger RNA splicing of exons 2, 3 and 10, a set of six protein isoforms ranging from 352 to 441 amino acids are generated in adult human brain. Tau isoforms differ by the absence or the presence of one or two inserts of 29 amino acids, encoded by the exons 2 (yellow box) and 3 (orange box), in combination with either three (R1, R2 and R3) or four (R1, R2, R3 and R4) repeat-regions (blue boxes) in the C-terminal region of the protein. The fourth microtubule-binding domain is encoded by the exon 10 (light blue box) (lower panel). (Adapted from Buée *et al*, 2000)

1.2. Localization, structure and functions of tau

Tau is a microtubule-associated protein of low molecular weight, highly expressed in both central and peripheral nervous system. It constitutes a major component of cytoskeletal structures. Primary sequence analysis demonstrates that tau consists of an N-terminal acidic portion followed by a proline rich region and a C-terminal tail, which is the basic part of the protein. Tau protein binds to the microtubules through the repeat regions R1-R4, encoded by exons 9-12 [16]. Each repeat region consists of stretches of eighteen, highly conserved residues [17]. The repeat domains are separated from each other by spacer regions of thirteen or fourteen residues [18-20].

The main function of tau is to promote tubulin polymerization, to stabilize the microtubules and to ensure their flexibility. Thereby tau is involved in the maintenance of axonal transport [7, 21-25]. Microtubules contribute to diverse cellular processes such as morphogenesis, cell division and intracellular trafficking [26, 27]. In cells, microtubules have the ability to change their length by dynamic instability [28]. The binding of tau protein to the microtubules is balanced by coordinated actions of kinases and phosphatases and is essential to maintain their integrity [29, 30]. Specific ATPase enzymes, including kinesin and dynein, serve as cellular motors that can transport their cargoes, such as mitochondria [31, 32], lysosomes [33], peroxisomes [34] as well as endocytotic and exocytotic vesicles [35], on the way to the cell periphery and back, towards the microtubule organizing center (MTOC) of the cell. Tau alters the intracellular traffic due to its tight binding to microtubules and possibly detaches the cargoes from kinesin, although the speed of kinesin does not seem to be influenced by tau protein [36] (Figure 3).

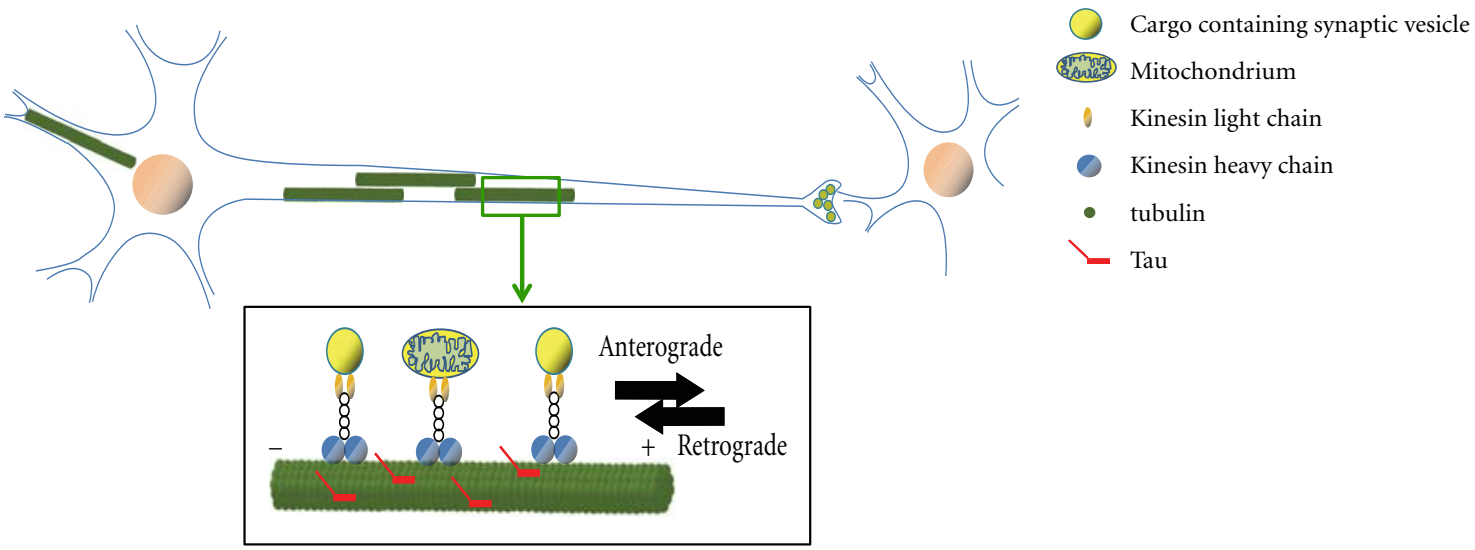

Figure 3: Microtubular transport

The presence of tau on microtubules modifies the dynamic of motor proteins such as dyneins and kinesins, which are using microtubules for retrograde or anterograde transport of cargoes, along the axon (Adapted from Jaworski *et al, 2010*).

1.3. Post-translational modifications of tau

Tau protein is subjected to diverse post-translational modifications and up to now it is very difficult to know which of them are crucial for the development of tauopathies. The mechanisms that lead to tau aggregation are not known but it is possible an interplay exists between several tau post-translational modifications that leads to tau accumulation and eventually the formation of neurofibrillary tangles (NFT). Here, only some of the identified post-translational modifications of tau will be described such as phosphorylation, glycosylation, ubiquitination or truncation.

1.3.1. Tau phosphorylation

Tau has been defined as a phosphoprotein by many different studies [37-39]. Most of them focused on the serine/threonine phosphorylation of the tau protein as well as phosphorylation

on tyrosine residues. The open structure of tau allowed for an access to a large number of potential phosphorylation domains. Two main groups of domains have been distinguished, depending on whether the Ser/Thr phosphorylation site targeting by the kinase is followed by a proline residue or not. Proline-directed kinases include the tau protein kinase I (also called glycogen synthase kinase 3, GSK3), tau protein kinase II (cdk5), kinases of the MAPK (p38) or JNK families, as well as other stress kinases, such as cdc2. In parallel, the protein kinase A (PKA), protein kinase C (PKC), calmodulin (CaM) kinase II, microtubule-affinity regulating kinase (MARK) and casein kinase II (CKII), which modifies residues close to acidic residues mainly in protein region corresponding to exons 2 and 3, define the non-proline-directed kinases [40]. It was suggested that changes in the phosphorylation of tau play an important role in the regulation of tau function by modifying its affinity to microtubules.

In particular, there is evidence that GSK3 plays an important role in regulation of tau phosphorylation under physiological and pathological conditions [41]. GSK3 is ubiquitously expressed and found at high levels in the brain where it localizes mostly in neurons [41, 42]. In 2003, Cho *et al*. demonstrated that GSK3 phosphorylates tau on both primed (following prior phosphorylation of the substrate by another kinase) and unprimed sites [43]. Consistently, several reports both *in vitro* and *in vivo* showed that tau phosphorylation increased following overexpression of GSK3 [44-47]. Inversely, reduction of tau phosphorylation has been detected in cells treated with lithium, a well-known inhibitor of GSK3 [48-50]. Together, this data suggest that GSK3 might be a potential target of tau phosphorylation *in vivo.*

Phosphorylation state of tau is determined by equilibrium of a different set of protein kinases and phosphatases. Dysfunction of this balance leads to the abnormal tau phosphorylation seen in AD.

1.3.2. Tau phosphatases

Several phosphatases (PP) have been related to tau dephosphorylation [51-53]. However, *in vitro* studies have shown that only three phosphatases, PP1, PP2A and PP2B, predominantly dephosphorylate tau [54, 55]. In the brain, tau dephosphorylation seems to be mainly regulated by PP2A, although not all of the phosphorylation sites depend on PP2A [56-58]. In addition to PP2A, another protein phosphatase playing an important role in the regulation of tau phosphorylation in the brain is PP5. PP5 is ubiquitously expressed in mammals and the expression levels of PP5 are especially high in the brain. *In vitro*, PP5 was shown to dephosphorylate tau and to interact with the microtubules [59].

1.3.3. Tau glycosylation

The addition of an O-linked N-acetylglucosamine (O-GlcNac) on Ser or Thr residues in the proximity of Proline amino acid is O-glycosylation, which is the dynamic and abundant post-translational modification [51]. Glycosylation is phosphorylation-dependent and aberrant glycosylation promotes hyperphosphorylation of tau by both increasing phosphorylation and by inhibiting dephosphorylation of tau [60].

1.3.4. Tau ubiquitination

Timely degradation of accumulating cytosolic proteins is crucial for the maintenance of cell homeostasis, particularly in non-dividing cells such as neurons. The ubiquitin-proteasome system (UPS) and autophagy are essential for the removal of unfolded proteins and allow an effective protein quality control. It has been shown that under physiological conditions tau is ubiquitinated and proteolytically processed by the UPS [61-64]. Both systems, UPS and autophagy, have recently been shown to be substantially involved in the pathogenesis of neurodegenerative proteinopathies, including Huntington's disease (HD), Parkinson's disease (PD) and AD [65-67]. While degradation of non-aggregated and soluble unfolded tau protein can be achieved by the proteasome, degradation of tau oligomers or aggregates is impossible due to the inaccessibility to the catalytic core of the 26S proteasome. Thus, since the UPS is in charge of tau degradation, its inhibition can enhance tau accumulation [62]. Despite ubiquitination, tau is not sufficiently degraded by the UPS and accumulates as NFT in the brain [65]. For this reason, dismantling of protein aggregates requires the autophagy machinery. In contrast to the proteasome, where ubiquitin tagged proteins are enzymatically degraded by the 26S proteasome, the autophagy system sequesters various forms of debris from proteins up to organelles by forming autophagosomes (see below, "Autophagy: an essential catabolic process").

1.3.5. Tau truncation

Not all of the post-translational tau modifications illustrated above would be required for tau aggregation. Accumulation of tau is dependent on its propensity to switch from its physiological random coil to a ß-sheet structure [68]. Proteolytic tau fragmentation results in an altered shape of tau molecule with potentially increased aggregation propensity [69]. Structures like paired helical filaments (PHF) found in AD consist of pathologically folded tau protein (PHF-tau) [70-72]. Several studies also reported the presence of truncated forms of

tau in PHF structures suggesting that tau truncation may be associated with tau aggregation in AD brains [73-75]. Nevertheless, the time course of the emergence of cleaved tau during the formation of NFT remains elusive [76, 77]. Recent reports have postulated that hyperphosphorylation of tau appears before its cleavage and that this fragmentation occurs before NFT formation [78-80]. Further reports indicated that cleavage of tau by caspases is related to cognitive decline of AD patients [80-83].

Evidence of tau cleavage by caspases was discovered in cultured cerebellar granule cells with the specific detection of a 17kD tau fragment during apoptosis [84]. *In vitro* experiments further revealed that tau truncated at its C-terminal domain was more toxic compared to the full-length form of tau, most probably due to its faster and greater aggregation propensity [85]. Moreover, cleavage of tau by caspase at C-terminal end, E391 (Glu^{391}) and D421 (Asp^{421}) promotes its accumulation and correlates with the progression of AD [86, 87]. Furthermore, truncation of tau in the N-terminal region has been previously reported [87] and this truncation may promote tau aggregation although its pathological significance remains to be proven.

The pathological role of tau fragmentation in the C-terminal region has been evaluated in cultured cells and transgenic animal models and multiple modifications in the organization and functions of membranous organelles (mitochondria and the endoplasmic reticulum) have been related to tau truncation [82, 84, 88-92]. Cognitive impairment associated with neuronal death and accumulation of misfolded truncated tau has also been reported in transgenic animals [93-99]. Moreover, clinicopathological analysis has been conducted for a better understanding of the role of tau fragmentation in the development of fibrillary structures in dementia and its pathological involvement in AD patients [77, 86, 100]. The evolution of AD correlates with the extent of tau fragmentation and precedes NFT formation [101]. Together, these data put emphasise on the pathophysiological importance of truncated tau in AD, which is of importance to identify novel diagnosis markers and to develop therapeutic tools.

PART II

Neurodegenerative disorders and animal models

The term “tauopathies” refers to the group of heterogeneous disorders clinically characterized by movement disturbances and the pathological accumulation of tau.
Over the past decade, the researchers have made their effort to develop animal models in order to mimic particular features of tauopathies, such as behavioural, histological and biochemical aspects. These models are useful to understand the pathomechanisms of tauopathies and to test potential therapeutic strategies.

2.1. Alzheimer’s disease

Alzheimer’s disease (AD) is a heterogeneous disorder in terms of clinical presentation and neuropathology. Its diagnosis is difficult due to the absence of specific disease markers and the overlap of clinical and pathological symptoms with those observed in non-demented elderly individuals and in patients affected by other types of dementia. In 1901, the german psychiatrist Alois Alzheimer (1864-1915) first met a patient named Mrs. Auguste D. at the Frankfurt Asylum (Figure 4). This 51 year-old woman suffered from a loss of short-term memory, among other cognitive symptoms that puzzled Dr. Alzheimer [102]. Five years later, the patient died and Dr. Alzheimer obtained her brain and medical records that were sent to him from Munich, where he was working with Dr. Emil Kraeplin. By staining sections of her brain, Dr. Alzheimer was, for the first time, able to identify and describe senile plaques and neurofibrillary tangles [103-105].

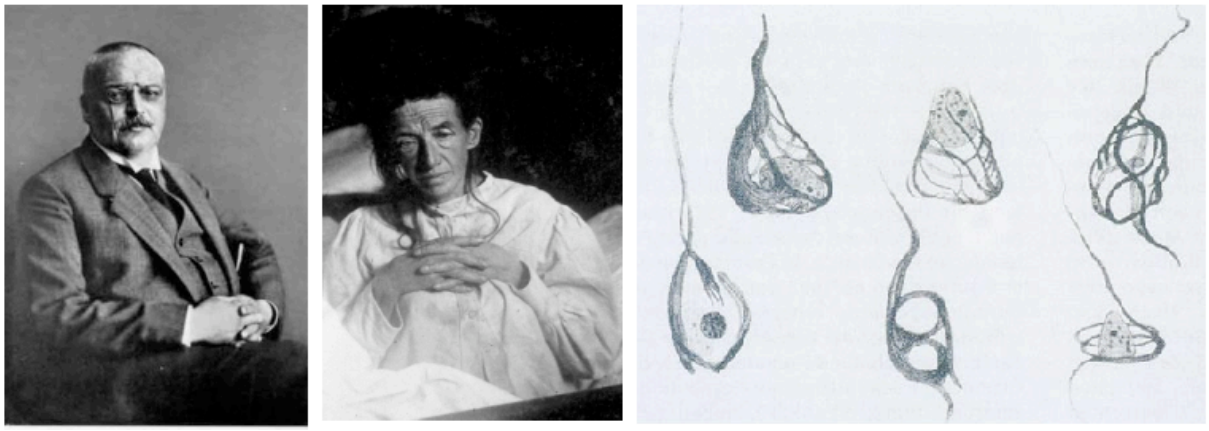

Figure 4: **Alois Alzheimer and Auguste D**

Alois Alzheimer (1864-1912) (**left image**) and his first patient (**middle image**), Auguste D., in whom he described the typical lesions due to the disease, now bearing his name. On the **right,** the original drawing by Alois Alzheimer shows the neurofibrillary tangles present in the brain of this patient.

The main pathological hallmarks of AD are i) the senile plaques composed of ß-amyloids (Aß), and ii) the neurofibrillary tangles (NFT) consisting of paired filaments of aggregated tau protein. The neuronal and dendritic loss in the perithinal and entorhinal cortex, the hippocampus and the cerebral cortex [106] as well as the synaptic damage [107-109] are also typical for this disease.

2.1.1 Senile plaques

In Alzheimer's original report senile plaques have been described as "miliary foci" (Figure 5) [103], which correspond to spherical lesions of 10-200 µm in diameter, today recognized as composed extracellular Aß deposit and cellular elements. The Bielschowsky silver technique has been used to identify and classify senile plaques. This method of staining is still in use nowadays [110]. It should be noted that before Alzheimer's report, Blocq and Marinesco had already described senile plaques in an elderly epileptic patient [111].

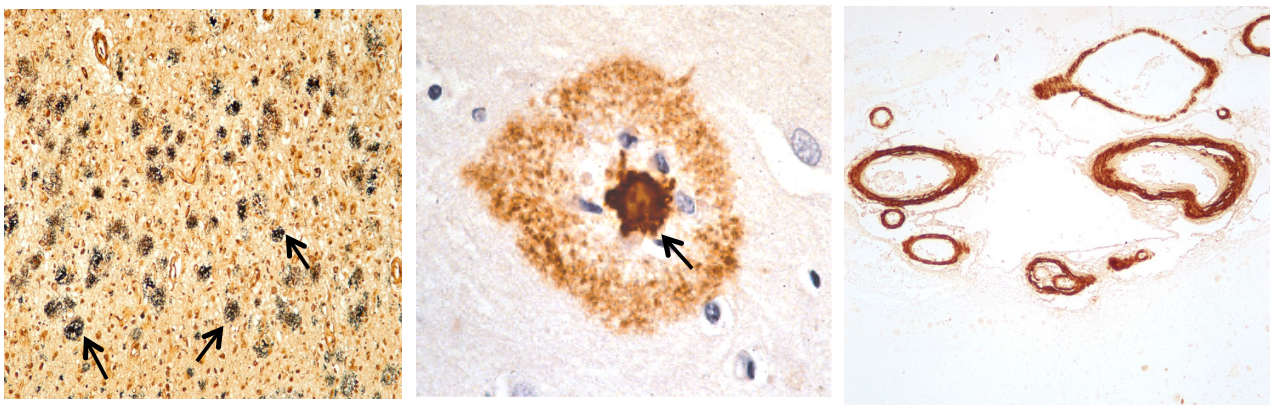

Figure 5: **Extracellular deposition of Aß**

Left panel: Bielschowsky silver impregnation is the technique used by Alzheimer in his original description of Auguste D. showing "miliary foci"(arrows) [112]. These typical foci were known to occur in association with "dementia senilis" before Alzheimer's description. **Middle and right panel**: Immunohistochemical staining of Aß showing the two main types of extracellular deposits encountered in AD: senile plaque with its compact amyloid core (middle, arrow) and Aß deposition in vessel walls (CAA; right) (Adapted from Castellani *et al.,* 2008).

There have been several pathological mechanisms postulated responsible for the generation of senile plaques. The main constituents of senile plaques are the extracellular deposits of aggregated Aß. These deposits are surrounded by dystrophic neurites, activated microglial cells and reactive astrocytes [113, 114]. In addition, Aß deposits are also present in the walls of cerebral [115, 116] and leptomeningeal blood vessels, now called cerebral amyloid angiopathy (CAA) [117, 118] (Figure 4).

The Aß peptide [119-121] is a 4 kDa protein fragment of 39-43 amino acids which results from the proteolysis of the amyloid precursor protein (APP) [122-125]. APP is a transmembrane glycoprotein, which can be proteolytically cleaved by the membrane-associated α-, β- and γ-secretases. The α-secretase cleaves APP within its Aß domain and produces soluble α-APP. This process is non-amyloidogenic, as the cleavage prevents the formation of Aß. In contrast to α-secretase cleavage, proteolysis may happen in the amyloidogenic endosomal-lysosomal pathway, triggered by ß-secretase and followed by γ-secretase, which together generate the highly fibrillogenic Aß peptide. Only one protein, BACE1, has been described so far to be required for ß-secretase activity, whereas γ-secretase

activity depends on the presence of a large heterotypic complex composed of presenilin, nicastrin, APH-1 and PEN-2 proteins [126, 127].

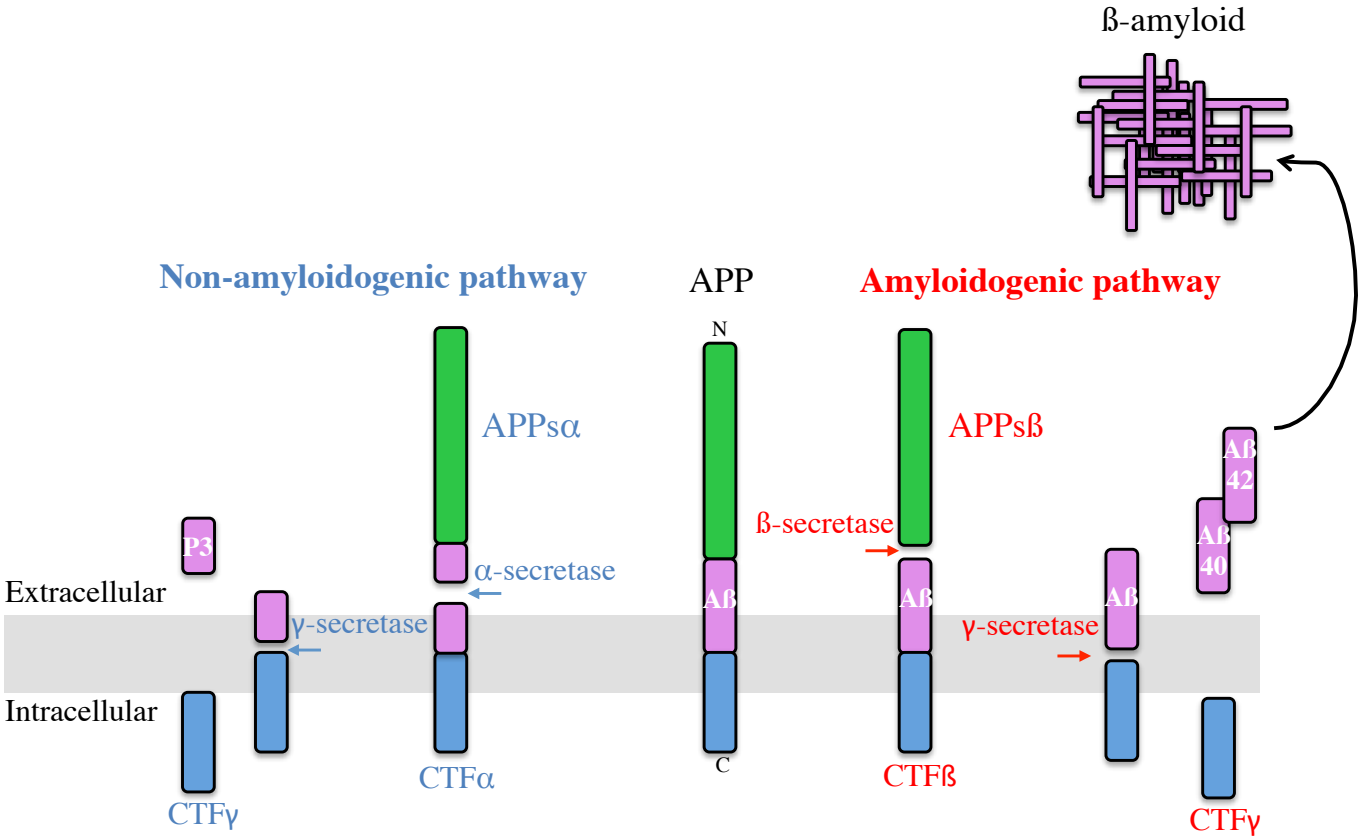

Figure 6: Schematic representation of APP processing by α-, ß-, γ-secretases

Cleavage by α-secretase (left panel) generates the large and soluble APPsα and the transmembrane C-terminal fragment (CTFα). Cleavage by ß-secretase (right panel) results in the production of soluble APPsß and production of C-terminal fragment (CTFß). Both CTFα and CTFß serve as substrates for γ-secretase, which gives, yields a 3 kDa peptide called p3 from cleavage of CTFα and Aß production from cleavage of CTFß. (Adapted from Kahle *et al.,* 2003).

The idea that the neurodegeneration in AD may be caused by the deposition of Aß peptide in plaques (the "*amyloid cascade*" hypothesis) has been first suggested in 1991 [128]. According to this hypothesis, the pathogenesis of AD is driven by the aggregation of Aß fibrils in the brain. The progression of the disease, including the formation of neurofibrillary lesions, microglia activation, synaptic dysfunction and neuronal loss, would then be an outcome of an imbalance between Aß production and clearance [129]. However, in elderly subjects presenting intact cognitive functions it is possible to find abundant cortical Aß aggregation [130, 131]. Several studies support a modification of the *amyloid cascade* hypothesis and suggest that Aß assembly into neurotoxic oligomers, and not into amyloid plaques, is the major toxic effector in AD pathogenesis [132-135]. Most probably fibrillar amyloid plaques serve as a container for the amyloid oligomers or constitute a pool of sequestered soluble and precipitated Aß. They would, therefore, have a protective rule or simply constitute the end stage of the Aß cascade [136].

2.1.2. Neurofibrillary lesions

Another hallmark of AD pathology is the intracellular accumulation of hyperphosphorylated tau proteins in NFT and the neuropil threads (NT) or dystrophic neurite associated with senile plaques (Figure 7). It has been suggested that Aß toxicity is tau dependent, even though the mechanism remains uncertain. Indeed, it has been shown that knocking out tau alleviates cognitive impairment without affecting Aß levels in an APP mouse model of AD [137]. Tau is normally localized in axon and has been shown to be mislocalized in dendrites and soma of neurons in AD. Tau in dendrites would interact with kinase protein and lead to Aß toxicity [138]. On the other hand, recent reports have shown that injection of Aß fibrils in P301L transgenic mice model increases the formation of NFT. In this study the authors demonstrated that the injection exaggerates hyperphosphorylation of tau and NFT formation [139].

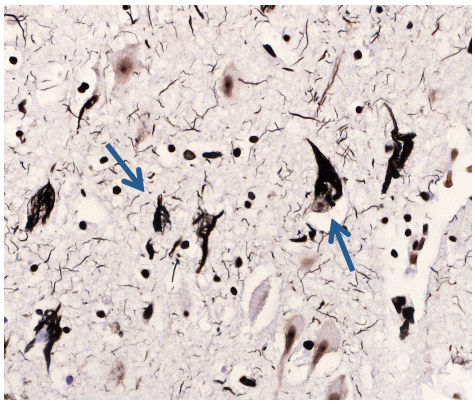

Figure 7: Intracellular lesions made of aggregated tau protein

Gallyas silver staining shows neurofibrillary tangles in the cortex of subjected with AD.

2.2. Other tauopathies

The central event leading to the formation of NFT and neuronal loss in AD is not exactly known. In AD, Aß peptides may play a central role in the formation of NFT [128]. However, as mentioned before, a number of neurodegenerative diseases known as tauopathies share the feature of tau inclusion in neurons and glial cells but in the absence of Aß pathology. Only the most frequent of them will be shortly described here.

2.2.1. Progressive supranuclear palsy

Progressive supranuclear palsy (PSP) is also known as Steele-Richardson-Olszewski syndrome. This neurodegenerative disorder is characterized by supranuclear vertical gaze palsy and motor impairment including axial rigidity and dystonia [140]. Neuropathologically, neuronal loss, gliosis and NFT formation are the characteristic symptoms of PSP. Since NFT appears first in the basal ganglia (mainly the globus pallidus and the subthalamic nucleus), brainstem and cerebellum [140]. PSP thus constitutes a "subcortical dementia" [141, 142]. Typical tau aggregates appear in different brain area as round or globose-type NFT and as NT [143, 144] as well as in astrocytes (tufted astrocytes) and oligodendrocytes (coiled bodies) [145] (Figure 8).

2.2.2. Corticobasal degeneration

Corticobasal degeneration (CBD) is an adult-onset, sporadic, slowly progressive neurodegenerative disorder. Clinically CBD is characterized by an extrapyramidal motor syndrome and cognitive dysfunction associated with aphasia and apraxia. In contrast to Parkinson's disease, this disorder is poorly responsive to dopaminergic drugs. [146-148]. In CBD, the dysfunction of the neurons is observed in many components of the basal ganglia including the substantia nigra. Thus, a treatment with dopamine agonist, unlike in Parkinson's disease, meets no intact effector cells in the striatum. Neuropathological observation of the brain reveals a frontoparietal, often asymmetrical atrophy together with neuronal and glial abnormalities including "astrocytic plaques" [149] (Figure 8).

2.2.3. Pick's disease

Pick's disease (PiD) is a rare, neurodegenerative disorder with a progressive clinical course characterized by frontal and temporal lobes symptoms with behavioural abnormalities, mood changing and impairment of language [150]. The specific pathological feature is an atrophy of the frontal and temporal lobes associated with severe neuronal loss, gliosis and argyrophilic. Even though Gallyas staining is negative, tau containing intraneuronal inclusions known as Pick bodies has been detected in both cortical and subcortical areas [151, 152], granule cells of the dentate gyrus and pyramidal neurons of the hippocampus [153, 154] (Figure 8).

2.2.4. Argyrophilic grain disease

Argyrophilic grain disease (AgD) is a common, sporadic dementia affecting elderly individuals, with a prevalence of 5% [155, 156]. AgD is characterized by an abundance of argyrophilic tau immunoreactive grains in the enthorinal cortex, hippocampus (CA1, subiculum) and amygdala [157, 158] often together with NFT typical of AD. The pathogenesis of AgD and the mechanisms leading to the accumulation of these grains remain unknown. The clinical symptoms of the pathology comprises a cognitive decline, dementia [156, 159] as well as behavioural changes like mood and emotional imbalance [155]. Besides, it has been shown that there is an occasional memory loss in AgD, making it difficult to distinguish from AD in some cases (Figure 8).

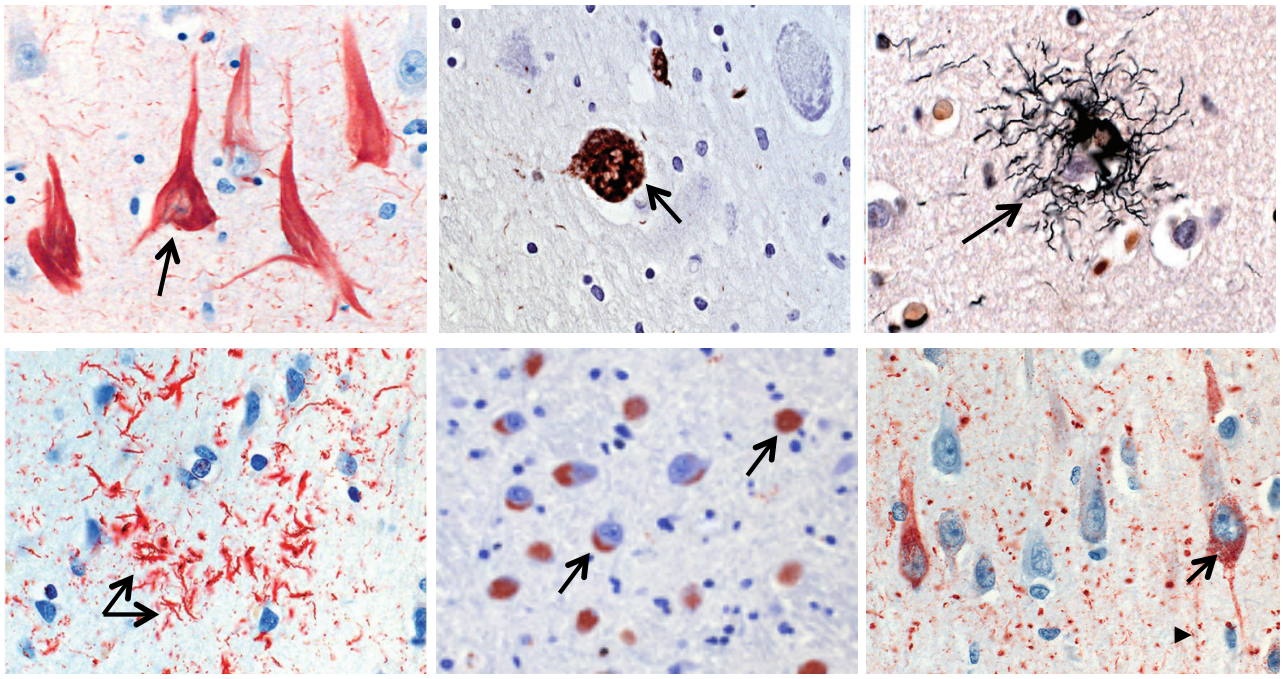

Figure 8: Different types of tau pathology in tauopathies

Upper panel, left: classical neurofibrillary tangles in AD revealed by immunohistochemistry with phosphorylation-dependent anti-tau antibody (arrow). **Middle**: Tau immunohistochemistry shows a globose tangle (arrow). **Right:** Tufted astrocytes in PSP revealed by Gallyas silver staining (arrow) (Adapted from M. Neumann *et al., 2009*). **Lower panel, left**: Tau immunohistochemistry shows astrocytic plaques in CBD (arrows) (Adapted from M. Neumann *et al., 2009*), **(middle)** pick bodies (spherical intraneuronal inclusions, arrows) using phospho-tau immunohistochemistry in Pick's disease. **Right**: Argyrophilic grain in the neuropil (arrowhead) and abnormal accumulation of hyperphosphorylated in hippocampal pyramidal cells in a case of argyrophilic grain disease (arrow).

2.2.5. Frontotemporal dementia and parkinsonism linked to chromosome 17

In 1994, a familial form of frontotemporal dementia with parkinsonism was linked to the locus 17q21.2 [160]. Mutations in the *TAU* genes were shown to be responsible for these pathological conditions which were gathered under the term of Fronto-Temporal Dementia and Parkinsonism linked to chromosome 17: FTDP-17 [161]. The neuropathological hallmarks of FTDP-17 are: neuronal loss, astrocytic gliosis and filamentous accumulation of hyperphosphorylated tau. The clinical features of this disease include personality changes, motor disturbances and cognitive decline, which leads to severe dementia. Depending on the mutation affecting the *TAU* gene, and the fact whether it is located in the coding or non-

coding region, tau aggregates can be constituted predominantly of 3R, 4R or a combination of 3R and 4R tau isoforms.

2.3. Development of experimental mouse models of tau pathology

Different transgenic mouse models of AD and other tauopathies have been generated over the last fifteen years. Several mouse models have been engineered and selected examples will be presented in the following part.

Transgenic mice with mutations present in familial forms of tauopathies develop a similar pathology as seen in human patients. The missense mutations substituting the proline 301 for a leucine (P301L) or serine (P301S) were discovered in FTDP-17 [162, 163]. These mutations affect *TAU* exon 10, which encodes the highly conserved microtubule-binding domain, and thereby only alter the 4R tau isoform. Transgenic mice expressing human 4R tau with FTDP-17 mutation P301L under the control of the mouse prion promoter (JPNL3 line) develop progressive motor and behavioural impairments [164]. Aggregated tau and NFT formations are found in the cortex, the hippocampus and the basal ganglia of these mice. JPNL3 mice show a sever phenotype at 6.5 months in hemizygous and 4.5 months in homozygous animals, even though the expression of the transgene is low. A similar model created in 2002 expresses the human *TAU* gene carrying the P301S mutation under control of the Thy 1.2 promoter [165]. In humans, this mutation causes an early onset form of FTDP-17. P301S mice develop a progressive motor deficit, which is related to the abundance of tau filaments inclusions in the brainstem and the spinal cord. These filaments contain hyperphosphorylated tau protein. While in FTDP-17 patients nerve and glial cells are affected [166], in P301S model the accumulation of tau is restricted to nerve cells which is due to the selective neuronal expression of the tau transgene by the Thy 1.2 promoter. These two murine models carrying mutation in the *TAU* gene (P301L and P301S) highlight the role of tau in neurodegenerative diseases and are currently being used for the development of possible therapeutic strategies against tauopathies.

Other mouse models have further established that an imbalance between the 3R/4R isoforms can be responsible for the development of tauopathies [18, 51, 167-169]. Notwithstanding, transgenic mice expressing the shortest 3R tau isoform under the HMG-

CoA reductase promoter [170] or under the Prnp promoter [171] recapitulate key features of tauopathy.

As mentioned before, tau can be cleaved by caspases at Asp^{421}. This fragmentation affects the conformation of the protein, which accumulates rapidly [74, 75], co-localizes with tangles and associates with degenerating neurons [93, 95, 96]. Interestingly, rTg(tau_{P301L}) 4510 mice showed a quick activation of the caspases, followed by the development of NFT in neurons. After tangle formation, caspase activity was suppressed in NFT-containing neurons without neuronal death. The authors established the hypothesis that the formation of NFT is not responsible *per se* or prerequisite for tau induced neurodegeneration or neuronal death. Furthermore, they demonstrated that NFT formation occurs after caspase activation [96]. In addition to cleavage at Asp421, tau can also be truncated at Glu^{391} at later stages in the progression of tau pathology. Recent studies showed that in rat models expressing fragmented human tau (3R or 4R), NF are widely accumulated in the brainstem and cortex [172, 173]. Moreover, these rat models developed muscle weakness and wasting, which might have caused their death. These studies highlight the major role of truncated tau in the development of pathologic condition by increasing the propensity for tau accumulation.

The main of our actual work is to understand the impact of fragmented tau on the pathogenesis of tauopathies. To this end, we have studied the toxicity of truncated tau in a novel inducible transgenic mouse in the presence of human full-length tau. In parallel, we have investigated whether increased autophagy can prevent tau aggregation in mouse models.

PART III

Autophagy: an essential catabolic process

Most neurodegenerative diseases share a similar pathogenesis with the occurrence of abnormal protein inclusions in the nervous system, containing specific misfolded proteins. Such human diseases, also called "proteinopathies", include Alzheimer's disease (AD), Parkinson's disease (PD), or Huntington's disease (HD). In these disorders, abnormal protein accumulation alters essential cellular functions and leads to neurological impairment and neuronal loss [174-177].

3.1. Mechanisms of the autophagy process

Autophagy (i.e. "self-eating" in greek) is a catabolic pathway conserved among eukaryotes, which allows cells to rapidly eliminate large, unwanted structures such as abnormal protein aggregates, damaged organelles and invading pathogens [178]. Three different types of autophagy can deliver cytoplasmic components into the lumen of lysosomes for degradation: macroautophagy, microautophagy and chaperone-mediated autophagy (Figure 9). Macroautophagy is considered to be the major type of autophagy occurring in cells and it has been more extensively studied than microautophagy and chaperone-mediated autophagy. Therefore, in the following part, the term "autophagy" will refer to macroautophagy for simplification.

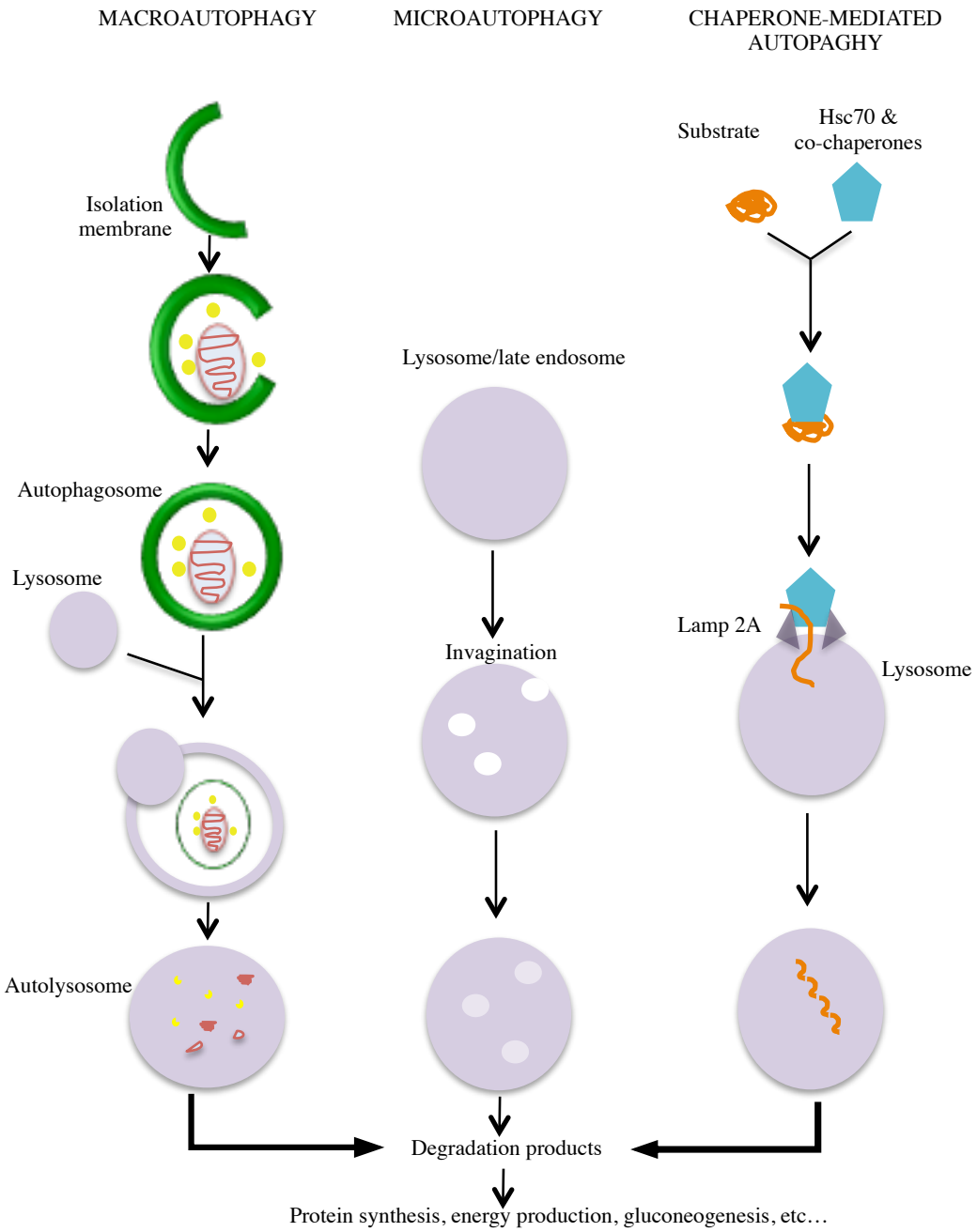

Figure 9: Different types of autophagy

During macroautophagy, a portion of cytoplasm, including organelles, is engulfed by a double-membrane vesicle, called autophagosome. Autolysosomes are formed by the fusion of the outer membrane of the autophagosome with lysosomes and allow the degradation of the sequestrated material. During microautophagy, small pieces of cytoplasm are directly engulfed by inward invagination of lysosomal or late endosomal membrane. During chaperone-mediated autophagy, specific substrate proteins containing a KFERQ-like pentapeptide sequence are first recognized by cytosolic Hsc70 and co-chaperones. After binding with lysosomal Lamp-2A, the complex substrate-Hsc70-co-chaperones are translocated into the lysosomal lumen (Adapted from N. Mizushima *et al.,* 2011).

At basal levels, autophagy can be considered as a housekeeping mechanism involved in the constitutive elimination of protein aggregates and other macromolecules inaccessible to the ubiquitin-proteasome pathway. Autophagy is dependent on the up-regulation of multiple autophagy-related genes (*ATG*) [179]. Autophagy starts with the formation of an isolating membrane, a crescent-shaped double membrane, which originates from the smooth ER or from another, not yet defined, subcellular location [180]. The isolating membrane completely surrounds cargoes targeted for degradation (Figure 10).

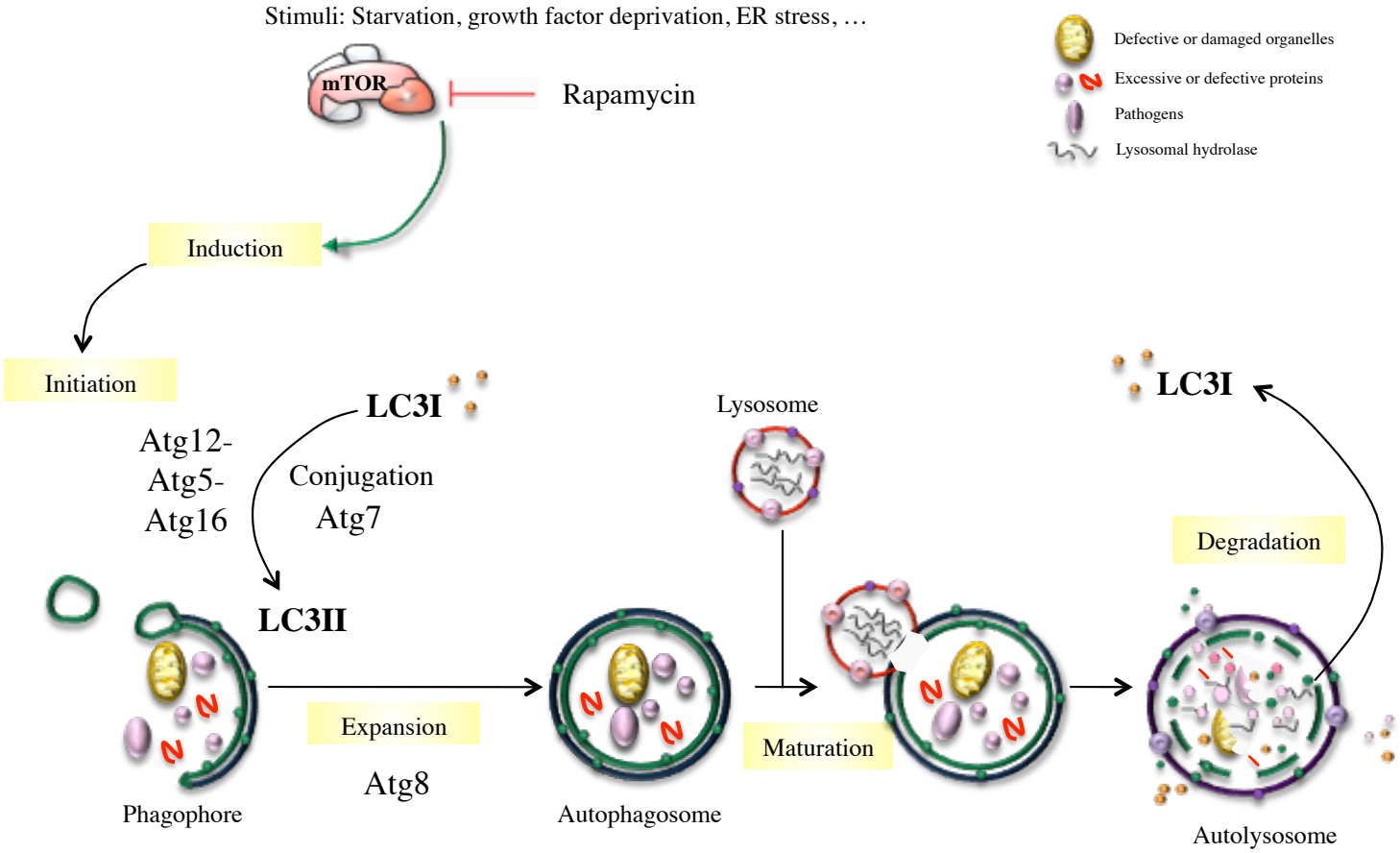

Figure10: The autophagy process

Autophagy occurs at low basal levels and can be activated by multiple stimuli such starvation or mTOR inhibition. It involves the sequestration of cytoplasmic material by an isolating membrane (derived from a crescent structure also termed a phagophore) to form a double-membrane vacuole, the autophagosome. Mature autophagosomes fuse with lysosomes containing lysosomal hydrolase to form autolysosomes, then degrading cargo and enabling components to be recycled.

The formation of the autophagosomes and the progression of the autophagy processing require two ubiquitin-like conjugation reactions: i) the formation of a Atg12–Atg5–Atg16 complex and ii) the conjugation of Atg7 (also known as microtubule-associated protein 1 light chain 3 protein or LC3) to phosphatidylethanolamine [181]. LC3 is commonly used as a biochemical marker for autophagy, since it is specifically lipidated and associated to autophagosomes during autophagy induction [182, 183]. Induction of autophagy by rapamycin (also known as sirolimus (Rapamune; Pfizer)) and CCI-779 is related to inhibition of TOR complex in yeast [184] and mTORC1 (mammalian target of rapamycin complex 1), a well-known, major inhibitor of autophagy, in mammals [185]. It should be noted, however, that some amino acid signalling can suppress autophagy in an mTOR-independent manner [186, 187]. Moreover, small molecule enhancers of the cytostatic effects of rapamycin (called SMERs) have been identified as inducers of autophagy independently of mTOR [188].

3.2. Autophagy in neurodegenerative disease

The accumulation of abnormally aggregated or mutant proteins plays a crucial role in neurodegenerative diseases [189]. On the other side, a dysfunction of autophagy, including accumulation of autophagosomes, has been reported in neuronal pathologies such as in Parkinson's, Huntington's and Alzheimer's diseases [190-192]. Induction of autophagy in these disorders can be interpreted in two ways. On one hand, increased activity of the autophagy machinery may be a primary element of the pathogenesis and could contribute to neurodegeneration e.g by the generation of toxic protein fragments or other yet unspecified mechanisms [193, 194]. On the other hand, autophagy induction may constitute an adaptative, protective response to activate the degradation of aggregate-prone proteins. Accordingly, impaired autophagy leads to the accumulation of neurotoxic proteins that later on become responsible for neuron death. In this light, modulation of the autophagic flux constitutes a potential therapeutic strategy to treat or ameliorate neurodegenerative disorders.

3.2.1. Parkinson's disease and the autophagy process

Parkinson's disease (PD) is a common neurodegenerative disorder of yet unknown origin. Clinical symptoms include resting tremor, slowness of movement, rigidity and postural instability. The symptoms are primarly attributed to a dramatic loss of dopamine containing

neurons in the substantia nigra pars compacta, leading to dopamine depletion in the striatum [195]. Histopathologically, PD is characterized by the presence of ubiquitinlated α-synuclein in cytoplasmic inclusions called Lewy bodies; however the origin and significance of Lewy bodies remain unclear. Cell models for PD revealed that the clearance of mutant forms of α-synuclein is highly dependends on autophagy [196, 197]. Hence, autophagy inhibitors, such as 3-methyladenine and bafilomycin A1, delay their degradation whereas autophagy inducers, including rapamycin, enhance their elimination [196, 197]. In a recent study, rapamycin was found to have beneficial effects in both *in vivo* and *in vitro* models of PD and to protect dopaminergic neuron cells from death [198]. In another study, the neuroprotective action of rapamycin in PD was related to an increase of autophagic degradation steps, the promotion of the autophagosome-lysosome fusion, and thereby to an enhanced clearance of the autophagosomes [199]. It remains difficult to rule out the contribution of the various other molecular pathways affected by rapamycin, however it is likely that the positive effects of rapamycin on PD are mainly mediated by an increase in the autophagy flux.

3.2.2. Huntington's disease and the autophagy process

Huntington's disease (HD) is an autosomal dominant neurodegenerative disorder characterized by progressive motor dysfunction, dementia and emotional disturbances [200]. HD is caused by an autosomal, dominant (CAG) triplet repeat expansion mutation in the *HTT* gene, encoding the ubiquitously expressed protein huntingtin (Htt). Mutated Htt (mtHtt) accumulates inside neurons and forms toxic oligomeric species and aggregates, which probably lead to cell death [200]. No effective treatment has been developed so far for the disease. Nonetheless, it has been demonstrated that rapamycin attenuates the neuronal toxicity of mtHtt fragment, both *in vitro* and in animal models of HD. In particular, efficiency of rapamycin has been proven using the powerful genetic model of *Drosophila melanogaster* visual system [185]. When these flies are fed with food containing rapamycin from the larval stage into adulthood, they present reduced degeneration of rhabdomere sensors of the visual neurons compared to untreated flies [185]. Rhabdomere degeneration and the associated cell death were also attenuated by genetic induction of autophagy [201]. The effects of rapamycin treatment were also tested and analyzed in a mouse model for HD expressing a mtHtt fragment in brain [185]. These mice display a drastic phenotype, reminiscent of that observed in human, including dyskinesia, tremors, weight loss and premature death [185]. Treatment with rapamycin reduced mTORC1 activity, attenuated protein aggregation and finally,

ameliorated the behaviour phenotype [185]. Taken together, most results indicate that pharmacological induction of autophagy by rapamycin or other comparable substances may constitute potential therapeutic strategies for HD by favouring the removal of mtHtt.

3.2.3. Alzheimer's disease and autophagy dysfunction

Alzheimer's disease (AD) is the most common neurodegenerative disorder and is characterized by memory loss and various cognitive dysfunctions. In AD brains, the two major pathological hallmarks are the extracellular deposition of amyloid plaques and the intracellular aggregation of tau [202]. In AD, massive accumulation of autophagosomes along dystrophic and degenerating neurites is caused by impaired maturation of the autophagosomes and their altered retrograde transport to the neuronal cell body [203]. Indeed, autophagosomes and endosomes actively form in synapses and along neuritic processes while lysosomes are concentrated in neuronal soma. Hence, autophagic degradation in neurons necessitate an efficient trafficking of autophagosomes along microtubules [66].

Several studies have reported a beneficial effect of autophagy induction in AD models. First of all, treatment with rapamycin was shown to decrease toxicity of mutated tau in transgenic flies [204, 205]. Induction of autophagy by using viral vector-mediated expression of beclin 1, also known as autophagy-related protein 6 (Atg6), reduced intracellular and extracellular ß-amyloid deposition in APP transgenic mice [206]. Similarly, enhancement of lysosomal activity in the transgenic mouse model of AD, (TgCRND8 line), decreased intraneuronal and extracellular Aß levels, and inhibited the progression of deficits of learning and memory in these animals [207]. Inversely, inhibition of autophagy increased Aß induced toxicity in neuron cell cultures [208]. Caccamo et al. using an AD mouse model found that mTORC1 inhibition with rapamycin improved cognitive deficits and alleviated tau pathology by enhancing autophagy [209]. Lastly, in two different genetic mouse models for AD, the PDAPP mice also known as hAPP (J20 line), which accumulate soluble and aggregated Aß, and the 3xTgAD mice expressing APP_{Swe}/P301L/mutant $PS1_{M146V}$, rapamycin restrained their cognitive deficits and attenuated amyloid and tau pathology by enhancing autophagy [209, 210].

It should be noted that imbalanced activity of mTORC1, which plays an important role in sensing nutrient and energy in cells, correlates with autophagy impairment in AD [203]. The mTORC1 pathway is more activated in the presence of Aß peptides accumulation whilst Aß levels are reduced with a decrease in signalling. Moreover, in AD brain, activity of

mTORC1 and levels of its downstream targets such as eukaryotic initiation factor 4E binding protein 1 (4EBP1), correlate with tau protein accumulation [211].

The importance of autophagy deficits in AD is not fully understood. It is well known that aging is an important risk factor for the development of AD and many other neurodegenerative diseases. Notably, rapamycin treatment in animals has been shown to prolonge lifespan in several recent studies, and to limit the development of age-related dysfunctions in several tissues, likely by promoting autophagy (see below, "Role of rapamycin in aging"). Hence, promoting autophagy in age-related neurodegenerative disorders constitutes a promising therapeutical strategy [212, 213].

3.3. The mTORC1 pathway and tau protein

mTOR is a 289kDa serine/threonine protein kinase that belongs to the phosphoinositide 3-kinase (PI3K)-related kinase family and serves as a main regulator of cell metabolism, growth, proliferation and survival [214-217]. Two main types of multi-protein complexes form with mTOR: the mTOR complex 1 (mTORC1) characterized by the raptor protein and the mTOR complex 2 (mTORC2) including the rictor protein [218]. mTORC1 positively regulates cell growth and proliferation by modulating anabolic processes such as protein synthesis and by blocking catabolic processes like autophagy. mTORC1 is recruited to and activated on lysosomal membranes in the presence of amino acids, and thereby can promote translation and inhibit autophagy [209, 219, 220].

Beyond its relation to tauopathy through the inhibition of autophagy (see above, "Autophagy in neurodegenerative disease"), mTORC1 pathway seems to play a role in neurodegenerative disorders by regulating tau translation, modulating its phosphorylation and thereby, the formation of PHF and NFT [221]. Moreover, tau phosphorylation has been shown to be regulated by the balance between PP2A and GSK3, which can be modulated through the PI3K/mTORC1 signalling [222]. All together, these data suggest that the mTORC1 pathway may be a potential, effective therapeutic target for tau-related pathological conditions.

3.3.1. Role of rapamycin in aging

Increased age is a risk factor shared by many neurodegenerative diseases, although the direct molecular link between ageing and neurodegeneration is still unknown. As mentioned before, several studies established that rapamycin extends life span in different species, including yeast [223], fruitflies [224] and mice [212]. Some of the reports also demonstrated that rapamycin exerts a beneficial effect on age-related neurodegeneration. According to these results, mTORC1 constitute a key player and a target for lifespan extension [225]. Anti-aging effects obtained by pharmacological or genetic inhibition of mTORC1 mainly rely on the induction of autophagy. However, it has also been suggested that lifespan extension promoted by rapamycin may be related to the reduction in protein synthesis in *D. melanogaster* [224]. Indeed, upregulation of S6K activity or genetic ablation of the translational suppressor 4E-BP abolished rapamycin mediated lifespan extension [224]. Furthermore, other reports proposed that increased lifespan in yeast are achieved due to the reduction in age-related genome instability [223]. In particular, ribosomal DNA (rDNA) recombination, associated with the formation of toxic repetitive extrachromosomal rDNA circles, can be repressed by the induction of sirtuin deacetylases, which belong to a family of key regulators of cell survival [226]. Interestingly, both caloric restriction and mTORC1 inhibition were shown to promote the activity of sirtuin enzymes.

Hence, the same molecular mechanisms may underlie the function of rapamycin on longevity and its neuroprotective effects in different models of neurodegeneration. This may shed light on the potential molecular link, still not yet identified, existing between aging and neurodegenerative disorders.

3.3.2. Rapamycin as a therapeutical approach

Rapamycin is an established Food and Drug Administration (FDA) approved drug. First identified as an antifungal and antibiotic drug, it is now recognized as a major immunosuppressor, and used to prevent transplant rejection [227, 228]. By inhibiting mTORC1, rapamycin may also limit tumor growth, in particular in the tuberous sclerosis complex (TSC) disease, and restrain cancers. Given the positive effect of the molecule on longetivity [212], one can suppose that rapamycin may also be used to fight against neurodegenerative disease such as AD [213, 229].

Preclinical tests also showed that rapamycin improves learning and restrains memory deficits, by promoting neuronal survival and plasticity and by reducing Aß and tau pathology [209, 210, 230]. Moreover, the accumulation of aggregated protein can be moderated through

the induction of autophagy, which can be in turn promoted by mTORC1 inhibition [231]. Together, these findings highlight that rapamycin or other analogue treatment targeting mTORC1 may constitute a basis for the development of treatment strategies that would improve proteinopathies such as AD.

RESULTS

Manuscript N°1:

Tau fragmentation exacerbates the toxicity of tau protein and participates in the onset of neuronal dysfunction

Publication N°2:

Rapamycin Attenuates the Progression of Tau Pathology in P301S Tau Transgenic Mice

Publication N°3:

Stimulation of autophagy reduces neurodegeneration in a mouse model of human tauopathy

Rationale and Aims of the thesis

1- Previous results

Before the beginning of this thesis, in autumn 2009, the impact of truncated forms of tau had been shown to favour tau aggregation [85], and tau fragmentation by proteases had been identified *in vitro*, in brain from AD patients, as well as in transgenic mouse models for AD [75, 86, 95]. In parallel, other groups had already suggested that induction of autophagy by rapamycin has a beneficial effect on age-related tissue dysfunction and on lifespan in various species, including yeast, fruitflies and mice [212, 223, 224]. Furthermore, in 2004, Ravikumar et al. also demonstrated in a pioneer study that mTORC1 inhibition and thereby autophagy induction is sufficient to limit the toxicity of polyglutamine expansions and to improve the associated HD-related phenotype of their fly model [185].

2- Specific questions

These prior reports opened interesting avenues regarding the mechanisms at play in the pathogenesis of tauopathies and potential therapeutical strategies [185]. To get further insight on the importance of tau fragmentation on the pathogenesis, we generated new transgenic mouse models, expressing a truncated form of tau (noted Δtau) in basal conditions (TAU62 mice) or concomitantly with the expression of full length forms of tau (P301SxTAU62 noted P62, ALZ17xTAU62). With this project, we wanted i) to test whether Δtau expression *in vivo* is sufficient to provoke characteristic tauopathy associated changes in mice, ii) to determine if Δtau modifies the toxicity of full length forms of tau protein and promotes the formation of tau aggregates, iii) to identify which forms (soluble/insoluble aggregates, oligomers, tangles, filaments) of tau are predominantly responsible for tau induced neuronal dysfunctions and iv) to further elucidate the cellular events at play in the onset and progression of tauopathies. The use of an inducible promoter in TAU62 mice furthermore allowed us to analyze the evolution of Δtau initiated pathology in the corresponding mice also when the expression of Δtau was stopped.

In parallel, as aging constitutes the most important risk factor for AD, and since autophagy impairment is thought to be involved in the onset of proteinopathies, it was of major interest to investigate the impact of autophagy inducers on the progression of

tauopathies. To shed light on this open question, we decided to study whether autophagy stimulation would promote tau clearance in a transgenic mouse model for tauopathy. To this end, P301S mutant tau mice, which were previously generated and characterized i.e. by Allen et al. [165], were treated with the autophagy-inducing agent rapamycin and the consequences on their phenotype were analyzed. The principal aim of the project was to determine whether mTORC1-dependent restoration of the autophagy process would reduce the accumulation of insoluble tau protein in the brain and spinal cord, and thereby ameliorate the associated neuron dysfunctions. In a comparable study, conducted in collaboration with the group of Dr. Michel Goedert (Cambridge, UK), P301S mice were treated with another well-known inducer of autophagy, trehalose, whose effect has been shown to be independent from mTORC1.

3- Publications arising from this work

This thesis is written in a manuscript-based format: the following part contains one manuscript in preparation and two published papers.

In the **Manuscript N°1** (*"Tau fragmentation exacerbates the toxicity of tau protein and participates in the onset of neuronal dysfunction"* - Sefika Ozcelik, Graham Fraser, Zhiva Skachokova, Dorothee Abramowski, Alphonse Probst, Ludwig Kappos, Stefan Frank, Matthias Staufenbiel, Michel Goedert, Markus Tolnay, David T. Winkler - in preparation), we demonstrate that Δtau fragment exerts a drastic toxic effect when co-expressed with full-length tau *in vivo*, and causes a severe but reversible motor phenotype associated with extensive neuronal changes in double transgenic mice. Notwithstanding, these Δtau-related defects were associated with the formation of toxic oligomers, in the absence of insoluble tau aggregates or tangles. Hence, this supports the hypothesis that tau fragmentation constitutes a central, determining event in the onset of tauopathies, and the prevention of tau cleavage may therefore be considered as a promising therapeutic strategy for these disorders.

In the **Publication N°2** (**"***Rapamycin Attenuates the Progression of Tau Pathology in P301S Tau Transgenic Mice*" - Ozcelik S, Fraser G, Castets P, Schaeffer V, Skachokova Z, Breu K, Clavaguera F, Sinnreich M, Kappos L, Goedert M, Tolnay M, Winkler DT. PLoS One. 2013 May 7;8(5):e62459.), we establish that rapamycin treatment significantly delayed the progression of tau pathology and the associated histopathological and biochemical changes in P301S mice. Comparable effects are described in the **Publication N°3** (*"Stimulation of autophagy reduces neurodegeneration in a mouse model of human*

tauopathy" - Schaeffer V, Lavenir I, Ozcelik S, Tolnay M, Winkler DT, Goedert M. Brain. 2012 Jul;135(Pt 7):2169-77) by using trehalose treatment, another inducer of autophagy. Together, these data encourage the development of drugs promoting the induction of autophagy for patients suffering from tauopathies, although side effects of such therapeutics should be carefully considered and examined.

Manuscript N°1

Tau fragmentation exacerbates the toxicity of tau protein and participates in the onset of neuronal dysfunction

Sefika Ozcelik, Graham Fraser, Zhiva Skachokova, Dorothee Abramowski, Alphonse Probst, Ludwig Kappos, Stefan Frank, Matthias Staufenbiel, Michel Goedert, Markus Tolnay, David T. Winkler

In preparation.

Tau fragmentation exacerbates the toxicity of tau protein and participates in the onset of neuronal dysfunction

Sefika Ozcelik[1, 2], M.Sc., Graham Fraser[3], PhD, Zhiva Skachokova[1], M.Sc., Dorothee Abramowski[4], M.Sc., Alphonse Probst[1], MD, Ludwig Kappos[2], MD, Stefan Frank[1], MD, Matthias Staufenbiel[4], PhD, Michel Goedert[3], PhD, Markus Tolnay[1], MD, David T. Winkler, MD, PhD[1, 2]

[1]Institute of Pathology and [2]Department of Neurology, University Hospital Basel, Petersgraben 4, CH-4031 Basel, Switzerland, [3]MRC, Laboratory of Molecular Biology, Hills Road, Cambridge CB2 0QH, UK, [4]Novartis Institute of Biomedical Research, Novartis Pharma AG, Forum 1, CH-4056 Basel, Switzerland

Key words: Alzheimer's disease; Tauopathy; Aggregation; Tau fragmentation; Axonopathy; Transgenic mouse models

Correspondence to:
D.T. Winkler, Institute of Pathology and Dept. of Neurology, University Hospital Basel, Petersgraben 4, CH-4031 Basel, Switzerland

Tel: 0041 61 328 61 62; Fax: 0041 61 265 41 00
Email: winklerd@uhbs.ch

Manuscript in preparation

Abstract

Hyperphosphorylation and aggregation of tau protein constitute the main pathological hallmark of tauopathies, including Alzheimer's disease (AD). Proteolytically derived, aggregation prone peptides e.g. amlyoid-β or cleaved Huntingtin substantially contribute to the pathogenesis of neurodegenerative proteinopathies. In this light, the role of tau fragmentation in the course of tauopathies is being debated. We here study the effects of tau truncation *in vivo*, by developing a novel inducible transgenic mouse model, called TAU62 mice, expressing the human $\Delta tau_{151\text{-}421}$ fragment. These mice show a slowly progressive motor phenotype and histopathological signs of axonal damage. To mimic the human situation, where tau fragmentation occurs in presence of full-length tau, we co-express Δtau with human full-length wild-type 2N4R or mutant 0N4R tau, by breeding TAU62 mice with ALZ17 and P301S mice, respectively. In those double transgenic mice, Δtau co-aggregates and co-accumulates with full-length tau and forms potentially toxic oligomers. This is associated with a severe axonopathy and a rapidly progressive, drastic motor impairment in P301SxTAU62 (abbreviated P62 mice) mice. Strikingly, these changes occur in absence of tau tangles and are widely reversible when Δtau expression is switched-off. Fragment-induced tau toxicity is less pronounced in ALZ17xTAU62 mice, although a subset of these mice also develops severe paralysis at about one month of age. In contrast, co-expression of the 0N4R (P301S mice) and 0N3R full-length isoforms (ALZ31 mice) does not result in any rapid motor disturbances. In conclusion, we demonstrate that Δtau exacerbates the toxicity of full-length forms of tau and favours the development of tauopathy typical changes, such as disruption of the Golgi network and microtubule dysfunction. Hence, our work underlines the importance of tau fragmentation in the context of the early pathogenesis of AD.

Introduction

Tau pathology is the hallmark of the most prevalent forms of dementia including Alzheimer's disease (AD), frontotemporal dementia (FTD) and less frequent disorders like corticobasal degeneration (CBD), progressive supranuclear palsy (PSP) and the amyotrophic lateral sclerosis/parkinsonism-dementia (ALS/PD) complex of Guam. Tau promotes microtubule (MT) growth, stabilizes MTs and limits their dynamics, thereby contributing to the maintenance of axonal growth, transport and polarity [1, 2]. Protein fragmentation has been implicated in the pathogenesis of many neurodegenerative disorders. Protein aggregates in neurodegenerative proteinopathies often consist either of fragments derived from longer precursor proteins, like amyloid-β (Aβ) in AD or amyloid-Bri (ABri) in Familial British Dementia (FBD) [3], or they comprise full-length proteins and cleaved fragments in parallel, e.g. for α-synuclein in Parkinson's disease (PD) [4, 5] or in TDP-43 related disorders [6, 7]. Aberrant protein cleavage also plays a prominent and early role in the pathogenesis of triplet expansion disorders including Huntington's disease (HD) [8], spinocerebellar-ataxia-3 (SCA3, Machado–Joseph disease) [9], and SCA7 [10].

Fragmentation of tau has been identified in patients suffering from AD, CBD, and PSP [11], *in vitro* [12], as well as in tau transgenic mouse models [13]. In AD, tau fragmentation occurs relatively early during the disease course and precedes tau tangle formation [14-20]. Tau fragments of various lengths involving different N- and C-terminal cleavage sites have been identified [15, 21, 22]. Caspase 3, caspase 6, and calpains are the main enzymes involved in tau cleavage, with the Asp421 being the most prominent caspase cleavage site [17, 23, for review see 24, 25]. However, it remains unclear whether tau truncation is part of the pathomechanism leading to the onset and progression of the disease, and what are the consequences of tau fragment expression on neuron homeostasis.

We here studied the impact of a short, wild-type Δtau fragment *in vivo,* using a novel inducible Δtau transgenic mouse model. These TAU62 mice overexpress a human, 3 repeat domains (3R) containing $\Delta tau_{151\text{-}421}$ fragment that spans from the two proline rich regions to the main C-terminal caspase cleavage site [2]. Δtau expression induces a slowly progressive axonopathy associated with a mild to moderate motor phenotype. Δtau, but not full-length wild-type 0N3R (ALZ31 mice) tau, drastically exacerbates the axonopathy and motor phenotype of mutant P301S full-length tau transgenic mice, resulting in early and severe palsy in absence of tau tangle formation. Importantly, Δtau-induced paralysis and the

associated changes in P62 mice are fully reversible when Δtau expression is halted. These findings reveal the extensive toxic potential of tau fragments by their vicious interaction with full-length tau *in vivo* and strengthen the view that tau cleavage may substantially contribute to the pathogenesis of tauopathies. The reversibility of even severe tau fragment induced changes gives hope that early inhibition of tau fragmentation might constitute a novel beneficial therapeutic approach.

Materials and Methods

Transgenic mice

Inducible Δtau expressing TAU62 transgenic mice have been generated by co-injection of two Thy 1.2 minigene based constructs into C57BL/6J oocytes. The Thy1.2-tTS construct was obtained by replacing exon 2 of the murine Thy 1.2 promoter by a tetracycline controlled transcriptional silencer element (tTS). The Thy1.2-TRE-Δtau construct contained a tetracycline responsive element (TRE) upstream of human wild-type Δtau cDNA encoding amino acids 151 to 421 of a 3-repeat domain spanning human wild-type tau fragment (0N3R $tau_{151-421}$). A total of 6 positive transgenic founder TAU62 mice (C57BL/6J-TgN(tTS-Thy1-$\Delta tau_{151-421}$) were identified and the inducible expression of human Δtau was assessed by western blot and immunohistochemistry. Lines 62-2 and 62-48 exhibited comparable and robust Δtau expression without leakage upon doxycycline withdrawal. All quantitative experiments were performed with mice of the TAU62-48 line, abbreviated TAU62 mice (C57BL/6J-TgN(tTS-Thy1-Tau)62). TAU62-2 mice were used in order to rule out an insertion side effect causing the drastic motor phenotype observed in P301SxTAU62-48 double transgenic mice.

Generation of P301S mutant 0N4R tau transgenic mice (C57BL/6J-TgN(Thy1-$hTau_{P301S}$)) [26] and ALZ17 wild-type 2N4R tau transgenic mice (C57BL/6J-TgN(Thy1-hTau)) [27] has been described previously.

For the generation of ALZ31 wild-type human 0N3R tau transgenic mice (C57BL/6J-TgN(Thy1-ALZ)31), 0N3R human cDNA was cloned into a standard neuron-specific Thy 1.2 promoter element [28] and injected into C57BL/6J oocytes.

P301SxTAU62 (called P62), ALZ17xTAU62 and P301SxALZ31 double transgenic mice have been obtained by crossing the respective single transgenic tau mouse lines. We will note $P62^{on}$ the mice receiving doxycycline, and $P62^{on\text{-}off}$ mice after the treatment was stopped. All double transgenic mice were heterozygous for the transgenes of interest. Chow containing 500mg/kg doxycycline was provided *ad libitum* to induce Δtau expression. All animal experiments were approved by the local Ethics and Animal Care and Use Committees.

Histology and immunohistochemistry

Mice were deeply anaesthetized with sodium pentobarbital (100mg/kg) and transcardially perfused with cold phosphate-buffered saline (PBS). Brains were removed and one half of the

brain was immersion fixed in 4% paraformaldehyde and embedded in paraffin. Sagittal serial sections of 4-20μm thickness were cut with a microtome throughout the hemisphere [29]. Hematoxylin and eosin (H&E), Holmes-Luxol (HL), Thioflavin S were done according to standard protocols [30]. Fibrillary tau tangle pathology was assessed by Gallyas silver staining. Antibodies used for immunohistochemistry: Tau-C3 (anti caspase-cleaved tau at Asp421, Santa Cruz Biotechnology, Texas), PHF1 (anti phospho-tau$^{Ser396/404}$, gift from Peter Davies, Albert Einstein College, NY), MC1 (conformation specific tau, gift from Peter Davies, Albert Einstein College, NY), AT100 (anti phospho-tau$^{Ser212/Thr214}$, Pierce, Rockford, IL), AT8 (phospho-tau$^{Ser202/Thr205}$, Pierce, Rockford, IL), anti-MG160 (gift from Nicholas Gonatas, Pathology and Laboratory Medecine, PA), anti-synaptophysin (Milipore Corporation, MA), anti-VAMP2/Synaptobrevin 2 (Synaptic System, Germany), anti-Cox subunit 1a (Abcam plc, UK), 2f11 (anti-neurofilament-light-chain protein , DakoCytomation, DK), NF200 (anti-neurofilament heavy-chain, [27]) and anti-GFAP (Clone Ab1, Thermo Scientific Freemont, CA).

Sarkosyl extraction and Western blot analysis

Following PBS perfusion, one half of the mouse brain was dissected into forebrain and brain stem and immediately frozen in liquid nitrogen. Sarkosyl extraction was performed as described previously [13]. Briefly, the brain tissue was homogenized in 3X volume (w/v) of 800mM NaCl, 10% sucrose, 10mM tris HCl pH 7.4, 1mM EGTA by using Ultraturrax T8 (IKA labortechnik) and then sonicated (Bandelin *Sonopuls*) at 90% power, 10% cycle and 10 pulses. Then the samples were centrifuged at 80 000g for 15 min by using ultracentrifuge (Beckman Coulter, Optima^{TM} L-70K Ultracentrifuge) by using SW55Ti rotor (Beckman Coulter). The supernatant was collected to use for the analysis of soluble tau and the remaining pellets are homogenized in A68 buffer (w/v). Samples were centrifuges at 5 000 rpm for 20 min and 1% of sarkosyl (N-laurylsarcosine, Sigma) added for 1h30 at 37 °C in thermoshaker under shaking. Samples were then centrifuged at 80 000g for 30 min and the pellet is resuspended in 150μl/g of tissue 50mM Tris HCl pH 7.4, considered as sarkosyl insoluble tau. Antibodies used for Western blotting are for detection of tau cleaved at Asp421 (Tau-C3 from Santa Cruz Biotechnology (Texas)), of human tau (HT7 antibody human tau, Pierce Biotechnology (Rockford, IL)) and of the human 3R isoform of tau (RD3 antibody from Milipore Corporation (Billerica, MA)).

Behavioural assessment

Phenotypic characterisation included the observation of motor behaviour including gait ataxia and tremor and testing of hind limb reflexes at ages of 12, 18 months old for TAU62 mice and 11 days up to 2 months old for P62. Quantitative motor testing was performed on a Rotarod® and a grid test. For Rotarod® testing, the mice were trained on 2 consecutive days on the accelerating Rotarod®. The day after, the mice were tested in 3 consecutive daily sessions over 3 days. The accelerating Rotarod was started at 4 rpm, increasing its speed over 2 minutes to a maximum speed. The time the mice were able to keep walking on the accelerating rod was noted. For the grid testing, mice were placed on a vertical mesh grid and the latency to fall of the grid was measured. Non-paralyzed mice attached to the grid climb towards the upper end of the grid and explore the whole grid, while paralyzed mice fall of the grid within the observation period of 180 seconds.

Statistical analysis

Statistical analysis was performed using IBM® SPSS® Statistics Version 19 for t-tests and ANOVA (see Supplementary Methods for details). P-values adjusted for multiple comparisons by the Holm-Bonferroni method are reported and outlined in all figures as follows: *=$p<0.05$, **=$p<0.01$, ***p=<0.001. The mean and SD are indicated in all figures.

Results

Δtau expression caused progressive motor phenotype associated with pretangle tau pathology

To test the toxicity of tau fragment on neuron cells *in vivo* and determine the role of tau truncation in the onset of tauopathies, we generated a novel transgenic mouse model (TAU62 mice), which overexpresses the human wild-type $tau_{151-421}$ fragment (Δtau) under the control of a transcriptional silencer element (tTS)-regulated Thy-1-promoter (Fig 1A). In TAU62 mice, this new, inducible, neuron-specific Thy-1.2 promoter element drives robust expression of Δtau when doxycycline is provided, while Δtau generation ceases completely when doxycycline is withdrawn (Fig 1B). Δtau expression was detected by immunohistochemistry with C3 antibody, throughout the nervous system including cortex, hippocampus and the brain stem region (Fig 1C). Continuous doxycycline administration maintained stable Δtau levels in heterozygous TAU62 mice up to high ages (data not shown).

At age of 3-6 months, a slowly progressive, initially mild motor phenotype became visible in TAU62 mice. Δtau-induced motor impairment started with mild tremor and gait ataxia (data not shown). At higher ages, a mild hind limb paralysis evolved and TAU62 mice showed an abnormal limb flexion (Fig S1A), comparable to earlier observations made in very aged transgenic mice expressing the human, full-length, wild-type tau [27]. Rotarod performance of TAU62 mice was still not significantly worsened by their paralysis at 18 months of age (data not shown). However, aged TAU62 mice failed to adhere to a vertical metal grid (grid test), while aged control mice were able to walk and climb on the grid for 180 seconds (Fig S1B).

The phenotype of 18-months-old TAU62 mice was associated with cerebral pretangle tau pathology. Widespread tau hyperphosphorylation at the AT8 epitope (phospho-$Tau^{Ser202/Thr205}$) with somato-dendritic redistribution of tau was most pronounced in the forebrain and the brain stem region, while being less dominant in the hippocampus (Fig 1D). While some brain stem neurons were positive with PHF1 antibody, detecting phospho-$Tau^{Ser396/404}$, in aged TAU62 mice (Fig 1E, upper), neither Gallyas stained tau tangles (data not shown) or tau hyperphosphorylated at late epitopes e.g. AT100 (phospho-$Tau^{Ser212/Thr214}$ - Fig 1E, left half) and MC1 (conformation specific tau, data not shown). It should be lastly noted that Δtau was also robustly expressed in spinal cord neurons (Fig 1F), where again pretangle tau pathology evolved with AT8 positive tau accumulation predominantly in motor

neurons (Fig 1F). Occasional axonal spheroids could be seen by Holmes Luxol staining (Fig 1F, right panel).

Δtau exacerbates the toxicity of P301S full-length form of tau *in vivo* and leads to severe neurologic phenotype

In man, tau fragmentation occurs in the presence of human full-length tau. In this light, we next co-expressed Δtau with human full-length tau *in vivo* by crossing P301S (0N4R) tau transgenic mice [26] with TAU62 mice, the resulting mice being called P62. Homozygous P301S mice developed a progressive motor phenotype with relevant hind limb palsy at age of 5 months and immobilizing limb paralysis at ages of 6-7 months (Fig 2A, upper, left half) as previously described [26]. Heterozygous P301S mice remained ambulatory up to more than 18 months of age (data not shown).

Co-expression of P301S full-length tau and Δtau resulted in an unexpectedly early and severe motor impairment in the $P62^{on}$ double transgenic mice. $P62^{on}$ mice showed mild gait ataxia at 9 days of age and reached complete hind limb palsy at about 3 weeks of age (Fig 2A, right half). Strikingly, this severe palsy was completely reversible when Δtau expression was stopped at age of 3 weeks (Fig 2A, down, left half). After stopping Δtau expression, the majority (5/9) of $P62^{on\text{-}off}$ mice rapidly recovered from their severe hind limb palsy, and their gait became normal within 2-3 weeks (Fig S2B). Moreover, upon Δtau switch-off, the small and low weight P62 mice steadily regained body weight (data not shown). The two $P62^{on\text{-}off}$ mice, which did not show signs of rapid recovery, were sacrificed for the reason of animal welfare (Fig S2B).

In order to rule out that an insertion site effect of the transgene underlies the observed phenotype in $P62^{on}$ mice, P301S mice were also crossed with the TAU62-2 line, what resulted in comparable phenotypic and histopathological findings (data not shown). Importantly, P301SxALZ31 mice, obtained by crossing P301S mice with 0N3R tau-expressing transgenic animals (ALZ31), did not develop a relevant motor phenotype up to adulthood, although high levels of the full-length 3R tau were detected in the mice (Fig S4). These results demonstrate that the drastic, reversible phenotype of P62 mice is induced by Δtau expression and caused by the specific toxicity conferred by tau fragment.

Δtau-derived phenotype is related to the formation of toxic oligomers, but not of tangles and insoluble aggregates

In P62 mice, the levels of Δtau fragment were significantly increased compared to heterozygous TAU62 single transgenic mice (Fig 2B and 2C). In parallel, levels of total tau exceeded even those measured in homozygous P301S mice of the same age, indicating an accumulation of both full-length tau and Δtau in P62 mice (Fig 2B and 2C). Western blots run under non-reducing conditions revealed an accumulation of higher molecular weight-tau forms, compatible with small oligomers with human tau HT7 antibody (Fig 2D). Antibody targeting 3R tau (RD3) confirmed the inclusion of 3R isoforms e.g. the Δtau fragment in the higher molecular aggregates (Fig 2D). By contrast, at the time point when P62 mice reached severe hind limb palsy, only mild AT8 hyperphosphorylation was observed in cortical, hippocampal and brain stem neurons. This hyperphosphorylation was widely reversible, when Δtau expression was switched-off (Fig 2E). No phosphorylation at so-called late epitopes e.g. PHF1 and AT100 was detectable (Fig 2F). Gallyas silver staining as well as Thioflavin S staining remained negative in all mice (Fig 2G). Correspondingly, no sarcosyl-insoluble tau aggregates formed in paralyzed P62 mice (data not shown). Together these results indicate that Δtau toxicity is related to the formation of oligomers but not to the presence of tangles or insoluble aggregates.

Interestingly, expression of the wild-type 2N4R tau with Δtau, by breeding TAU62 mice with ALZ17 animals [27], resulted in severe paralysis only in a subset of these double transgenic mice at age of about 1 month. In paralyzed ALZ17xTAU62 mice, comparably to P62 mice, pretangle tau pathology was present without signs of Gallyas positive structures (data not shown). Although a milder toxicity of Δtau is observed in the presence of the full-length, wild-type form of tau, this observation further confirms that the pathology is arising independently from tangle and aggregate formation.

Δtau-induced neuronal dysfunction is associated with reversible disruption of the Golgi network, deregulation of synaptic proteins and mitochondrial mislocation

Although only mild tau hyperphosphorylation was noted in the hippocampus of P62^{on} mice, detailed analysis revealed a disruption of the Golgi network as shown in CA1 pyramidal cells: the Golgi apparatus, stained with antibodies directed against MG160 protein, became fragmented and swollen compared to controls (Fig 3). When Δtau expression was halted, the

Golgi structure normalized (Fig 3). Compatible with a disturbed protein sorting, synaptophysin, a protein associated with presynaptic vesicles, was dislocated and accumulated within the soma of the pyramidal cells in $P62^{on}$ mice, which was restored in $P62^{on\text{-}off}$ (Fig 3). There were furthermore signs of missorting of the vesicular protein VAMP2 that was extensively lost from CA1 dendrites when Δtau was expressed (Fig 3). Interestingly, mitochondria also reversibly agglomerated within the soma of the pyramidal cells as well as in patchy axonal clusters with cox antibody (Fig 3). These results indicate that Δtau toxicity is related to altered Golgi and mitochondria dynamics and/or localization, which likely modify the synaptic functioning.

Δtau expression in P301S mice causes severe axonal damage of spinal cord neurons

Δtau was widely expressed in the spinal cord of $P62^{on}$ mice (Fig 4A) and associated with reversible tau hyperphosphorylation at the AT8 epitope (Fig 4B). Again, no AT100, MC1 or Gallyas positive structures were observed (data not shown). In parallel with the massive motor impairment, spinal cord neurons exhibited signs of severe dysfunction with pathological swelling, beginning chromatolysis, as shown with Holmes Luxol staining (Fig 4C). Axonal damage with extensive accumulation of neurofilaments stained with 2f11 and NF200 antibodies were also observed and sometimes formed axonal spheroids (Fig 4D-E). These changes as well as the accompanying astrogliosis (Fig 4F) recovered with motor improvement in $P62^{on\text{-}off}$ mice. Electron microscopy further confirmed that axonal spheroids comprised massed neurofilaments and multiple small, congested mitochondria (Fig 4G).

P301SxTAU62^{on} transgenic mice develop a drastic but reversible neuro- and myopathy

The changes at the spinal cord level were accompanied by substantial axonal neuropathy in paralyzed $P62^{on}$ mice. As observed with Holmes Luxol, Masson Trichrome, which stains myelinated axons, and p-Phenyldiamine staining, which reacts with collagen, the sciatic nerves exhibited pathological vacuolization of nerve fibres, collapses of myelin sheets and loss of fibres (Fig 5A). Upon recovery, no more vacuolization was noted in $P62^{on\text{-}off}$ mice, the myelin debris were removed and intact fibres of apparently smaller diameters were seen (Fig 5A).

The rapidly progressive hind limb palsy in $P62^{on}$ mice was associated with severe muscle wasting (Fig S3). Compared to controls, Hematoxylin and Eosin staining revealed marked muscle fibre atrophy (Fig 5B). Both types I and II fibres were severely affected, as shown by the ATPase coloration (Fig 5B). Atrophic and angulated fibre profiles were also noted, which was compatible with an atrophy related to both neuropathy and disuse. In parallel to the motor improvement of $P62^{on\text{-}off}$ mice, the muscles macroscopically widely recovered (Fig S3) and they histologically comprised hypertrophic muscle fibres, predominantly of type II, with centralized nuclei consistent with a regenerative step involved in the restoration of the fibres (Fig 5B).

Figures Legends

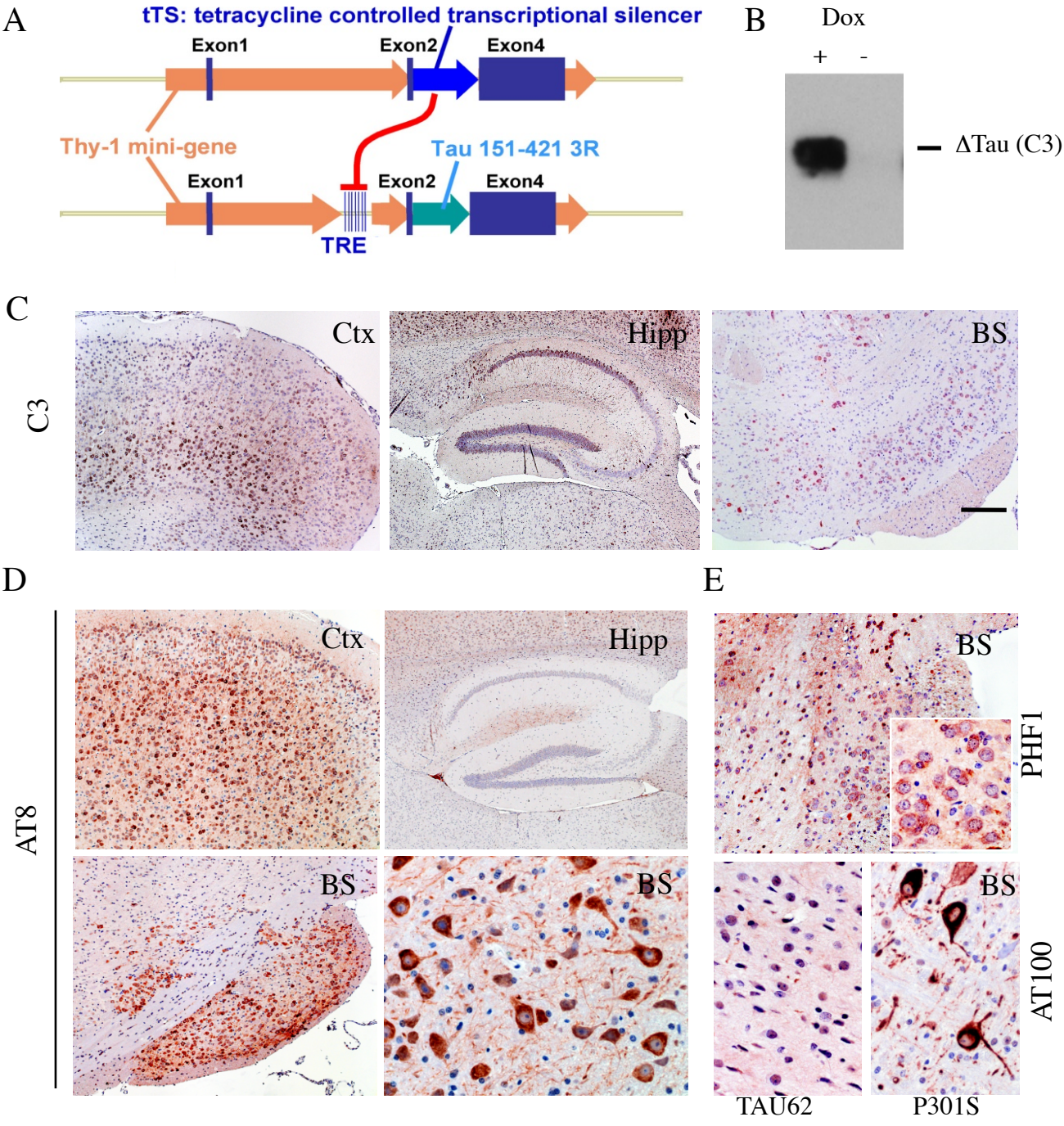

Figure 1: Tau fragmentation is sufficient to induce pretangle pathology

(A) In TAU62 mice, neuronal ΔTau expression is driven by a novel inducible Thy1.2 promoter element that includes a tetracycline responsive element (TRE).

(B) Western blot analysis with C3 antibody directed against Δtau (cleaved at Asp421) shows that the robust ΔTau generation is fully halted when doxycycline (Dox) treatment is withdrawn (-).

(C-F) Tau protein immunoreactivity in brains and spinal cords from TAU62 mice. C3 antibody reveals ΔTau expression in the cortex (Ctx), the hippocampus (Hipp), the brain stem (BS) from 12 month-old TAU62 mice (C) and spinal cord (SPC) from 18 month-old mutant mice (F). AT8 antibody recognizing phospho-tau$^{Ser202/Thr205}$ was used to stain the cerebral Ctx, Hipp and BS (D) and SPC (F) from 18 month-old mice. In **D,** higher magnification shows somato-dendritic redistribution of hyperphosphorylated tau in BS. **(E)** PHF-1 and AT100 antibodies directed against phospho-tau$^{Ser212/Thr214}$ protein were used to stain the brainstem (BS) from 18 month-old of TAU62 mice. Aged tangle bearing P301S homozygous mouse 5 month-old are used as positive control. In **(F**) Holmes Luxol (HL) staining shows axonal spheroid formation in SPC from 18 month-old of TAU62 mice. Scale bar in C equals 200µm in Ctx and BS, 400µm in Hipp; Scale bar in D equals 100µm in Ctx, BS (left panel), and 50µm in BS (right panel), 100µm in Hipp; Scale bar in E equals 100µm in BS (PHF-1), 100µm in BS (TAU62 and P301S; AT100); Scale bar in F (HL) equals 100µm in SPC (C3), and 50µm (C3 and AT8).

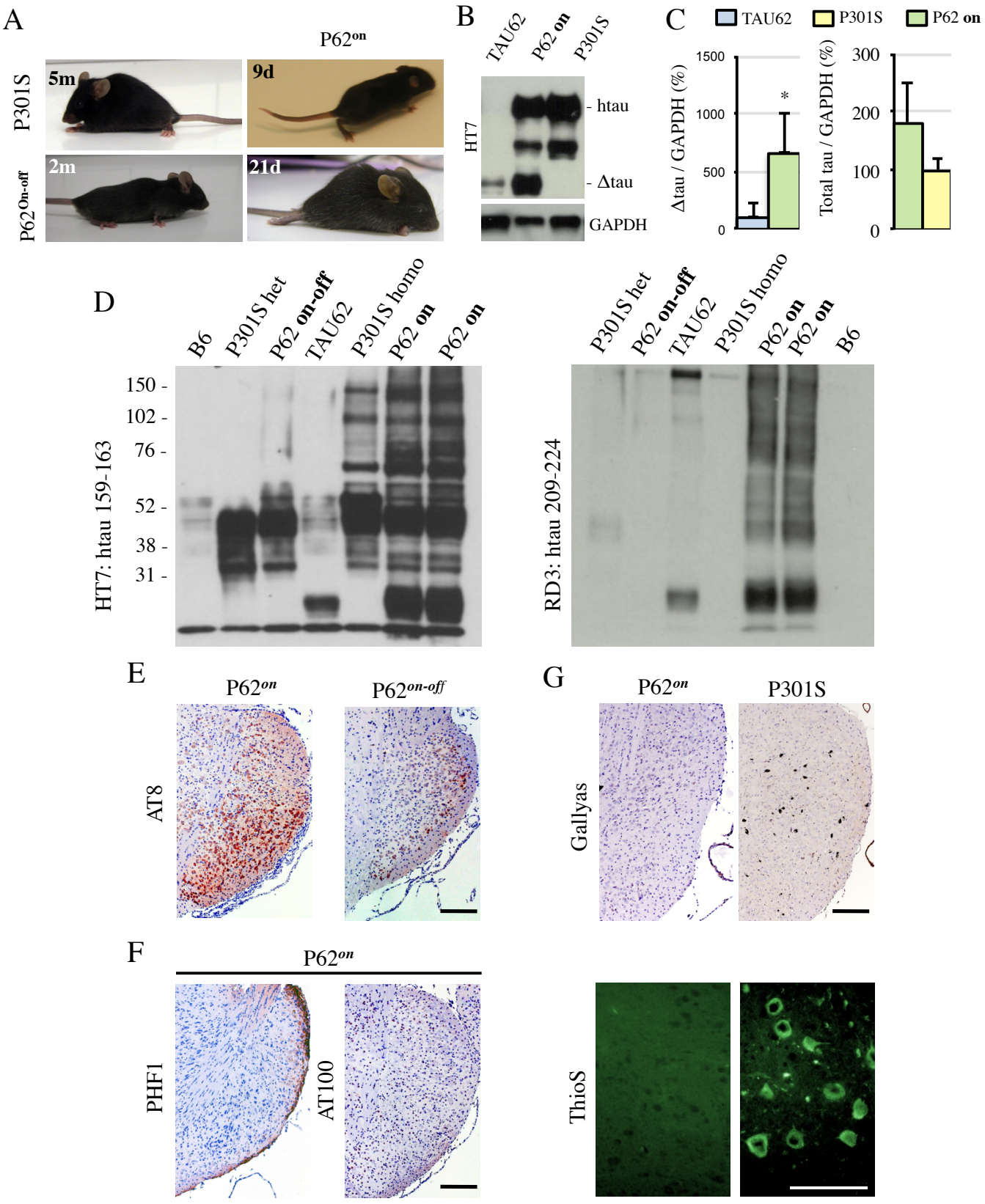
A
P62on
P301S
5m
9d
P62On-off
2m
21d
B
TAU62
P62 on
P301S
HT7
- htau
- Δtau
GAPDH
C
TAU62
P301S
P62 on
Δtau / GAPDH (%)
1500
1000
500
0
*
Total tau / GAPDH (%)
300
200
100
0
D
B6
P301S het
P62 on-off
TAU62
P301S homo
P62 on
P62 on
HT7: htau 159-163
150 -
102 -
76 -
52 -
38 -
31 -
P301S het
P62 on-off
TAU62
P301S homo
P62 on
P62 on
B6
RD3: htau 209-224
E
P62on
P62on-off
AT8
G
P62on
P301S
Gallyas
F
P62on
PHF1
AT100
ThioS

Figure 2: Co-expression of P301S full-length tau with ΔTau provokes severe neuronal dysfunction, in the absence of tangles and insoluble aggregates

(A) Global appearance of the transgenic mice generated 5 month-old P301S homozygous mice develop progressive gait disturbances. $P62^{on}$ double transgenic mice, heterozygous for both transgenes, show after 9 days progressive gait ataxia and reach severe hind limb palsy resulting in dragging their hind limbs at age of 3 weeks. The severe motor phenotype of 2 month-old $P62^{on-off}$ is almost fully reversible when ΔTau expression is stopped.

(B) Immunoblot analysis of tau protein in brains from TAU62, $P62^{on}$ and P301S mice show accumulation of ΔTau and total tau with anti-tau antibody HT7 targeting the human tau form.

(C) ΔTau expression quantified by Western blot is 6 times higher in $P62^{on}$ mice compared to heterozygous TAU62 mice and total tau levels in $P62^{on}$ animals exceed the levels measured in homozygous P301S mice.

(D) Western blot under non-reducing conditions show tau isoforms with higher molecular weight in young paralyzed $P62^{on}$ mice, using HT7 antibody specific for human tau. Similar oligomers-like tau forms are detected in aged homozygous P301S mice. Immunoblot does not reveal oligomers in young single transgenic TAU62 mice, heterozygous P301S mice and in $P62^{on-off}$ mice. In $P62^{on}$ mice, the high molecular tau forms also contain 3R tau isoforms detected with RD3 antibody.

(E) Staining of the brainstem region of 3 week-old P62 mice with anti-tau antibody AT8. The phosphorylation-dependent anti-tau antibody AT8 shows accumulation of hyperphosphorylated tau, which is almost fully reversible when ΔTau expression is stopped ($P62^{on-off}$ mice) even though P301S tau expression is maintained.

(F) Immunohistochemistry with PHF-1 and AT100 antibodies shows no accumulation of the phosphorylated tau forms (at $Ser^{396/404}$ and phospho-$tau^{Ser212/Thr214}$, respectively) in the brainstem of 3 week-old $P62^{on}$ mice.

(G) Gallyas-Braak silver and Thioflavine S stainings reveal the absence of tangle formation in 3 week-old $P62^{on}$ mice, while strong positive signal is detected in 5 month-old P301S homozygous mice. Scale bar in E equals 100µm in F and G and scale bar for Thioflavin S equals 50µm.

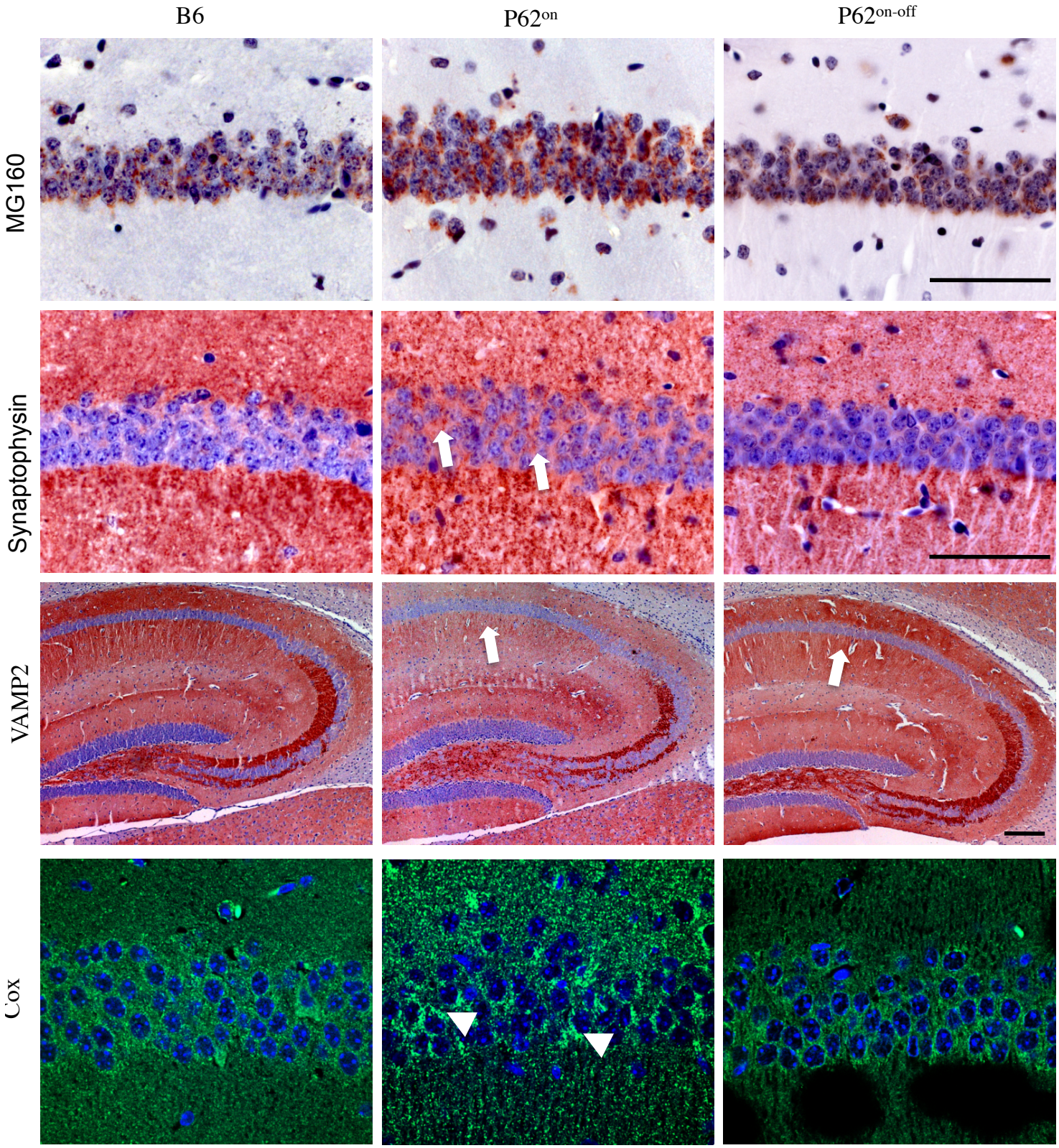
B6
P62on
P62on-off
MG160
Synaptophysin
VAMP2
Cox

Figure 3: Expression of P301S full-length tau with ΔTau leads to Golgi disruption and mitochondria mislocation

Immunohistochemistry using Golgi-specific MG160 antibody reveals fragmented and enlarged Golgi structures in CA1 (cornu ammonis 1) pyramidal layer in 3 week-old $P62^{on}$ mice, while normal organization is observed in 2 month-old $P62^{on\text{-}off}$ mice. C57/Bl6 (B6) mice are used as control. In parallel, the abnormal accumulation of synaptic protein synaptophysin (arrows) within the soma of CA1 pyramidal cells of $P62^{on}$ mice is also reversed in $P62^{on\text{-}off}$ mice. The vesicular protein VAMP2 is widely lost in CA1 dendrites in $P62^{on}$ mice (arrow) but restored after stopping ΔTau expression (arrow). Lastly, perisomatic clustering of mitochondria, detected by immunofluorescence staining for cox protein (arrowhead), in CA1 pyramidal neurons of paralyzed $P62^{on}$ mice is not observed anymore in $P62^{on\text{-}off}$ mice. Scale bar equals 100µm in MG160, Synaptophysin and 100µm in VAMP2.

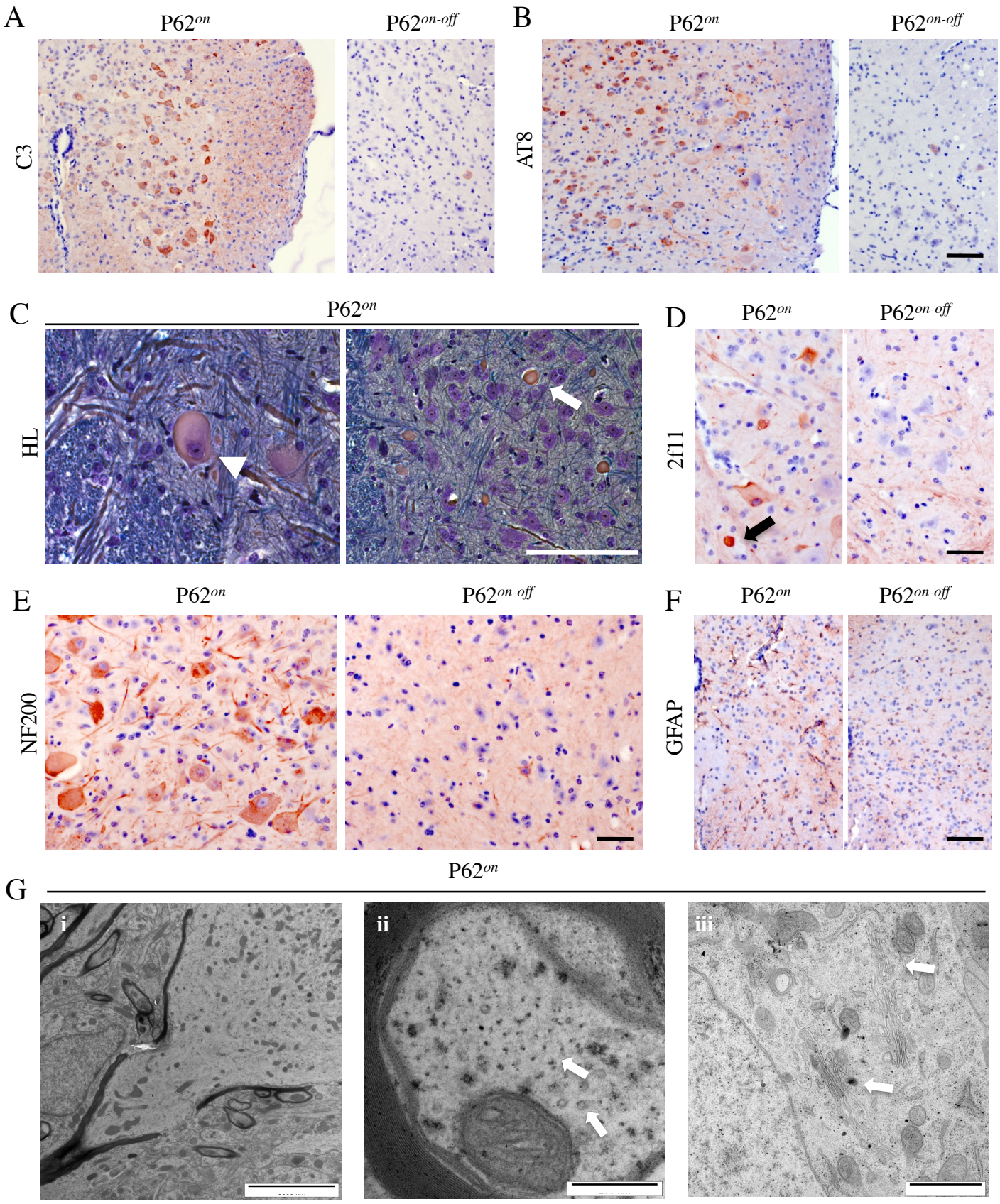
A
P62on
P62on-off
C3
B
P62on
P62on-off
AT8
C
P62on
HL
D
P62on
P62on-off
2f11
E
P62on
P62on-off
NF200
F
P62on
P62on-off
GFAP
G
P62on
i
ii
iii

Figure 4: ΔTau expression in spinal cord causes severe axonal damage

(A, B) ΔTau, detected by immunohistochemistry with C3 antibody, is widely expressed in the spinal cord **(A)** and associated with moderate hyperphosphorylation at the AT8 epitope in 3 week-old $P62^{on}$ mice **(B)**. Upon cessation of ΔTau generation in 2-month-old $P62^{on\text{-}off}$ mice, no more ΔTau **(A)** nor AT8 hyperphosphorlyated tau **(B)** are detectable. Scale bar equals 100μm.

(C) Holmes Luxol (HL) staining is used to reveal axonal spheroids (arrow), chromatolysis and ballooned neurons (arrowhead) in spinal cord of 3 week-old $P62^{on}$ mice. Scale bar equals 100μm.

(D, E) Immunohistochemistry with 2f11 antibody recognizes the 200kDa and 68kDa neurofilament proteins **(D, left)** and NF200 antibody directed against NFH (high-molecular weight neurofilament subunit; 200kD) **(E, left)** reveals the accumulation of neurofilaments in neurons of $P62^{on}$ mice. Axonal spheroids containing neurofilaments are observed in $P62^{on}$ (arrow) and widely disappear in $P62^{on\text{-}off}$ mice in parallel with the normalization of the neurofilament distribution **(D, E, right)**. Scale bar equals 50μm in D and 20μm in E.

(F) Immunohistochemistry directed against the glial GFAP shows reversible astrogliosis, which parallels with the neuronal dysfunction in P62 mice. Scale bar equals 50μm.

(G) Electron microscopy of the nerve cells in spinal cord from mice of $P62^{on}$ line. Higher magnification of axonal spheroids shows accumulated poorly oriented neurofilaments intermingled with multiple small, mitochondria (i). Sparse microtubular profiles in a myelinated axon of the spinal cord (ii, arrows) and abundant neurofilaments (iii, arrows) in a 3 week-old $P62^{on}$ mice.

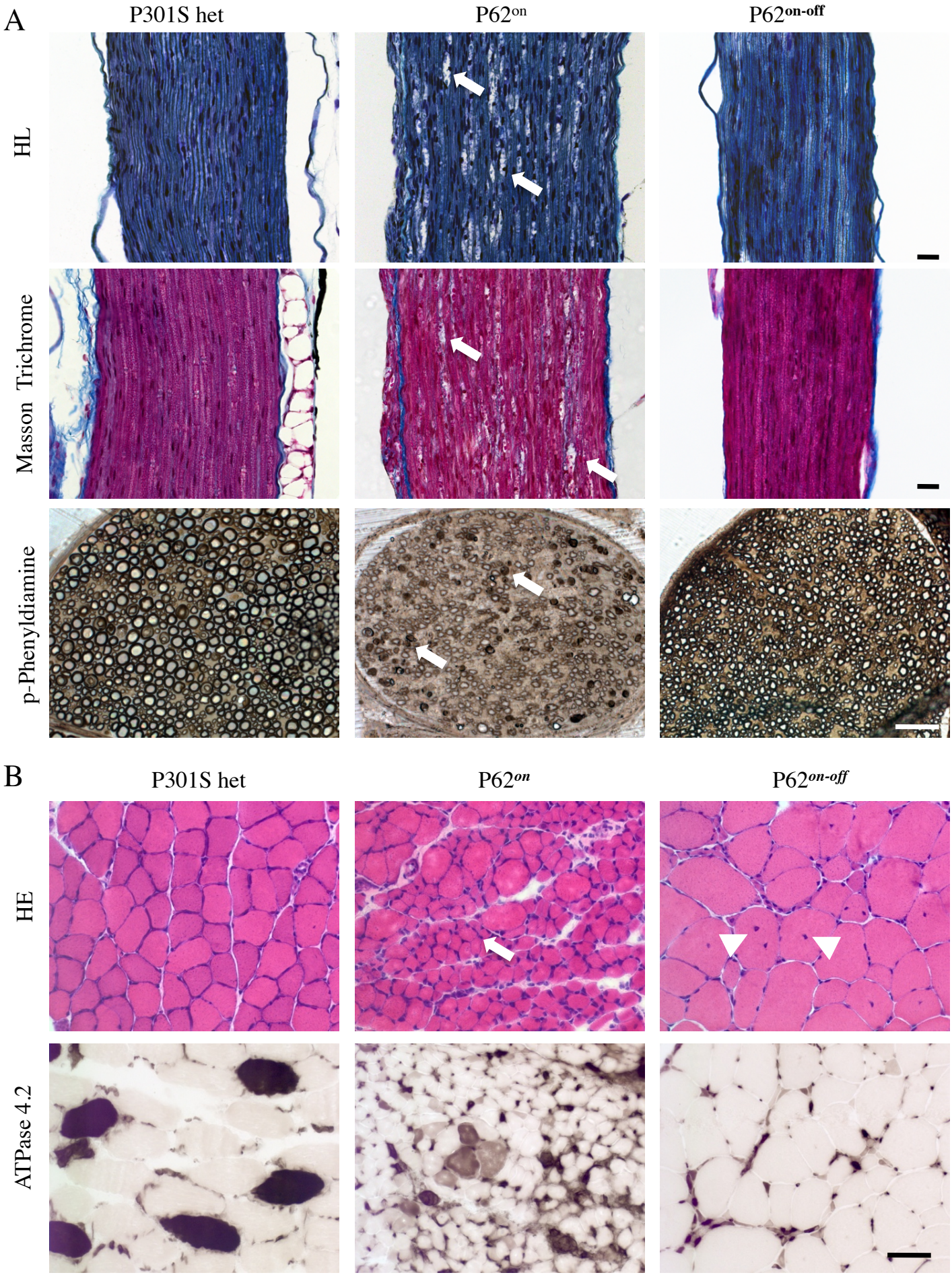
A
P301S het
P62on
P62on-off
HL
Masson Trichrome
p-Phenyldiamine
B
P301S het
P62on
P62on-off
HE
ATPase 4.2

Figure 5: Paralyzed P301SxTAU62^{on} mice exhibit extensive signs of peripheral neuropathy

(A) Holmes Luxol (HL) and Masson Trichrome stainings of the sciatic nerve of 3 week-old P62^{on} mice show vacuolar degeneration of nerve fibres (arrows) and digestion chambers along nerve fibres indicative of Wallerian degeneration (arrows), respectively. Paraphenylenediamine staining (p-Phenyldiamine) further reveals collapsed myelin sheets and signs of fibre loss (arrows). When ΔTau expression was stopped (P62$^{on\text{-}off}$ mice), the nerve largely recovered but contained much larger amounts of small myelinated fibres. Scale bar equals 20μm.

(B) The severe palsy of P62^{on} mice at 3 weeks of age is associated with marked neurogenic muscle atrophy in gastrocnemius muscles. HE and ATPase pH4.2 stainings show that both fibres are atrophic. Small angular shaped muscle fibres are organized into large groups (arrow), consistent with disuse and neurogenic muscle atrophy. After stopping ΔTau expression (P62$^{on\text{-}off}$ mice), some muscle fibres become hypertrophic and display internalized nuclei (arrowheads), whereas others remain as atrophic (grouped) fibres with mostly angulated fibre profiles. Scale bar equals 50μm.

Supplementary figures

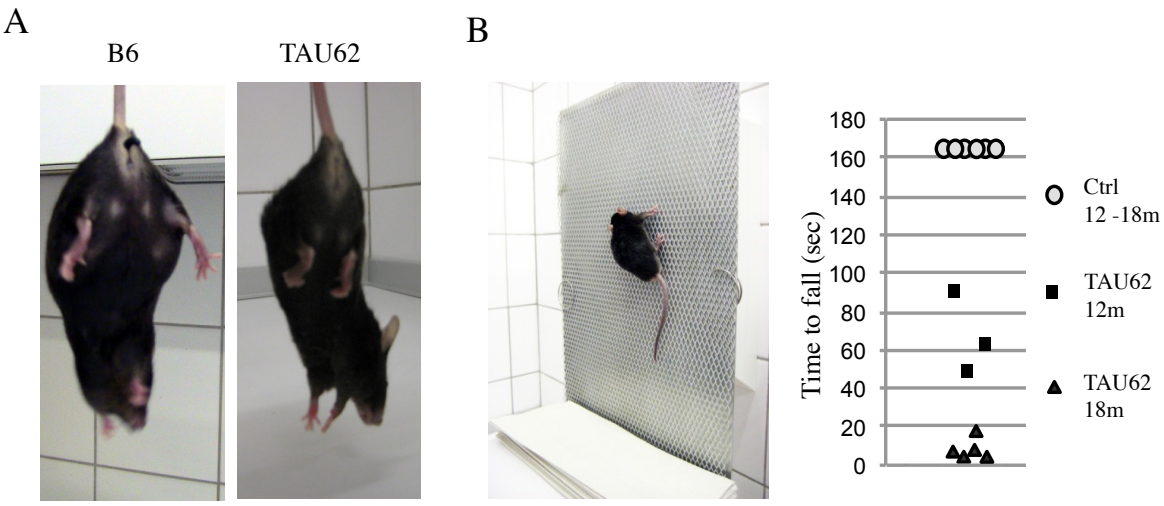

Figure S1: Neurologic phenotype in mice of the TAU62 line

Tail suspension test with normal spreading of the hind limbs in 18 month aged B6 mice and pathological retraction of the hind limbs in aged TAU62 mice **(A)**. TAU62 mice show a slowly progressive motor palsy and the time they walk on a vertical grid is reduced at higher ages **(B)**.

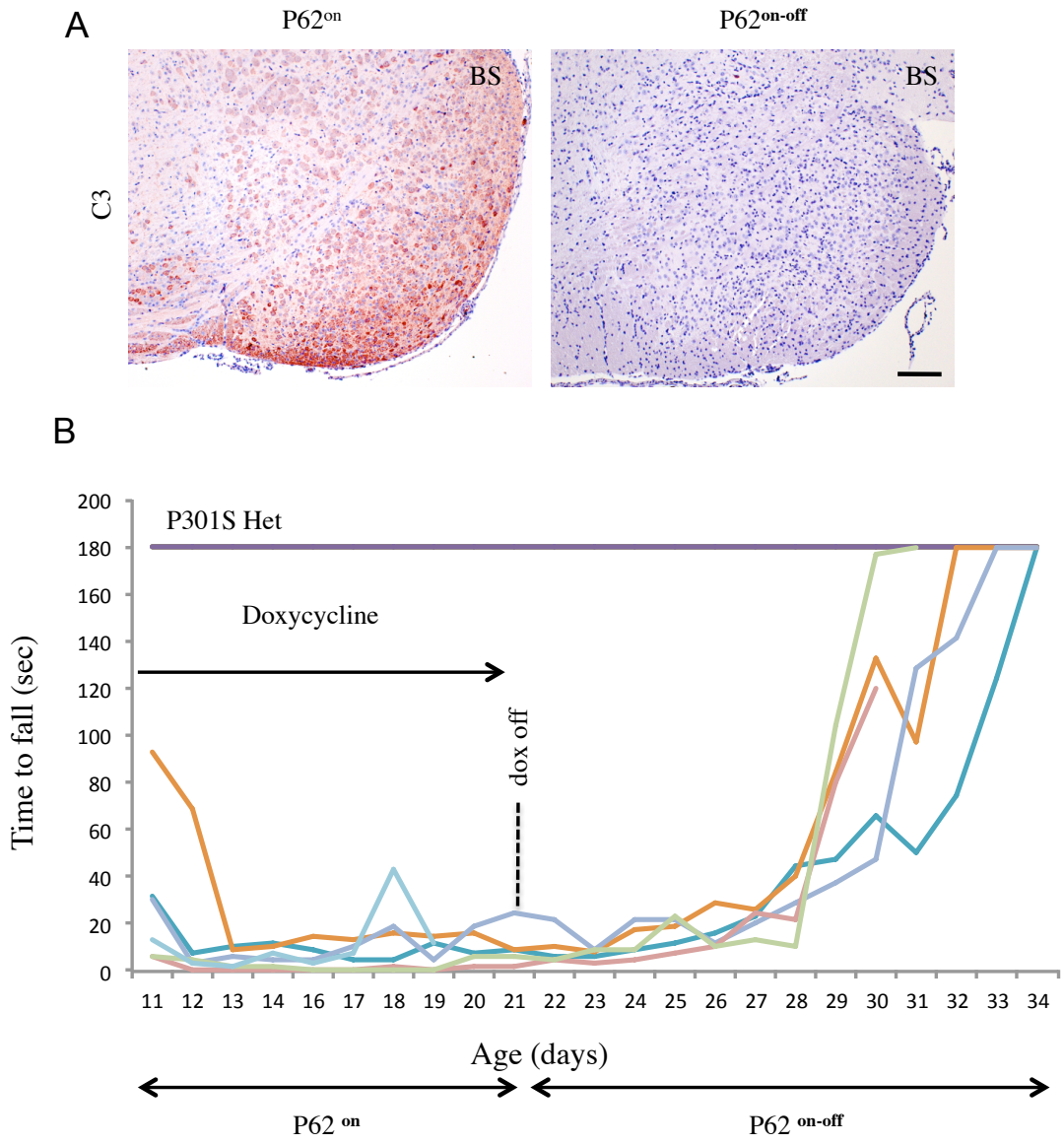

Figure S2: ΔTau expression in P62 mice impairs motor function

Expression of ΔTau is detected in the brainstem (BS) of 3 week-old P62^{on} and 2 month-old P62$^{on\text{-}off}$ mice by immunohistochemistry with C3 antibody **(A)**. The majority (5/9) of formerly severely paralyzed P62 mice become able to climb successfully on a vertical grid 1-2 weeks after the stop of ΔTau expression **(B)**, even though P301S tau expression is maintained (Grid-Test: course of recovery of paralyzed P62 mice; P301S heterozygous controls (n=8)). Scale bar equals 100µm in A.

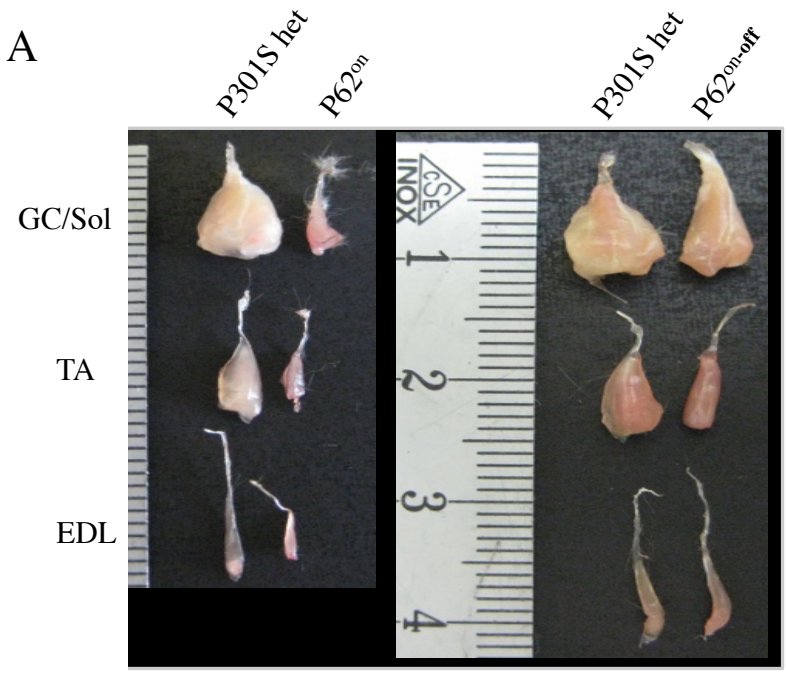

Figure S3: Macroscopic picture of muscles in P62 mice

Severe muscle atrophy is observed in paralyzed, 3 week-old P62^{on} mice (left half panel) compared to heterozygous P301S heterozygous mouse (P301S het). From top: gastrocnemius and soleus, tibialis anterior and extensor digitorum longus. Within 4 weeks upon stop of ΔTau expression, the hind limb musculature widely recovers (right half panel) and becomes macroscopically comparable to control muscles (P301S het).

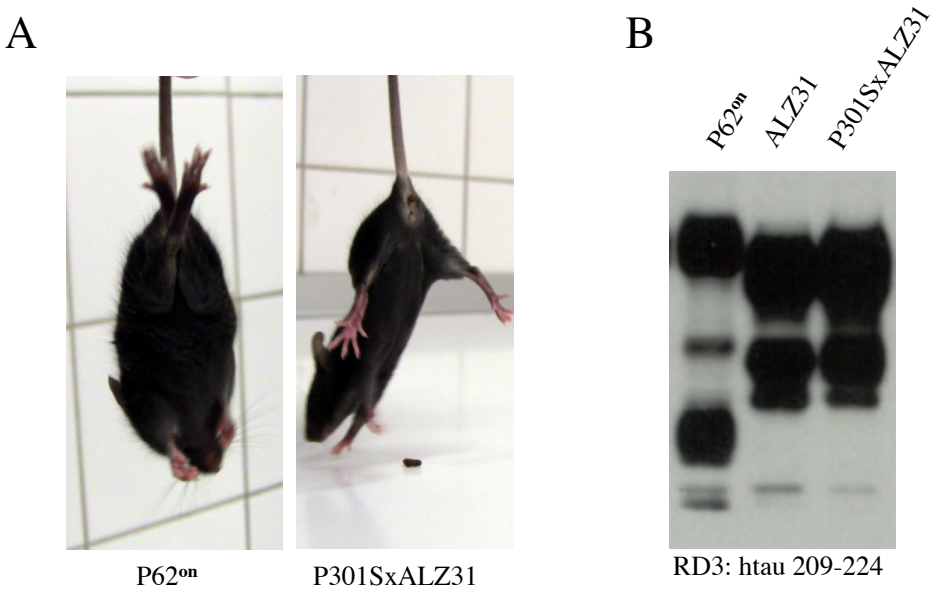

Figure S4: Co-expression of full-length 0N4R and 0N3R tau with ΔTau

A 3 week-old P62^{on} mouse fails to spread its hind limbs when suspended by the tail **(A)**, contrasting with a 3 week-old P301SxALZ31. **(B)** Immunoblot analysis of tau protein in brain from P62^{on}, ALZ31 and P301SxALZ31 mice show the expression of tau using anti-tau antibody HT7 targeting the human tau form.

Discussion

Protein fragments play a major role in neurodegenerative disorders and the relevance of proteolysis in the pathogenesis of tauopathies is increasingly being recognized. Here, we establish for the first time that tau truncation exacerbates the toxicity of full-length forms of tau promoting the onset of pretangle pathology with severe neuronal dysfunction.

To study the effects of a tau fragment *in vivo*, we firstly established a novel inducible TAU62 transgenic mouse line that overexpresses a human wild-type $\Delta tau_{151\text{-}421}$ fragment in a neuron-specific manner. Sheer $\Delta tau_{151\text{-}421}$ expression in TAU62 mice causes a mild, rather slowly progressive motor phenotype associated with pretangle stage histological features including tau hyperphosphorylation and axono-dendritical redistribution of tau, similar as that observed in the full-length wild-type ALZ17 transgenic mouse model [27]. In contrast to reports on overexpression of tau fragments in rats [31, 32], but similarly to findings in mice expressing a C-terminally cleaved 1N4R $tau_{1\text{-}391}$ fragment [33], TAU62 mice stay devoid of tau tangle formation up to high ages of 26 months and do not accumulate relevant amounts of sarkosyl insoluble tau. In absence of full-length human tau, the toxicity of $\Delta tau_{151\text{-}421}$ in TAU62 mice does not exceed the effects of full-length 3R tau reported previously in mice [34].

In order to mimic the situation of human tauopathies, where tau fragments are co-occurring with full-length human tau, we next crossed full-length human tau expressing P301S mice with TAU62 mice. While our homozygous P301S mice start to develop a visible motor phenotype with trembling and mild hind limb palsy at ages of 4-6 months, heterozygous P301S mice can reach more than 15 months of age without limiting paralysis. Unexpectedly, a much more drastic phenotype evolves in P62 double transgenic mice, although heterozygous for each transgene, which reach almost complete hind limb palsy at 3 weeks of age. Δtau thus exponentiates the toxicity of full-length tau and both tau forms co-accumulate in the brain and spinal cord of the mice. This results in extensive neuronal dysfunction and neuropathological findings typically found in human tauopathies and tauopathy models such as Golgi network disruption and mitochondria mislocation and axonal transport deficits. Eventually, co-expression of full-length 0N3R tau with P301S full-length tau does not result in any severe phenotype up to the age of 3 months in ALZ31xP301S mice, which underscores the importance of the fragment for the induced toxicity.

Biochemical analysis reveals increased levels of Δtau and total tau in P62 mice compared to the respective levels in TAU62 or even in homozygous P301S mice. This points towards a direct interaction of Δtau with human full-length tau, which results in stabilization of both tau variants. This *in vivo* interaction of two amyloidogenic proteins is comparable to findings reported earlier in amyloid-β (Aβ) overexpressing mice, where intraneuronal co-expression of $A\beta_{42}$ with $A\beta_{40}$ resulted in the stabilization and accumulation of $A\beta_{40}$ [35]. Interestingly, tau isoforms of higher molecular weight were detected in the brain of P62 mice, which was compatible with small oligomeric tau forms. In contrast, there was no sign, using biochemical and histochemical analyses, of overt tau aggregation into sarcosyl insoluble forms or tangle formation in paralyzed P62 mice. The absence of tangles, even when the mice reached severe palsy, is thereby in line with the hypothesis that tangles are not the main toxic agents in tauopathies [36-39]. Inversely, the sheer accumulation of Δtau induced toxic or dysfunctional oligomeric tau species seems to be sufficient to provoke severe neuronal dysfunction. This confirms the recently recognized importance of sarcosyl-soluble but oligomeric tau species for the pathogenesis of tauopathies [40-42]. Formation of tau dimers and subsequent oligomerization has been observed early in the cascade of AD pathology [43, 44]. Although late tangled tau aggregates correlate with disease progression in man, cognitive deficits and neuronal dysfunction precede and exceed tau tangle pathology in man and transgenic models, including P301S mice [36, 45, 46]. In tangle bearing mouse models e.g. rTG4510 mice, the toxicity of tau oligomers has been shown to correlate better with neuronal dysfunction than the extent of tau tangles [47]. The absence of extensive tau hyperphosphorylation in parallel to the observed severe neuronal dysfunction is compatible with the hypothesis that tau hyperphosphorylation is a secondary reactive measure of the cell in order to cope the accumulation of excessive tau, rather than being a primary pathogenic event. This would be comparable to the situation of TDP-43 associated disorders, where fragmentation of TDP-43 protein has been shown to precede its phosphorylation and aggregation into insoluble forms [48].

Δtau induced tau accumulation results in extensive neuronal dysfunction and histopathological changes of tauopathy typical character in P62 mice. A part of the lower motor neurons degeneration is indicated by the partly neurogenic muscular atrophy present in these mice. Furthermore, multiple axonal spheroids, filled with small jammed mitochondria, and accumulated neurofilaments similar to findings in human AD [49] are consistent with transport deficits in spinal cord axons. Notwithstanding, even in the hippocampus, where only

very limited tau hyperphosphorylation is noted, we observed dislocated and clustered mitochondria in CA1 pyramidal neurons, similar to findings in AD brain tissue [50]. Interestingly, comparable perinuclear mitochondrial clumping has also been found in rTg4510 tau transgenic mice where it was shown to correlate primarily with the presence of soluble tau species but not with tau tangles [50]. Most prominently, we find dispersed and swollen Golgi networks associated with somatic accumulation of synaptophysin pointing towards congested Golgi pathways, comparable to previously reported findings in JLNP3 mice [51]. This fragmentation of the Golgi apparatus, the central sorting machinery for all newly generated proteins destined for fast axonal transport [52], is comparable with findings in AD patients [53, 54]. Disruption of Golgi traffic has been observed in various neurodegenerative disorders and it may be directly linked to a dysfunction of microtubular structure, on which the Golgi assembly is dependent [55, 56].

These pathological changes observed in paralyzed P62 mice point towards a widespread cellular transport disruption. Axonal transport deficits have been reported in a broad spectrum of neurodegenerative diseases and the term dysferopathies has been proposed to summarize these disorders [57]. In agreement with the hypothesis that tauopathies are associated with a disrupted microtubule network, recent studies in transgenic mouse models reported behavioral and histopathological improvements of P301S transgenic mice following the administration of microtubule stabilizing drugs e.g. Epothilone D [58-60] or Paclitaxel [61]. The consequences of microtubule disruption, Golgi network alteration and obstruction of axonal transport are far reaching and may result in the depletion of synaptic protein pools, energy depletion by a lack of mitochondria at distal site and eventually cause overt neuronal dysfunction and even degeneration as seen in our P62 mice.

Importantly, we here showed that most of these events are widely reversible when the generation of dysfunctional tau is halted. Although P301S tau expression is ongoing, cessation of Δtau expression is sufficient to decrease the levels of toxic tau forms below a threshold that allows neurons in $P62^{on\text{-}off}$ mice to cope with P301S tau and even to recover functionally. This firstly outlines the importance of Δtau for the maintenance of tau toxicity in this model. Secondly, it proofs the reversibility of the toxicity of soluble oligomeric tau forms in a more drastic way than previously shown in inducible tau transgenic mice and in the absence of overt tau tangle aggregates [38, 62]. It remains however yet unclear, how soluble toxic tau species cause the disruption of axonal transport. Even total absence of tau in mice affects only subtypes of neurons and causes a reduction in microtubules, but does not lead to a severe phenotype [63, 64]. This implies that toxic di- or oligomeric tau species might exert a

toxic gain of function by interfering dysfunctionally with MT assembly, e.g. with end-binding proteins [65], and cause "catastrophe" events with MT breakdowns [66]. This hypothesis might explain the rapid recovery noted in our P62 model. Consistently, when co-expressing less aggregation prone 0N4R wild-type human full-length tau with Δtau, only a subset of such ALZ17xTAU62 mice develop severe motor impairments; this would be compatible with the existence of a threshold level of dysfunctional oligomeric tau, which cannot be coped by the cellular degradation pathways.

Most neurodegenerative disorders share the important role of small aggregation prone protein fragments in their pathogenesis. Cleaved proteins are substantially involved in Alzheimer's disease (Aβ), Huntington's disease (Huntingtin) [67], Parkinson's disease (PD) [4, 5], TDP-43 related disorders [48], Familial British Dementia (FBD) [3], Familial Danish Dementia (FDD) [68], and triplet repeat disorders e.g. SCA3 [9] or SCA7 [10]. While in a subset of hereditary variants of these diseases the causes of increased or altered cleavage have been identified, e.g. for presenilin mutations in AD or the frame shift mutations in FBD, the causes for the accumulation of the cleaved products has yet remained elusive in most of the sporadic forms of these disorders. Here, we established that tau truncation harbours the potential to provoke the aggregation of tau isoforms with drastic dysfunctional consequences. The initiation of tau fragmentation in human tauopathies has yet remained unclear. Tau is mainly cleaved by caspases and calpain. Caspase activation has been shown to precede tangle formation in transgenic mice and to potentially persist for a long time without direct induction of cell death [19]. Aberrant caspase cleavage within the lysosomal system has been shown to induce toxic oligomer formation *in vitro,* and disturbed lysosomal function increase tau cleavage and toxicity in a Drosophila model [69, 70]. Moreover, tau fragmentation is being observed widely and early in the pathogenesis of human tauopathies [11, 14-20, 71].

In light of our *in vivo* findings, reduction of tau cleavage may constitute a promising therapeutic target, which might be comparably effective as secretase inhibition in the case of APP. Our novel, severely affected P62 tauopathy model constitute an ideal tool to test such therapeutical strategies or to screen potential drugs addressing other pathomechanistic targets, e.g. increasing tau clearance by immunotherapy or autophagy activation.

MT and DTW are supported by the Swiss National Science Foundation (310030_135214 to MT and 32323B_123812 to D.T.W.) and by the Velux Foundation, Switzerland.

References

1. Caceres, A. and K.S. Kosik, *Inhibition of neurite polarity by tau antisense oligonucleotides in primary cerebellar neurons.* Nature, 1990. **343**(6257): p. 461-3.
2. Trinczek, B., et al., *Domains of tau protein, differential phosphorylation, and dynamic instability of microtubules.* Mol Biol Cell, 1995. **6**(12): p. 1887-902.
3. Vidal, R., et al., *A stop-codon mutation in the BRI gene associated with familial British dementia.* Nature, 1999. **399**(6738): p. 776-81.
4. Liu, C.W., et al., *A precipitating role for truncated alpha-synuclein and the proteasome in alpha-synuclein aggregation: implications for pathogenesis of Parkinson disease.* J Biol Chem, 2005. **280**(24): p. 22670-8.
5. Dufty, B.M., et al., *Calpain-cleavage of alpha-synuclein: connecting proteolytic processing to disease-linked aggregation.* Am J Pathol, 2007. **170**(5): p. 1725-38.
6. Neumann, M., et al., *Ubiquitinated TDP-43 in frontotemporal lobar degeneration and amyotrophic lateral sclerosis.* Science, 2006. **314**(5796): p. 130-3.
7. Zhang, Y.J., et al., *Aberrant cleavage of TDP-43 enhances aggregation and cellular toxicity.* Proc Natl Acad Sci U S A, 2009. **106**(18): p. 7607-12.
8. Wellington, C.L., et al., *Caspase cleavage of mutant huntingtin precedes neurodegeneration in Huntington's disease.* J Neurosci, 2002. **22**(18): p. 7862-72.
9. Jung, J., et al., *Preventing Ataxin-3 protein cleavage mitigates degeneration in a Drosophila model of SCA3.* Hum Mol Genet, 2009. **18**(24): p. 4843-52.
10. Mookerjee, S., et al., *Posttranslational modification of ataxin-7 at lysine 257 prevents autophagy-mediated turnover of an N-terminal caspase-7 cleavage fragment.* J Neurosci, 2009. **29**(48): p. 15134-44.
11. Arai, T., et al., *Identification of amino-terminally cleaved tau fragments that distinguish progressive supranuclear palsy from corticobasal degeneration.* Ann Neurol, 2004. **55**(1): p. 72-9.
12. Gamblin, T.C., et al., *Caspase cleavage of tau: linking amyloid and neurofibrillary tangles in Alzheimer's disease.* Proc Natl Acad Sci U S A, 2003. **100**(17): p. 10032-7.
13. Delobel, P., et al., *Analysis of tau phosphorylation and truncation in a mouse model of human tauopathy.* Am J Pathol, 2008. **172**(1): p. 123-31.
14. Gastard, M.C., J.C. Troncoso, and V.E. Koliatsos, *Caspase activation in the limbic cortex of subjects with early Alzheimer's disease.* Ann Neurol, 2003. **54**(3): p. 393-8.
15. Horowitz, P.M., et al., *Early N-terminal changes and caspase-6 cleavage of tau in Alzheimer's disease.* J Neurosci, 2004. **24**(36): p. 7895-902.
16. Rohn, T.T., et al., *Caspase-9 activation and caspase cleavage of tau in the Alzheimer's disease brain.* Neurobiol Dis, 2002. **11**(2): p. 341-54.
17. Guillozet-Bongaarts, A.L., et al., *Tau truncation during neurofibrillary tangle evolution in Alzheimer's disease.* Neurobiol Aging, 2005. **26**(7): p. 1015-22.
18. Rissman, R.A., et al., *Caspase-cleavage of tau is an early event in Alzheimer disease tangle pathology.* J Clin Invest, 2004. **114**(1): p. 121-30.
19. de Calignon, A., et al., *Caspase activation precedes and leads to tangles.* Nature, 2010. **464**(7292): p. 1201-4.
20. Basurto-Islas, G., et al., *Accumulation of Aspartic Acid421- and Glutamic Acid391-Cleaved Tau in Neurofibrillary Tangles Correlates With Progression in Alzheimer Disease.* J Neuropathol Exp Neurol, 2008. **67**(5): p. 470-483.
21. Novak, M., J. Kabat, and C.M. Wischik, *Molecular characterization of the minimal protease resistant tau unit of the Alzheimer's disease paired helical filament.* EMBO J, 1993. **12**(1): p. 365-70.

22. Corsetti, V., et al., *Identification of a caspase-derived N-terminal tau fragment in cellular and animal Alzheimer's disease models.* Mol Cell Neurosci, 2008. **38**(3): p. 381-92.
23. Guo, H., et al., *Active caspase-6 and caspase-6-cleaved tau in neuropil threads, neuritic plaques, and neurofibrillary tangles of Alzheimer's disease.* Am J Pathol, 2004. **165**(2): p. 523-31.
24. Avila, J., *Alzheimer disease: caspases first.* Nat Rev Neurol, 2010. **6**(11): p. 587-8.
25. Fasulo, L., G. Ugolini, and A. Cattaneo, *Apoptotic effect of caspase-3 cleaved tau in hippocampal neurons and its potentiation by tau FTDP-mutation N279K.* J Alzheimers Dis, 2005. **7**(1): p. 3-13.
26. Allen, B., et al., *Abundant tau filaments and nonapoptotic neurodegeneration in transgenic mice expressing human P301S tau protein.* J Neurosci, 2002. **22**(21): p. 9340-51.
27. Klionsky, D.J., A.M. Cuervo, and P.O. Seglen, *Methods for monitoring autophagy from yeast to human.* Autophagy, 2007. **3**(3): p. 181-206.
28. Sturchler-Pierrat, C., et al., *Two amyloid precursor protein transgenic mouse models with Alzheimer disease-like pathology.* Proc Natl Acad Sci U S A, 1997. **94**(24): p. 13287-92.
29. Winkler, D.T., et al., *Thrombolysis induces cerebral hemorrhage in a mouse model of cerebral amyloid angiopathy.* Ann Neurol, 2002. **51**(6): p. 790-3.
30. Carson, F.L., *Histotechnology, 2nd edition, ASCP Press, Chicago, USA.* 1996.
31. Zilka, N., et al., *Truncated tau from sporadic Alzheimer's disease suffices to drive neurofibrillary degeneration in vivo.* FEBS Lett, 2006. **580**(15): p. 3582-8.
32. Filipcik, P., et al., *First transgenic rat model developing progressive cortical neurofibrillary tangles.* Neurobiol Aging, 2012. **33**(7): p. 1448-56.
33. McMillan, P.J., et al., *Truncation of tau at E391 promotes early pathologic changes in transgenic mice.* J Neuropathol Exp Neurol, 2011. **70**(11): p. 1006-19.
34. Kaushik, S., A.C. Massey, and A.M. Cuervo, *Lysosome membrane lipid microdomains: novel regulators of chaperone-mediated autophagy.* EMBO J, 2006. **25**(17): p. 3921-33.
35. Abramowski, D., et al., *Transgenic expression of intraneuronal Abeta42 but not Abeta40 leads to cellular Abeta lesions, degeneration, and functional impairment without typical Alzheimer's disease pathology.* J Neurosci, 2012. **32**(4): p. 1273-83.
36. Yoshiyama, Y., et al., *Synapse loss and microglial activation precede tangles in a P301S tauopathy mouse model.* Neuron, 2007. **53**(3): p. 337-51.
37. Leroy, K., et al., *Early axonopathy preceding neurofibrillary tangles in mutant tau transgenic mice.* Am J Pathol, 2007. **171**(3): p. 976-92.
38. Santacruz, K., et al., *Tau suppression in a neurodegenerative mouse model improves memory function.* Science, 2005. **309**(5733): p. 476-81.
39. Spires-Jones, T.L., et al., *Are tangles as toxic as they look?* J Mol Neurosci, 2011. **45**(3): p. 438-44.
40. Brunden, K.R., J.Q. Trojanowski, and V.M. Lee, *Evidence that non-fibrillar tau causes pathology linked to neurodegeneration and behavioral impairments.* J Alzheimers Dis, 2008. **14**(4): p. 393-9.
41. Spires-Jones, T.L., et al., *Tau pathophysiology in neurodegeneration: a tangled issue.* Trends Neurosci, 2009. **32**(3): p. 150-9.
42. Lasagna-Reeves, C.A., et al., *Preparation and characterization of neurotoxic tau oligomers.* Biochemistry, 2010. **49**(47): p. 10039-41.
43. Maeda, S., et al., *Granular tau oligomers as intermediates of tau filaments.* Biochemistry, 2007. **46**(12): p. 3856-61.

44. Patterson, K.R., et al., *Characterization of prefibrillar Tau oligomers in vitro and in Alzheimer disease.* J Biol Chem, 2011. **286**(26): p. 23063-76.
45. Spires, T.L., et al., *Region-specific dissociation of neuronal loss and neurofibrillary pathology in a mouse model of tauopathy.* Am J Pathol, 2006. **168**(5): p. 1598-607.
46. Gomez-Isla, T., et al., *Neuronal loss correlates with but exceeds neurofibrillary tangles in Alzheimer's disease.* Ann Neurol, 1997. **41**(1): p. 17-24.
47. Berger, Z., et al., *Accumulation of pathological tau species and memory loss in a conditional model of tauopathy.* J Neurosci, 2007. **27**(14): p. 3650-62.
48. Igaz, L.M., et al., *Expression of TDP-43 C-terminal Fragments in Vitro Recapitulates Pathological Features of TDP-43 Proteinopathies.* J Biol Chem, 2009. **284**(13): p. 8516-24.
49. Schmidt, M.L., V.M. Lee, and J.Q. Trojanowski, *Relative abundance of tau and neurofilament epitopes in hippocampal neurofibrillary tangles.* Am J Pathol, 1990. **136**(5): p. 1069-75.
50. Kopeikina, K.J., et al., *Tau accumulation causes mitochondrial distribution deficits in neurons in a mouse model of tauopathy and in human Alzheimer's disease brain.* Am J Pathol, 2011. **179**(4): p. 2071-82.
51. Liazoghli, D., et al., *Fragmentation of the Golgi apparatus induced by the overexpression of wild-type and mutant human tau forms in neurons.* Am J Pathol, 2005. **166**(5): p. 1499-514.
52. Hammerschlag, R., et al., *Evidence that all newly synthesized proteins destined for fast axonal transport pass through the Golgi apparatus.* J Cell Biol, 1982. **93**(3): p. 568-75.
53. Stieber, A., Z. Mourelatos, and N.K. Gonatas, *In Alzheimer's disease the Golgi apparatus of a population of neurons without neurofibrillary tangles is fragmented and atrophic.* Am J Pathol, 1996. **148**(2): p. 415-26.
54. Gonatas, N.K., A. Stieber, and J.O. Gonatas, *Fragmentation of the Golgi apparatus in neurodegenerative diseases and cell death.* J Neurol Sci, 2006. **246**(1-2): p. 21-30.
55. Cooper, A.A., et al., *Alpha-synuclein blocks ER-Golgi traffic and Rab1 rescues neuron loss in Parkinson's models.* Science, 2006. **313**(5785): p. 324-8.
56. Lin, X., et al., *Leucine-rich repeat kinase 2 regulates the progression of neuropathology induced by Parkinson's-disease-related mutant alpha-synuclein.* Neuron, 2009. **64**(6): p. 807-27.
57. Morfini, G.A., et al., *Axonal transport defects in neurodegenerative diseases.* J Neurosci, 2009. **29**(41): p. 12776-86.
58. Zhang, B., et al., *The microtubule-stabilizing agent, epothilone D, reduces axonal dysfunction, neurotoxicity, cognitive deficits, and Alzheimer-like pathology in an interventional study with aged tau transgenic mice.* J Neurosci, 2012. **32**(11): p. 3601-11.
59. Brunden, K.R., et al., *Epothilone D improves microtubule density, axonal integrity, and cognition in a transgenic mouse model of tauopathy.* J Neurosci, 2010. **30**(41): p. 13861-6.
60. Barten, D.M., et al., *Hyperdynamic microtubules, cognitive deficits, and pathology are improved in tau transgenic mice with low doses of the microtubule-stabilizing agent BMS-241027.* J Neurosci, 2012. **32**(21): p. 7137-45.
61. Zhang, B., et al., *Microtubule-binding drugs offset tau sequestration by stabilizing microtubules and reversing fast axonal transport deficits in a tauopathy model.* Proc Natl Acad Sci U S A, 2005. **102**(1): p. 227-31.

62. Sydow, A., et al., *Tau-induced defects in synaptic plasticity, learning, and memory are reversible in transgenic mice after switching off the toxic Tau mutant.* J Neurosci, 2011. **31**(7): p. 2511-25.
63. Harada, A., et al., *Altered microtubule organization in small-calibre axons of mice lacking tau protein.* Nature, 1994. **369**(6480): p. 488-91.
64. Dawson, H.N., et al., *Inhibition of neuronal maturation in primary hippocampal neurons from tau deficient mice.* J Cell Sci, 2001. **114**(Pt 6): p. 1179-87.
65. Maurer, S.P., et al., *EBs recognize a nucleotide-dependent structural cap at growing microtubule ends.* Cell, 2012. **149**(2): p. 371-82.
66. Brun, L., et al., *A theory of microtubule catastrophes and their regulation.* Proc Natl Acad Sci U S A, 2009. **106**(50): p. 21173-8.
67. Miller, J.P., et al., *Matrix metalloproteinases are modifiers of huntingtin proteolysis and toxicity in Huntington's disease.* Neuron, 2010. **67**(2): p. 199-212.
68. Vidal, R., et al., *A decamer duplication in the 3' region of the BRI gene originates an amyloid peptide that is associated with dementia in a Danish kindred.* Proc Natl Acad Sci U S A, 2000. **97**(9): p. 4920-5.
69. Khurana, V., et al., *Lysosomal dysfunction promotes cleavage and neurotoxicity of tau in vivo.* PLoS Genet, 2010. **6**(7): p. e1001026.
70. Wang, Y., et al., *Tau fragmentation, aggregation and clearance: the dual role of lysosomal processing.* Hum Mol Genet, 2009. **18**(21): p. 4153-70.
71. Wray, S., et al., *Direct analysis of tau from PSP brain identifies new phosphorylation sites and a major fragment of N-terminally cleaved tau containing four microtubule-binding repeats.* J Neurochem, 2008. **105**(6): p. 2343-52.

Publication N°2

Rapamycin Attenuates the Progression of Tau Pathology in P301S Tau Transgenic Mice

Sefika Ozcelik, Graham Fraser, Perrine Castets, Véronique Schaeffer, Zhiva Skachokova, Karin Breu, Florence Clavaguera, Michael Sinnreich, Ludwig Kappos, Michel Goedert, Markus Tolnay, David Theo, Winkler

Plos One 2013 May 7;8(5):e62459

OPEN ACCESS Freely available online

PLOS ONE

Rapamycin Attenuates the Progression of Tau Pathology in P301S Tau Transgenic Mice

Sefika Ozcelik[1,2], Graham Fraser[3], Perrine Castets[2,4], Véronique Schaeffer[3], Zhiva Skachokova[1,2], Karin Breu[1,2], Florence Clavaguera[1], Michael Sinnreich[2,4], Ludwig Kappos[2], Michel Goedert[3], Markus Tolnay[1], David Theo Winkler[1,2]*

1 Institute of Pathology, University Hospital Basel, Basel, Switzerland, **2** Department of Neurology, University Hospital Basel, Basel, Switzerland, **3** MRC, Laboratory of Molecular Biology, Cambridge, United Kingdom, **4** Neuromuscular Research Centre, Department of Biomedicine, University Hospital Basel, Basel, Switzerland

Abstract

Altered autophagy contributes to the pathogenesis of Alzheimer's disease and other tauopathies, for which curative treatment options are still lacking. We have recently shown that trehalose reduces tau pathology in a tauopathy mouse model by stimulation of autophagy. Here, we studied the effect of the autophagy inducing drug rapamycin on the progression of tau pathology in P301S mutant tau transgenic mice. Rapamycin treatment resulted in a significant reduction in cortical tau tangles, less tau hyperphosphorylation, and lowered levels of insoluble tau in the forebrain. The favourable effect of rapamycin on tau pathology was paralleled by a qualitative reduction in astrogliosis. These effects were visible with early preventive or late treatment. We further noted an accumulation of the autophagy associated proteins p62 and LC3 in aged tangle bearing P301S mice that was lowered upon rapamycin treatment. Thus, rapamycin treatment defers the progression of tau pathology in a tauopathy animal model and autophagy stimulation may constitute a therapeutic approach for patients suffering from tauopathies.

Citation: Ozcelik S, Fraser G, Castets P, Schaeffer V, Skachokova Z, et al. (2013) Rapamycin Attenuates the Progression of Tau Pathology in P301S Tau Transgenic Mice. PLoS ONE 8(5): e62459. doi:10.1371/journal.pone.0062459

Editor: Mel B. Feany, Brigham and Women's Hospital, Harvard Medical School, United States of America

Received January 31, 2013; **Accepted** March 21, 2013; **Published** May 7, 2013

Funding: MT and DTW are supported by the Swiss National Science Foundation (310030_135214 to MT and 32323B_123812 to D.T.W.), and by the Velux Foundation, Switzerland. The funders had no role in study design, data collection and analysis, decision to publish, or preparation of the manuscript.

Competing Interests: The authors have declared that no competing interests exist.

* E-mail: winklerd@uhbs.ch

Introduction

Alzheimer's disease (AD) and fronto-temporal dementia with tau inclusions (FTD-T) are the most frequent types of dementia [1]. They are characterized by intraneuronal accumulation, hyperphosphorylation and aggregation of tau protein. Despite of intense research efforts, causative treatments are still lacking [2] and the pathogenesis of sporadic AD and FTD-T has yet remained only partly understood. Autophagy dysfunction however is known to contribute to the evolution of different neurodegenerative proteinopathies including tauopathies [3,4,5,6].

We have recently reported beneficial effects of autophagy activation by trehalose on tau pathology *in vivo* [7], and others have shown similar effects *in vitro* [8]. Autophagy can be pharmacologically stimulated by the FDA approved drug rapamycin that inhibits the mammalian target of rapamycin complex 1 (mTORC1) and thereby facilitates the formation of autophagosomes. First studies investigating the use of rapamycin for the cure of neurodegenerative disorders in transgenic mouse models reported reduced neuronal protein aggregation following rapamycin administration in a murine model of Huntington's disease [9], a triple transgenic model of Alzheimer's disease [10,11], and recently in a model of spinocerebellar ataxia type 3 [12].

We here studied the effect of rapamycin on tau pathology in a pure tauopathy mouse model. We find a significant reduction of cortical tau tangle pathology in P301S mice after long- and short-term rapamycin treatment. Furthermore, astrogliosis was reduced and accumulation of the autophagy associated proteins p62 and LC3 in aged tangle bearing P301S mice was lowered. The FDA-approved drug rapamycin might thus be evaluated as a therapeutic approach for tauopathies, in particular for patients suffering from hereditary tauopathies.

Materials and Methods

Transgenic Mice

A total of 49 homozygous P301S tau transgenic and non-transgenic control mice ranging from 3 weeks to 5.5 months of age were included in the present study. Generation of P301S transgenic mice overexpressing the shortest human four-repeat tau isoform (0N4R) under the control of a neuron-specific Thy-1.2 promoter element has been described previously [13]. This study was carried out in strict accordance with the recommendations in the Guide for the Care and Use of Laboratory Animals of the Swiss Federal Veterinary Office. The protocol was approved by the Committee on the Ethics of Animal Experiments of the University of Basel and the Federal Veterinary Office of the Kanton Basel-Stadt (Permit Number: 2364).

Rapamycin Treatment

In brief, P301S mice were treated twice weekly intraperitoneally with 15 mg rapamycin per kg body weight or vehicle from the age of 3 weeks to 5.5 months of age (group 5-months treatment, 5MT; n = 6 rapamycin; n = 5 vehicle), and from 3 months to 4.5 months

of age (6-weeks treatment, 6WT; 6/6). For a detailed study outline including further control groups see Fig. S1.

Rapamycin powder (LC Laboratories, Woburn, MA) was dissolved at 20 mg/ml in ethanol and stored at −70°C. Before each administration, rapamycin was diluted in 5%Tween 80, 5% polyethylene glycol monolaurate (Sigma-Aldrich, Saint Louis, MO) [14,15]. Vehicle contained comparable amounts of ethanol, Tween 80, and polyethylene glycol monolaurate as the rapamycin solution. Levels of rapamycin were measured by HPLC in blood and perfused brain tissue as published previously [16].

Histology and Immunohistochemistry

Mice were deeply anaesthetized with sodium pentobarbital (100 mg/kg body weight) and transcardially perfused with cold phosphate-buffered saline (PBS). Brains were removed and one half of the brain was immersion fixed in 4% paraformaldehyde and embedded in paraffin. Sagittal serial sections of 20 µm thickness were cut with a microtome throughout the hemisphere [17]. Fibrillary tau tangle pathology was assessed by Gallyas silver staining. Immunohistochemistry on paraffin fixed sections was done according to previously published protocols [18] using the avidin–biotin–peroxidase complex method and VECTOR NovaRED kits (Vector Laboratories, Burlingame, CA) as chromogen. Samples of rapamycin and vehicle treated mice were processed pairwise in parallel. AT8 (ptau Ser202/Thr205, Pierce, Rockford, IL), AT100 (ptau Ser212/Thr214, Pierce, Rockford, IL), and GFAP (Clone Ab1; Thermo Scientific Freemont, CA) antibodies were used. Cortical GFAP staining was assessed qualitatively by three independent raters (S.O., K.B., D.W.). Blinded sets comprising every fifth 20 µm section of 5MT mice were rated from – to +++ and mean scores of the three raters were obtained (see also Fig. S2).

Stereology

Quantification of tau tangles was performed on Gallyas silver stained sections using the Optical Fractionator [19]. In the 5MT group, cortex, hippocampus and brain stem were taken into account for stereological analysis, while in the 6WT group the quantification was limited to the cortex. AT8 positive cortical cells were quantified in both groups. In brief, every 5th section of 20 µm thickness throughout the left hemisphere was assessed using a Zeiss Axioplan microscope and StereoInvestigator software (Version 9.14; MicroBrightField, Williston, VT).

Sarkosyl Extraction and Western Blot Analysis

Following PBS perfusion, one half of the mouse brain was dissected into forebrain and brain stem and immediately frozen in liquid nitrogen. Sarkosyl extraction was performed as described previously [20]. The brain tissue was homogenized in 0.5 ml of 800 mM NaCl, 10% sucrose, 10 mM tris HCl pH 7.4, 1 mM EGTA using a Kinetica polytron. Samples were centrifuged at 5000 rpm for 15 min. The supernatant was collected and sarkosyl added to 1% for 1 hour, shaking. Samples were then centrifuged at 80,000 rpm for 30 min and the pellet resuspended in 150 µl/g of tissue 10 mM Tris HCl pH 7.4. Antibodies used for Western blotting are listed in detail including the targeted epitopes in Methods S1. In brief, we used for detection of tau: BR134 [21]; RD3 from Millipore Corporation (Billerica, MA); T49 [22,23], a kind gift of Prof. Virginia Lee, CNDR, University of Pennsylvania School of Medicine, Philadelphia, PA; AT8 and AT100 from Pierce Biotechnology (Rockford, IL). For evaluation of mTORC1 signalling and autophagy were used: anti-S6 Ribosomal Protein (#2217), anti-Phospho-S6 Ribosomal Protein Ser235/236 (#2211), anti-LC3B (#2775), from Cell Signaling Technology (Danvers, MA); anti-Phospho-S6 Ribosomal anti-p62 (GP62-C) from Progen Biotechnik (Heidelberg, Germany).

Statistical Analysis

Statistical analysis was performed using IBM® SPSS® Statistics Version 19. Biochemical data of tau Western blots was subjected to unpaired T-tests and T-tests adjusted for unequal variances (Welch-Test), yielding both similar results. Holm-Bonferroni corrections were applied. Biochemical data of p62 and LC3-levels was analyzed by ANOVA. Stereological samples of vehicle and rapamycin treated mice were stained in parallel. Accordingly, the pairwise reduction of Gallyas or AT8 positive counts was analysed using one-sample T-tests per brain region. Significant p-values adjusted for multiple comparisons by the Holm-Bonferroni method are reported and outlined in all figures as follows: * = $p<0.05$, ** = $p<0.01$, *** = $p<0.001$. The mean and SD are indicated in all figures.

Results

Aged vehicle treated P301S tau transgenic mice developed extensive tau pathology, spreading throughout the central nervous system including the forebrain, comparable with previous reports [13] (Fig. 1A). Preventive long-term rapamycin administration initiated at 3 weeks of age resulted in a marked reduction of cortical tau tangles at age of 5.5 months (Fig. 1B). While in vehicle treated mice, abundant Gallyas stain positive tangle pathology was seen throughout the cortex, pronounced in rostral motor cortex, only few isolated tangles formed in the cortex of rapamycin treated 5MT P301S mice (Fig. 1C). In parallel, cortical tau phosphorylation at the early hyperphosphorylated AT8 epitope and the late AT100 epitope was diminished by rapamycin treatment (1D, E). With the evolution of tau tangle pathology, P301S mice develop progressive astrogliosis [24]. In parallel to the marked reduction in cortical tangle load, we noted a qualitative alleviation of cortical astrogliosis in long-term rapamycin treated mice (Fig. 1F, Fig. S2).

While in the hippocampus of vehicle treated 5MT P301S mice, only sparse tangles and limited tau hyperphosphorylation were seen, there was a markedly advanced tangle formation affecting the brain stem region. Only a mild qualitative reduction of the sparse hippocampal and the extensive brain stem tau pathology became visible following rapamycin administration (Fig. 1G, H).

We further studied whether a favourable effect on tau pathology progression could also be attained when treatment was started only after the onset of tau hyperphosphorylation in P301S mice. A short 6 weeks treatment with rapamycin was initiated at 3 months of age (6WT group) and again resulted in a notable reduction of cortical tau hyperphosphorylation and tangles (Fig. 1I).

Quantitative stereological analysis confirmed a significant reduction in cortical tangles by 86% comparing long-term rapamycin treated mice to vehicle treated mice (5MT group, $n = 5$, Gallyas positive tangle count reduced to $13.7\% \pm 18.8\%$, $p<0.001$) (Fig. 2). Cortical tau hyperphosphorylation, assessed by neuronal AT8 positivity, was reduced to $29.5 \pm 28.9\%$ ($p = 0.02$) in long-term rapamycin treated mice (5MT). While a trend towards a reduction of tau tangles was noted in the hippocampus ($p = 0.05$), the lowering of the marked tangle pathology observed in the brain stem region did not reach statistical significance (Fig. 2).

The short 6 weeks treatment started at 3 months of age significantly reduced cortical tangles (6WT group, $n = 6$, tangle count reduced to $38.9\% \pm 25.7\%$, $p = 0.004$) and lowered tau hyperphosphorylation at the AT8 epitope (reduction to $45.5 \pm 32.7\%$; $p = 0.04$; Fig. 2).

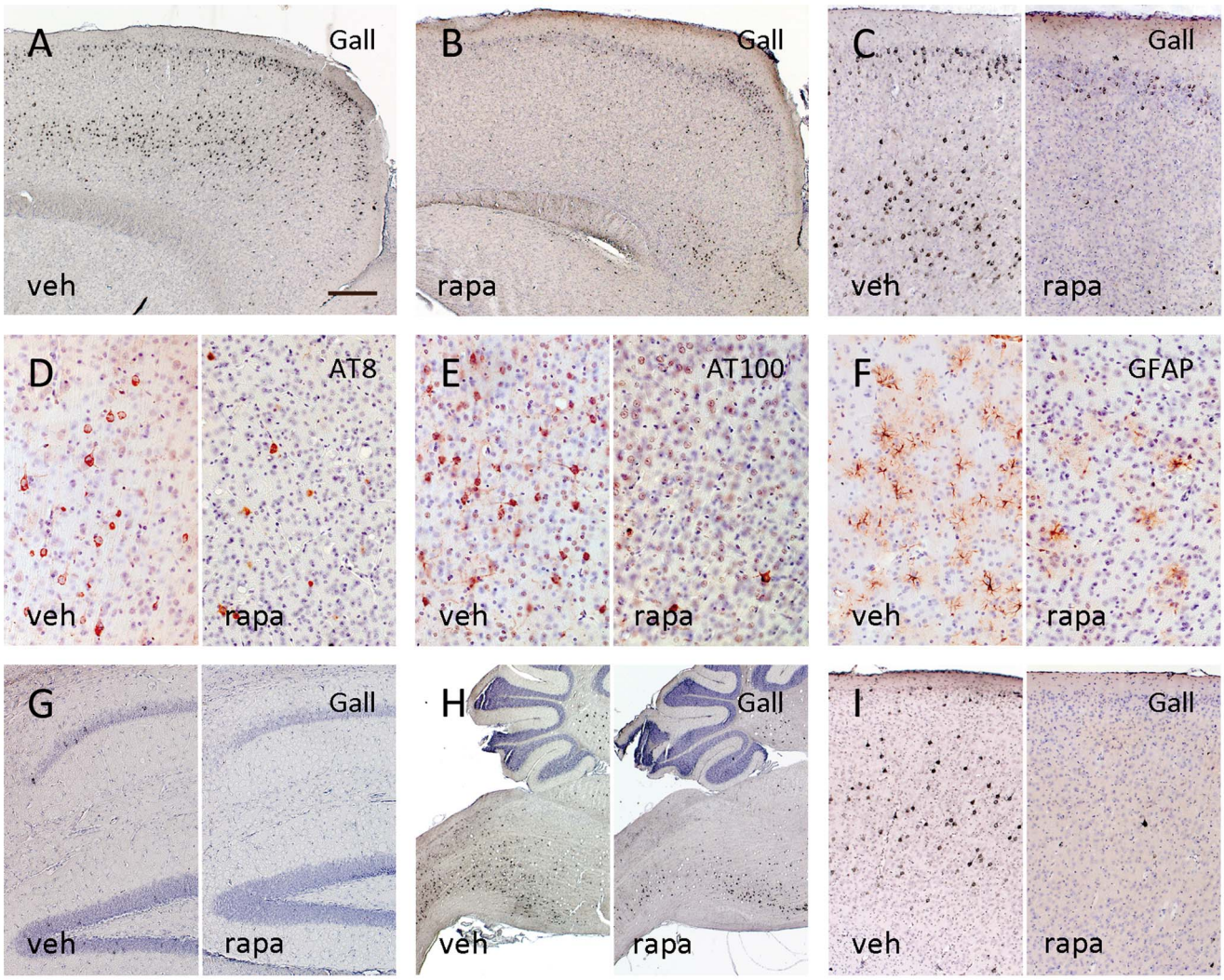

Figure 1. The extensive cortical tau tangle pathology present in 5.5 months old vehicle (veh) treated P301S mice (A) was widely attenuated in long-term rapamycin (rapa) treated mice (B). The lowering in tangle formation was most pronounced in the motor cortex (C: left vehicle treated/right rapamycin) and associated with reduced pathological tau hyperphosphorylation at the AT8 and AT100 epitopes (D, E). In parallel, cortical astrogliosis was diminished following rapamycin treatment (F). While there was a trend towards a reduction of the sparse tangles in the hippocampus, the advanced tau pathology in the brain stem however was not significantly ameliorated by rapamycin (G, H). Short-term treatment at 3 months of age for 6 weeks again resulted in a marked reduction of cortical tangles (I) (A–H: 5MT group; I: 6WT. A–C, G–I: Gallyas silver stain; D: AT8 IHC; E: AT100 IHC; F: GFAP IHC. Bar in A equals 300 µm in A and B, 150 µm in C, G and I, 75 µm in D–F, 600 µm in H).
doi:10.1371/journal.pone.0062459.g001

In parallel to the observed attenuation in cortical tau tangle pathology in the stereological assessment, biochemical analysis revealed a significant reduction of sarkosyl insoluble tau in the forebrain of long- and short-term treated P301S mice (5MT: rapamycin group: percentage of vehicle treated mice: 56.7±17.5%, $p = 0.03$, Fig. 3A; 6WT: 28.0±36.2%, $p = 0.004$, Fig. 3B). Tau hyperphosphorylated at AT8 and AT100 was significantly lowered upon 6 weeks of rapamycin treatment as measured by Western blotting (6WT: rapamycin group: percentage of vehicle treated mice: AT8:11.2±42.3%, $p = 0.004$; AT100:4.1±17.9%, $p = 0.04$, Fig. 3C). In contrast, no decrease of forebrain soluble tau levels was noted in these aged mice, and no acute suppression of soluble tau protein generation occurred after rapamycin administration in pretangle P301S mice (Fig. S3A). Endogenous murine tau furthermore remained unchanged after acute and chronic rapamycin administration in P301S mice as assessed by the mouse tau specific antibody T49 [22] (Fig. S3B).

High levels of rapamycin were measured in the brain following its intraperitoneal administration, in confirmation that rapamycin penetrates the blood-brain barrier (Fig. S4A). Rapamycin induced inhibition of the mTORC1 pathway in the brain of treated mice resulted in significantly reduced phosphorylation of ribosomal S6 protein (S6) (5MT, Fig. 4A). S6 suppression by rapamycin was comparable in the forebrain and the brain stem (Fig. S4B).

In line with the activation of autophagy by rapamycin, a significant increase in LC3II by 229% was found in rapamycin treated P301S mice (6WT, $p = 0.02$, Fig. 4B). High levels of the autophagy associated proteins p62 and LC3 in a set of vehicle treated old tangle bearing P301S mice furthermore pointed towards a disturbed autophagy flux in our tauopathy model. This accumulation of p62 and LC3 was prevented by rapamycin treatment (Fig 4C).

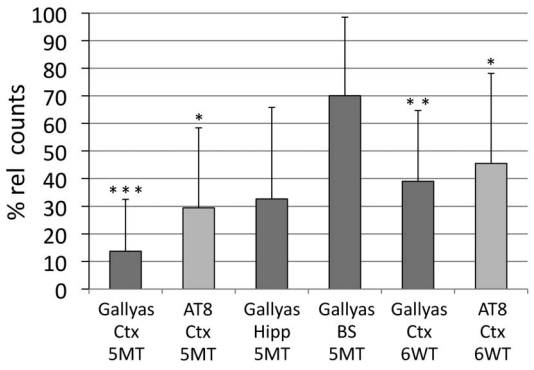

Figure 2. After long-term rapamycin treatment (n = 6), unbiased stereology confirmed a significant reduction of cortical tau tangles to only 14% of the amount of tangles seen in vehicle treated (n = 5) P301S mice (vehicle = 100%). The number of AT8 stained cells containing hyperphosphorylated tau was reduced to 30% in aged rapamycin treated mice compared to controls (100%) (5MT group). A significant attenuation of Gallyas-stained (to 39% of controls) and AT8-positive cells (to 46% of controls) was also achieved by late short-term rapamycin treatment (6WT, n = 6/6). The reduction of tangles in the hippocampus (to 33% of controls) and the brain stem (to 72% of controls) did not reach the level of significance adjusted for multiple testing. Pairwise reduction of Gallyas or AT8 positive counts was analysed using one-sample T-tests per brain region. Significant p-values, adjusted for the multiple comparisons of all 6 tested groups by the Holm-Bonferroni method, are outlined as follows: *$p<0.05$, **$p<0.01$, and ***$p<0.001$.
doi:10.1371/journal.pone.0062459.g002

Discussion

We report a significant alleviation of cortical tau pathology in a murine tauopathy model following long- and short-term administration of the autophagy inducing drug rapamycin. Alzheimer's disease (AD) and other tauopathies including fronto-temporal dementia with tau pathology (FTD-T) constitute the most prevalent forms of neurodegenerative disorders [1]. Despite a broad range of concepts, only few tau targeting approaches such as tau directed immunotherapy [25,26] and administration of lithium chloride [27], sodium selenate [28] or methylene blue [29] have been effective *in vivo*.

Disturbed autophagy is known to be involved in the pathogenesis of AD [4,30]. We have recently shown that trehalose alleviates tau pathology by autophagy stimulation *in vivo* [7]. A beneficial effect of autophagy induction on amyloid-β and associated tau pathology has furthermore been found in a triple transgenic mouse model of AD [10,11].

We here studied the effect of the FDA approved drug rapamycin on tau pathology in absence of amyloid-β pathology, using the P301S mutant tau transgenic mouse model. Vehicle treated P301S mice develop extensive tau pathology with tau redistribution towards the cell body and dendrites, early tau hyperphosphorylation at 4–6 weeks of age, and subsequently, at ages of 3 months, progressive aggregation of tau into tangles. We show that long-term rapamycin treatment reduces cortical tau tangle burden by more than 80% and levels of sarkosyl insoluble tau in the forebrain by 70%. In parallel to the attenuation of tau pathology, we note reduced astrogliosis following rapamycin administration. Rapamycin is also able to alleviate tau tangle pathology when a short-term treatment is started after tau hyperphosphorylation has already been initiated. These findings extend previous observations in rodent models on beneficial effects of rapamycin for cerebral proteinopathies e.g. polyglutamine disorders [9,12] and the amyloid-β cascade [10] to tauopathies.

Comparably to trehalose treatment [7], rapamycin does not fully prevent the formation of tau pathology in P301S mice. Particularly in the brain stem, the persisting tangle formation might be caused by the extensive basal tau pathology present in this brain region in P301S mice that could overrun the benefical effect of autophagy induction in this brain area [13]. Rapamycin treatment thus seems to be subjected to a ceiling effect that does not allow coping with a very high tau load. As a limitation of our present study, the rapidly progressive brain stem pathology

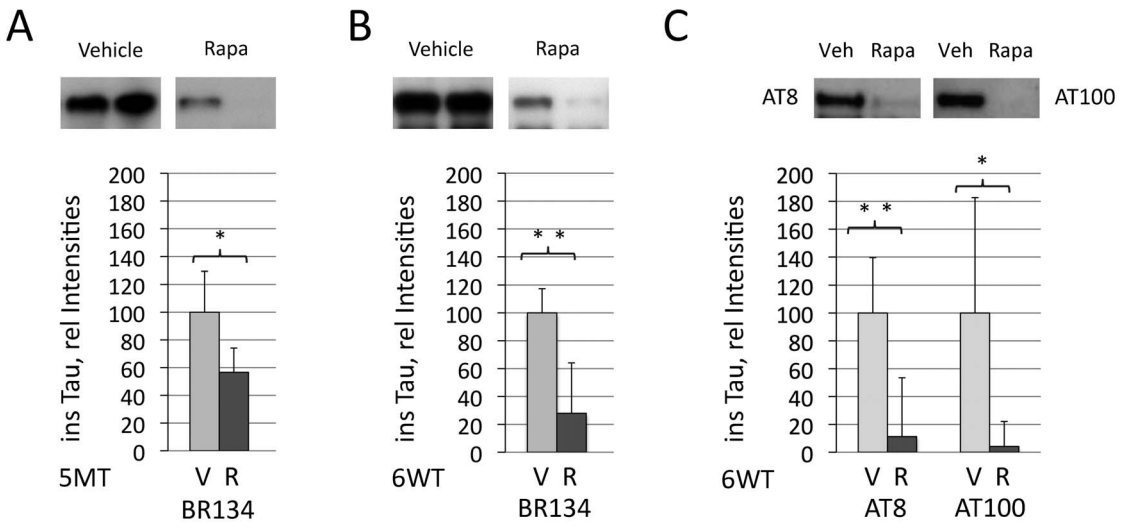

Figure 3. Levels of sarkosyl extracted insoluble tau were significantly reduced in the forebrain of P301S mice after 5 months of long-term rapamycin treatment (R, n = 6) when compared to vehicle treated mice (V, n = 5) (A, 5MT group; Western blot using BR134 antibody). A comparable lowering of insoluble tau was obtained by late short-term rapamycin administration over 6 weeks (B; 6WT group, n = 6/6). In parallel, the accumulation of tau hyperphosphorylated at the AT8 and AT100 epitopes was significantly lowered (C; 6WT group, n = 6/6). Quantification of tau Western blots was subjected to unpaired T-tests and T-tests adjusted for unequal variances (Welch-Test), yielding both similar results. *$p<0.05$ and **$p<0.01$.
doi:10.1371/journal.pone.0062459.g003

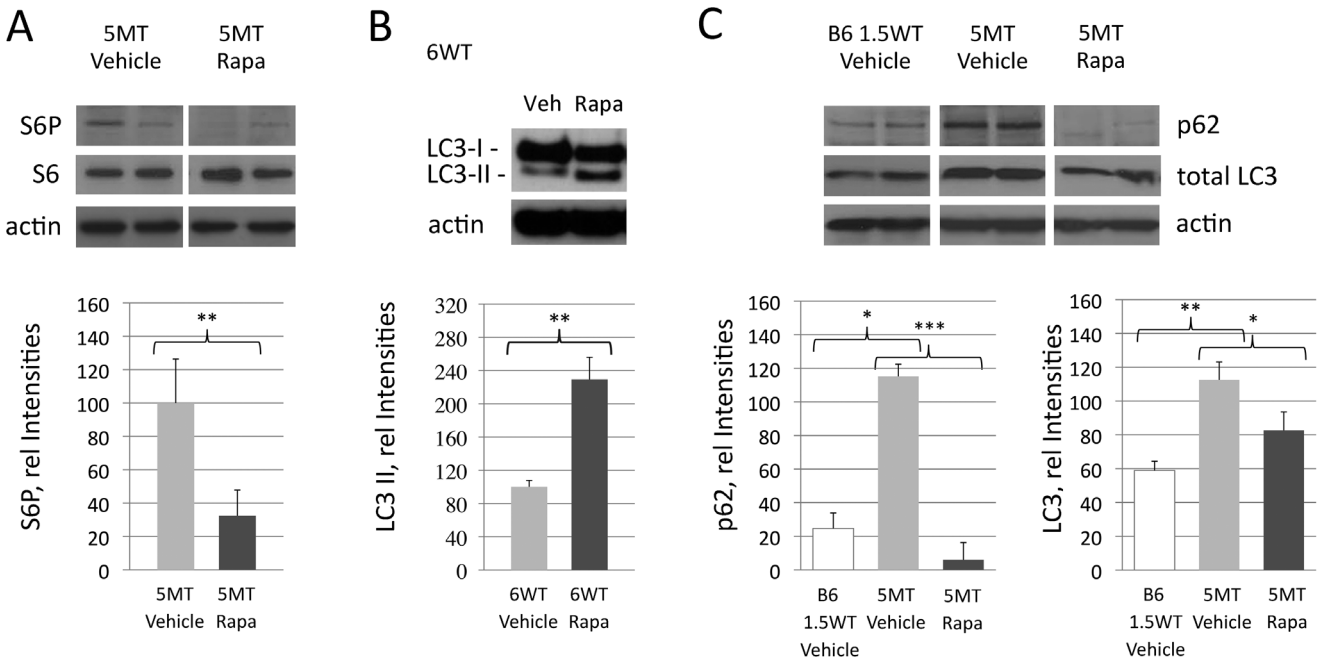

Figure 4. Consistent with cerebral mTOR inhibition, phosphorylation of S6 (S6P) was significantly reduced following rapamycin administration (A, 5MT group, n = 4/4). Compatible with an induced autophagy pathway, LC3II levels were increased upon rapamycin treatment (B, 6WT group, n = 6/6). High levels of the autophagy associated proteins p62 and LC3 were measured in aged vehicle treated P301S transgenic mice (C; 5MT Vehicle, n = 4). This accumulation of p62 and LC3 was prevented by long-term rapamycin administration, pointing towards a restored autophagic flux (C; 5MT Rapa, n = 4). Forebrain tissue was used and data was analyzed by ANOVA. *$p<0.05$, **$p<0.01$, and ***$p<0.001$.
doi:10.1371/journal.pone.0062459.g004

furthermore precludes the observation of a significant clinical improvement in the P301S model. Detailed analysis of behavioural and functional parameters including the characterization of early effects on tau metabolism following rapamycin treatment should therefore be addressed in future studies.

Prevention from protein aggregation by rapamycin in different models of neurodegenerative disorders has mainly been attributed to its autophagy inducing property [5,10]. Here we show that intraperitoneally administrated rapamycin penetrates the blood-brain-barrier in mice. It reaches effective levels in the brain to inhibit mTOR and stimulate autophagy. Our analysis of autophagic flux is limited by the *ex vivo* nature of our specimen and the long-term treatment effects. However, in vehicle treated, tangle bearing P301S mice, we observe an accumulation of LC3 protein and the autophagy substrate protein p62, similar to reports on findings in human tauopathy patients' brains [31]. Lowered levels of p62 and LC3 in our rapamycin treated P301S mice thus may point towards a restoration of the autophagic flux, comparable to a recent observation in APP transgenic, amyloid-ß depositing CRND8 mice [32]. Besides autophagy stimulation, rapamycin can attenuate tauopathy progression also by its immunosuppressive properties. The later mechanism may underlie the observed reduction in astrogliosis, as tau associated gliosis has earlier been reported to be responsive to immunosuppression [33]. Rapamycin has furthermore been shown to modulate tau phosphorylation *in vitro* during neuronal development [34,35]. A favorable effect on tau phosphorylation may therefore contribute to the attenuation of tau pathology in our model. It has furthermore been reported that rapamycin can inhibit protein synthesis [36]. We however see no reduction in endogenous mouse tau nor in transgenic human tau following short-term rapamycin administration, precluding that the observed favourable effects on tau pathology evolution are primarily based on a reduced generation of tau in our model.

Rapamycin is an established FDA-approved drug. Its use as an mTOR inhibitor for the treatment of tuberous sclerosis has recently been translated from transgenic mouse models to man [37]. The beneficial effects of rapamycin on the progression of tau pathology in our murine model may encourage the development of autophagy inducing agents for patients suffering from tauopathies.

Supporting Information

Figure S1 Scheme of the study indicating the treatment schedules of the different groups of rapamycin (R) or vehicle (V) treated P301S mutant tau transgenic mice and non-transgenic C57BL/6J mice. P301S mice were treated twice weekly intraperitoneally with 15 mg rapamycin per kg body weight or vehicle from 3 weeks to 5.5 months of age (group 5-months treatment, 5MT; n = 6 rapamycin; n = 5 vehicle), and from 3 months to 4.5 months of age (6-weeks treatment, 6WT; 6/6). Additional P301S mice were treated at age of 3 months for 1.5 weeks in order to analyze the immediate effects on soluble tau levels (1.5-weeks-treatment, 1.5WT; 5/5). Furthermore, non-transgenic C57BL/6J mice were treated accordingly at the age of 3 months for 1.5 weeks (B6-1.5WT; 2/2). A total of 8 adult C57BL/6J mice (4 rapamycin, 4 vehicle) have been used to measure the levels of rapamycin in blood and brain (B6 sir; 4/4). A total of 4 additional rapamycin treated mice died during the experiments and could therefore not be included for data collection.
(PDF)

Figure S2 For the qualitative assessment of astrogliosis in long-term rapamycin treated mice, blinded sets comprising every 5th

20 μm section of 5MT mice were rated from – (A), + (B), ++ (C) to +++ (D) by three independent raters (S.O., K.B., D.W.). The median rating of the GFAP stainings of all sections was listed per brain region and mouse for a qualitative comparison of the 5 vehicle treated to the 6 rapamycin treated mice (E).
(TIF)

Figure S3 Forebrain levels of soluble tau protein remained unchanged after both, 5 months or 6 weeks of rapamycin treatment (A; 5 MT, $p = 0.35$; 6 WT, $p = 0.18$). We also analyzed the immediate effects of a short rapamycin treatment of 1.5 weeks duration on forebrain tau levels in pretangle P301S mice. There again was no reduction of soluble tau by rapamycin treatment (A; 1.5 WT, $p = 0.53$). Furthermore, unchanged levels of mouse tau following rapamycin administration indicate that there is no suppression of endogenous tau synthesis by rapamycin in our model (D; T49 antibody (kindly provided by Prof. V. Lee); 1.5 WT, $p = 0.20$; 6 WT, $p = 0.86$).
(TIF)

Figure S4 Intraperitoneal rapamycin administration resulted in high cerebral rapamycin levels as measured by HPLC. Similar levels were achieved in the forebrain and the brain stem (A; B6 1.5 WT; FB = forebrain, BS: brain stem, BL: blood). Consistent with cerebral mTOR inhibition, Western blotting of forebrain tissue showed significantly reduced phosphorylation of S6 following rapamycin administration (see Fig. 4A). Suppression of the phosphorylation of S6 (S6P) was comparable in brain stem and forebrain tissue, compatible with a similar effect of rapamycin on mTOR in both brain regions.
(TIF)

Methods S1
(DOCX)

Acknowledgments

We thank Dr. L. Slomianka, Institute of Anatomy, University of Zürich, for his expert advice and help pertaining to stereological procedures. We acknowledge A. Schötzau and U. Simmen (www.schoetzau-simmen.ch) for statistical advice. We thank Prof. Virginia Lee, CNDR, University of Pennsylvania School of Medicine, for the T49 antibody and Dr. D. Mueller, Institute of Pharmacology and Toxicology, University Hospital Zürich, for the measurement of rapamycin by HPLC.

Author Contributions

Critical revision and extension of the drafted manuscript: PC ZS MS LK MG MT. Conceived and designed the experiments: SO GF PC VS MS MG DW. Performed the experiments: SO GF PC VS KB MS DW. Analyzed the data: SO GF PC VS KB MS MG DW. Contributed reagents/materials/analysis tools: PC FC MS MG MT. Wrote the paper: DW SO.

References

1. Goedert M, Spillantini MG (2006) A century of Alzheimer's disease. Science 314: 777–781.
2. Citron M (2010) Alzheimer's disease: strategies for disease modification. Nat Rev Drug Discov 9: 387–398.
3. Boland B, Kumar A, Lee S, Platt FM, Wegiel J, et al. (2008) Autophagy induction and autophagosome clearance in neurons: relationship to autophagic pathology in Alzheimer's disease. J Neurosci 28: 6926–6937.
4. Pickford F, Masliah E, Britschgi M, Lucin K, Narasimhan R, et al. (2008) The autophagy-related protein beclin 1 shows reduced expression in early Alzheimer disease and regulates amyloid beta accumulation in mice. J Clin Invest 118: 2190–2199.
5. Rubinsztein DC (2006) The roles of intracellular protein-degradation pathways in neurodegeneration. Nature 443: 780–786.
6. Mizushima N, Levine B, Cuervo AM, Klionsky DJ (2008) Autophagy fights disease through cellular self-digestion. Nature 451: 1069–1075.
7. Schaeffer V, Lavenir I, Ozcelik S, Tolnay M, Winkler DT, et al. (2012) Stimulation of autophagy reduces neurodegeneration in a mouse model of human tauopathy. Brain 135: 2169–2177.
8. Kruger U, Wang Y, Kumar S, Mandelkow EM (2012) Autophagic degradation of tau in primary neurons and its enhancement by trehalose. Neurobiol Aging 33: 2291–2305.
9. Ravikumar B, Vacher C, Berger Z, Davies JE, Luo S, et al. (2004) Inhibition of mTOR induces autophagy and reduces toxicity of polyglutamine expansions in fly and mouse models of Huntington disease. Nat Genet 36: 585–595.
10. Caccamo A, Majumder S, Richardson A, Strong R, Oddo S (2010) Molecular interplay between mammalian target of rapamycin (mTOR), amyloid-beta, and Tau: effects on cognitive impairments. J Biol Chem 285: 13107–13120.
11. Majumder S, Richardson A, Strong R, Oddo S (2011) Inducing autophagy by rapamycin before, but not after, the formation of plaques and tangles ameliorates cognitive deficits. PLoS One 6: e25416.
12. Menzies FM, Huebener J, Renna M, Bonin M, Riess O, et al. (2010) Autophagy induction reduces mutant ataxin-3 levels and toxicity in a mouse model of spinocerebellar ataxia type 3. Brain 133: 93–104.
13. Allen B, Ingram E, Takao M, Smith MJ, Jakes R, et al. (2002) Abundant tau filaments and nonapoptotic neurodegeneration in transgenic mice expressing human P301S tau protein. J Neurosci 22: 9340–9351.
14. Hegedus B, Banerjee D, Yeh TH, Rothermich S, Perry A, et al. (2008) Preclinical cancer therapy in a mouse model of neurofibromatosis-1 optic glioma. Cancer Res 68: 1520–1528.
15. Meikle L, Pollizzi K, Egnor A, Kramvis I, Lane H, et al. (2008) Response of a neuronal model of tuberous sclerosis to mammalian target of rapamycin (mTOR) inhibitors: effects on mTORC1 and Akt signaling lead to improved survival and function. J Neurosci 28: 5422–5432.
16. Mueller DM, Rentsch KM (2010) Sensitive quantification of sirolimus and everolimus by LC-MS/MS with online sample cleanup. J Chromatogr B Analyt Technol Biomed Life Sci 878: 1007–1012.
17. Winkler DT, Bondolfi L, Herzig MC, Jann L, Calhoun ME, et al. (2001) Spontaneous hemorrhagic stroke in a mouse model of cerebral amyloid angiopathy. J Neurosci 21: 1619–1627.
18. Jucker M, Walker LC, Schwarb P, Hengemihle J, Kuo H, et al. (1994) Age-related deposition of glia-associated fibrillar material in brains of C57BL/6 mice. Neuroscience 60: 875–889.
19. West MJ, Slomianka L, Gundersen HJ (1991) Unbiased stereological estimation of the total number of neurons in thesubdivisions of the rat hippocampus using the optical fractionator. Anat Rec 231: 482–497.
20. Delobel P, Lavenir I, Fraser G, Ingram E, Holzer M, et al. (2008) Analysis of tau phosphorylation and truncation in a mouse model of human tauopathy. Am J Pathol 172: 123–131.
21. Goedert M, Spillantini MG, Jakes R, Rutherford D, Crowther RA (1989) Multiple isoforms of human microtubule-associated protein tau: sequences and localization in neurofibrillary tangles of Alzheimer's disease. Neuron 3: 519–526.
22. Mawal-Dewan M, Henley J, Van de Voorde A, Trojanowski JQ, Lee VM (1994) The phosphorylation state of tau in the developing rat brain is regulated by phosphoprotein phosphatases. J Biol Chem 269: 30981–30987.
23. Forman MS, Lal D, Zhang B, Dabir DV, Swanson E, et al. (2005) Transgenic mouse model of tau pathology in astrocytes leading to nervous system degeneration. J Neurosci 25: 3539–3550.
24. Hampton DW, Webber DJ, Bilican B, Goedert M, Spillantini MG, et al. (2010) Cell-mediated neuroprotection in a mouse model of human tauopathy. J Neurosci 30: 9973–9983.
25. Asuni AA, Boutajangout A, Quartermain D, Sigurdsson EM (2007) Immunotherapy targeting pathological tau conformers in a tangle mouse model reduces brain pathology with associated functional improvements. J Neurosci 27: 9115–9129.
26. Bi M, Ittner A, Ke YD, Gotz J, Ittner LM (2011) Tau-targeted immunization impedes progression of neurofibrillary histopathology in aged P301L tau transgenic mice. PLoS One 6: e26860.
27. Noble W, Planel E, Zehr C, Olm V, Meyerson J, et al. (2005) Inhibition of glycogen synthase kinase-3 by lithium correlates with reduced tauopathy and degeneration in vivo. Proc Natl Acad Sci U S A 102: 6990–6995.
28. van Eersel J, Ke YD, Liu X, Delerue F, Kril JJ, et al. (2010) Sodium selenate mitigates tau pathology, neurodegeneration, and functional deficits in Alzheimer's disease models. Proc Natl Acad Sci U S A 107: 13888–13893.
29. Hosokawa M, Arai T, Masuda-Suzukake M, Nonaka T, Yamashita M, et al. (2012) Methylene Blue Reduced Abnormal Tau Accumulation in P301L Tau Transgenic Mice. PLoS One 7: e52389.
30. Pritchard SM, Dolan PJ, Vitkus A, Johnson GV (2011) The toxicity of tau in Alzheimer disease: turnover, targets and potential therapeutics. J Cell Mol Med 15: 1621–1635.
31. Kuusisto E, Salminen A, Alafuzoff I (2001) Ubiquitin-binding protein p62 is present in neuronal and glial inclusions in human tauopathies and synucleinopathies. Neuroreport 12: 2085–2090.

32. Yang DS, Stavrides P, Mohan PS, Kaushik S, Kumar A, et al. (2011) Reversal of autophagy dysfunction in the TgCRND8 mouse model of Alzheimer's disease ameliorates amyloid pathologies and memory deficits. Brain 134: 258–277.
33. Yoshiyama Y, Higuchi M, Zhang B, Huang SM, Iwata N, et al. (2007) Synapse loss and microglial activation precede tangles in a P301S tauopathy mouse model. Neuron 53: 337–351.
34. Meske V, Albert F, Ohm TG (2008) Coupling of mammalian target of rapamycin with phosphoinositide 3-kinase signaling pathway regulates protein phosphatase 2A- and glycogen synthase kinase-3 -dependent phosphorylation of Tau. J Biol Chem 283: 100–109.
35. Morita T, Sobue K (2009) Specification of neuronal polarity regulated by local translation of CRMP2 and Tau via the mTOR-p70S6K pathway. J Biol Chem 284: 27734–27745.
36. Wyttenbach A, Hands S, King MA, Lipkow K, Tolkovsky AM (2008) Amelioration of protein misfolding disease by rapamycin: translation or autophagy? Autophagy 4: 542–545.
37. Franz DN, Leonard J, Tudor C, Chuck G, Care M, et al. (2006) Rapamycin causes regression of astrocytomas in tuberous sclerosis complex. Ann Neurol 59: 490–498.

Supplementary Materials

Supplementary Figure S1

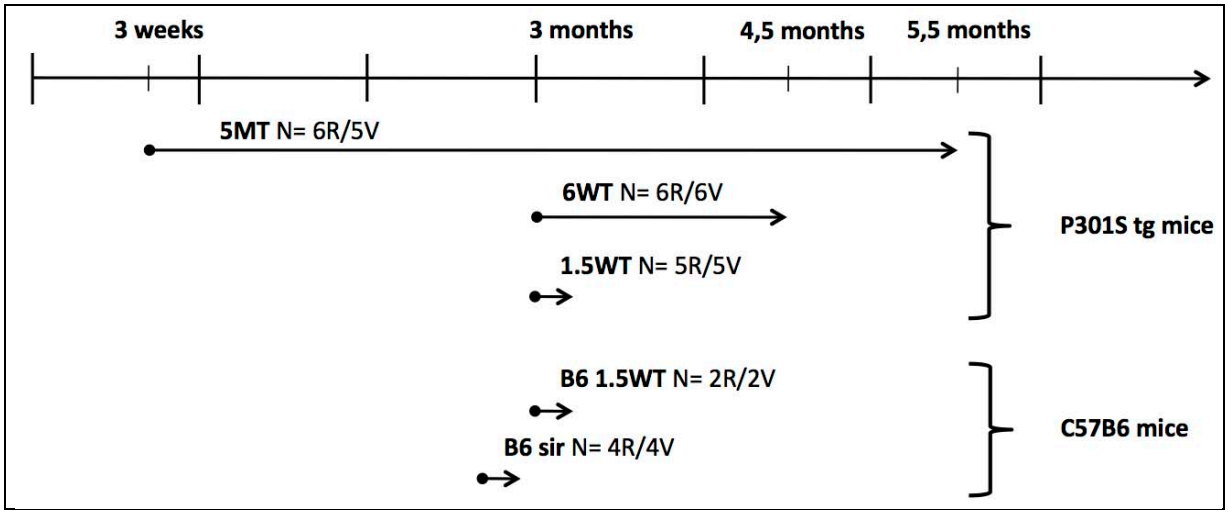

Scheme of the study indicating the treatment schedules of the different groups of rapamycin (R) or vehicle (V) treated P301S mutant tau transgenic mice and non-transgenic C57BL/6J mice.
P301S mice were treated twice weekly intraperitoneally with 15mg rapamycin per kg body weight or vehicle from 3 weeks to 5.5 months of age (group 5-months treatment, 5MT; n=6 rapamycin; n=5 vehicle), and from 3 months to 4.5 months of age (6-weeks treatment, 6WT; 6/6). Additional P301S mice were treated at age of 3 months for 1.5 weeks in order to analyze the immediate effects on soluble tau levels (1.5-weeks-treatment, 1.5WT; 5/5). Furthermore, non-transgenic C57BL/6J mice were treated accordingly at the age of 3 months for 1.5 weeks (B6-1.5WT; 2/2). A total of 8 adult C57BL/6J mice (4 rapamycin, 4 vehicle) have been used to measure the levels of rapamycin in blood and brain (B6 sir; 4/4). A total of 4 additional rapamycin treated mice died during the experiments and could therefore not be included for data collection.

Supplementary Figure S2

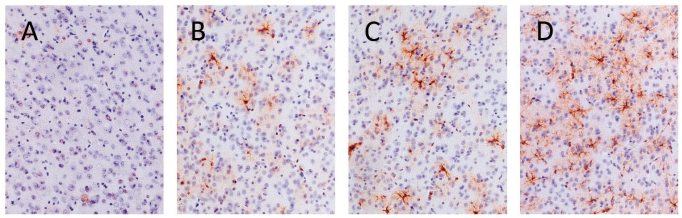

E

Cortex	Hippocampus	
-/+	-/+	Vehicle 5MT
+/++	++	
+/++	++	
++	++	
++	++/+++	
-	+/++	Rapa 5MT
-	-	
+	+/++	
+/++	+	
+/++	+/++	
++	-/+	

For the qualitative assessment of astrogliosis in long-term rapamycin treated mice, blinded set comprising every 5th 20μm section of 5MT mice were rated from – (A), + (B), ++ (C) to +++ (D) by three independent raters (S.O., K.B., D.W.). The median rating of the GFAP stainings of all sections was listed per brain region and mouse for a qualitative comparison of the 5 vehicle treated to the 6 rapamycin treated mice (E).

Supplementary Figure S3

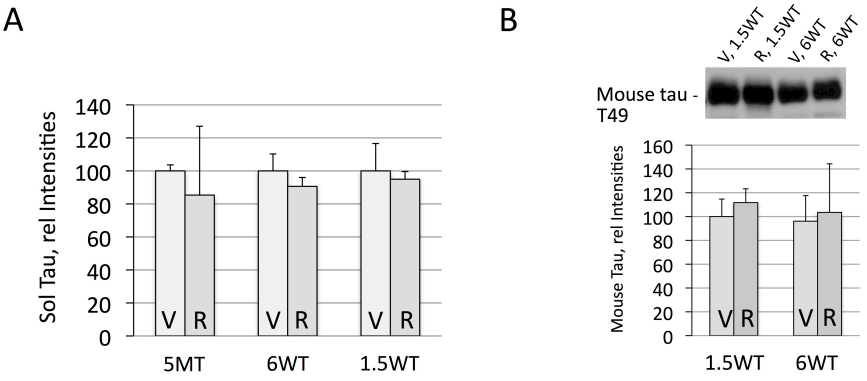

Forebrain levels of soluble tau protein remained unchanged after both, 5 months or 6 weeks of rapamycin treatment (A; 5MT, p=0.35; 6WT, p=0.18). We also analyzed the immediate effects of a short rapamycin treatment of 1.5 weeks duration on forebrain tau levels in pretangle P301S mice. There again was no reduction of soluble tau by rapamycin treatment (A; 1.5WT, p=0.53). Furthermore, unchanged levels of mouse tau following rapamycin administration indicate that there is no suppression of endogenous tau synthesis by rapamycin in our model (D; T49 antibody (kindly provided by Prof. V. Lee); 1.5WT, p=0.20; 6WT, p=0.86).

Supplementary Figure S4

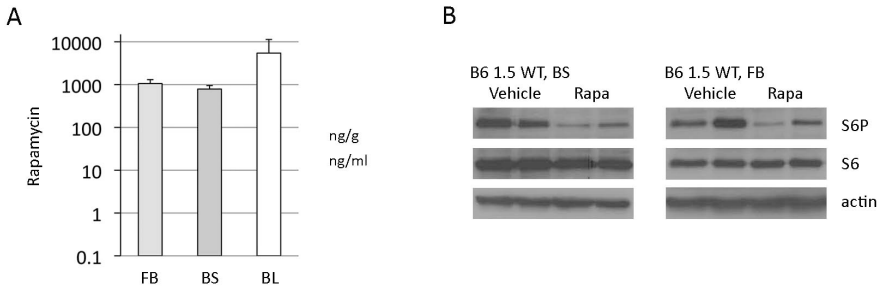

Intraperitoneal rapamycin administration resulted in high cerebral rapamycin levels as measured by HPLC. Similar levels were achieved in the forebrain and the brain stem (A; B6 1.5WT; FB= forebrain, BS: brain stem, BL: blood). Consistent with cerebral mTOR inhibition, Western blotting of forebrain tissue showed significantly reduced phosphorylation of S6 following rapamycin administration (see Fig 2C). Suppression of the phosphorylation of S6 (S6P) was comparable in brain stem and forebrain tissue, compatible with a similar effect of rapamycin on mTOR in both brain regions.

Supplementary Methods

Rapamycin quantification in brain tissue and blood by HPLC

In order to measure brain levels of rapamycin, a total of 8 C57BL/6J mice were treated for 1.5 weeks with rapamycin or vehicle (4/4). The mice then were deeply anesthetized, blood was collected in EDTA tubes following cardiac puncture, and the mice were perfused with NaCl before removing and immediately freezing their brains. The forebrain halves were homogenized and subjected to HPLC measurement of rapamycin according to a previously published protocol [1]. Brain halves and blood samples of vehicle treated mice were used to calibrate the HPLC system.

Antibodies used for Western blotting

For Western blotting, the following antibodies were used:

i) for detection of tau: BR134 detecting the C terminus of human and murine tau independently of its phosphorylation [2], RD3 targeting aa209-220 of human tau and recognizing 3-repeat human and murine tau isoforms from Millipore Corporation (Billerica, MA), T49 [3,4] specific for mouse tau (kind gift of Prof. Virginia Lee, CNDR, University of Pennsylvania School of Medicine, Philadelphia, PA), AT8 against the phosphorylated Ser202 tau residue from Endogen (Woburn, MA), and AT100 against tau phosphorylated at Ser212 and Thr214 from Pierce Biotechnology (Rockford, IL),

ii) for evaluation of mTORC1 signalling and autophagy: anti-S6 Ribosomal Protein (#2217), anti-Phospho-S6 Ribosomal Protein Ser235/236 (#2211), anti-LC3B (#2775), from Cell Signaling Technology (Danvers, MA), anti-Phospho-S6 Ribosomal anti-p62 (GP62-C) from Progen Biotechnik (Heidelberg, Germany),

iii) as loading controls: anti-GAPDH ((#32233) from Santa Cruz Biotechnology (Santa Cruz, CA), and anti-beta-Actin (#A5316) from Sigma-Aldrich (Saint Louis, MO).

Statistics

Statistical analysis was performed using IBM® SPSS® Statistics Version 19. Biochemical data of tau Western blots was subjected to unpaired T-tests and T-tests adjusted for unequal variances (Welch-Test), yielding both similar results. Holm-Bonferroni corrections were applied. Biochemical data of p62 and LC3-levels was analyzed by ANOVA. Stereological samples of vehicle and rapamycin treated mice were stained in parallel. Accordingly, the pairwise reduction of Gallyas or AT8 positive counts was analysed using one-sample T-tests per brain region. Significant p-values adjusted for multiple comparisons by the Holm-Bonferroni method are reported and outlined in all figures as follows: *=$p<0.05$, **=$p<0.01$, ***p=<0.001. The mean and SD is indicated in all figures.

1. Mueller DM, Rentsch KM (2010) Sensitive quantification of sirolimus and everolimus by LC-MS/MS with online sample cleanup. J Chromatogr B Analyt Technol Biomed Life Sci 878: 1007-1012.
2. Goedert M, Spillantini MG, Jakes R, Rutherford D, Crowther RA (1989) Multiple isoforms of human microtubule-associated protein tau: sequences and localization in neurofibrillary tangles of Alzheimer's disease. Neuron 3: 519-526.
3. Mawal-Dewan M, Henley J, Van de Voorde A, Trojanowski JQ, Lee VM (1994) The phosphorylation state of tau in the developing rat brain is regulated by phosphoprotein phosphatases. J Biol Chem 269: 30981-30987.
4. Forman MS, Lal D, Zhang B, Dabir DV, Swanson E, et al. (2005) Transgenic mouse model of tau pathology in astrocytes leading to nervous system degeneration. J Neurosci 25: 3539-3550.

Publication N°3

Stimulation of autophagy reduces neurodegeneration in a mouse model of human tauopathy

Véronique Schaeffer, Isabelle Lavenir, **Sefika Ozcelik**, Markus Tolnay, David T. Winkler and Michel Goedert

Brain 2012 Jul;135(Pt 7):2169-77

doi:10.1093/brain/aws143 Brain 2012: 135; 2169–2177 | 2169

BRAIN
A JOURNAL OF NEUROLOGY

Stimulation of autophagy reduces neurodegeneration in a mouse model of human tauopathy

Véronique Schaeffer,[1] Isabelle Lavenir,[1] Sefika Ozcelik,[2,3] Markus Tolnay,[3] David T. Winkler[2,3] and Michel Goedert[1]

1 MRC Laboratory of Molecular Biology, Cambridge CB2 0QH, UK
2 Department of Neurology, University Hospital Basel, CH-4031 Basel, Switzerland
3 Institute of Pathology, University Hospital Basel, CH-4031 Basel, Switzerland

Correspondence to: Michel Goedert,
Medical Research Council Laboratory of Molecular Biology,
Hills Road, Cambridge CB2 0QH,
UK
E-mail: mg@mrc-lmb.cam.ac.uk

The accumulation of insoluble proteins is a pathological hallmark of several neurodegenerative disorders. Tauopathies are caused by the dysfunction and aggregation of tau protein and an impairment of cellular protein degradation pathways may contribute to their pathogenesis. Thus, a deficiency in autophagy can cause neurodegeneration, while activation of autophagy is protective against some proteinopathies. Little is known about the role of autophagy in animal models of human tauopathy. In the present report, we assessed the effects of autophagy stimulation by trehalose in a transgenic mouse model of tauopathy, the human mutant P301S tau mouse, using biochemical and immunohistochemical analyses. Neuronal survival was evaluated by stereology. Autophagy was activated in the brain, where the number of neurons containing tau inclusions was significantly reduced, as was the amount of insoluble tau protein. This reduction in tau aggregates was associated with improved neuronal survival in the cerebral cortex and the brainstem. We also observed a decrease of p62 protein, suggesting that it may contribute to the removal of tau inclusions. Trehalose failed to activate autophagy in the spinal cord, where it had no impact on the level of sarkosyl-insoluble tau. Accordingly, trehalose had no effect on the motor impairment of human mutant P301S tau transgenic mice. Our findings provide direct evidence in favour of the degradation of tau aggregates by autophagy. Activation of autophagy may be worth investigating in the context of therapies for human tauopathies.

Keywords: autophagy; neurodegenerative disorders; neuroprotection; protein aggregation; tau
Abbreviation: LC3 = microtubule-associated protein light chain 3

Introduction

Most neurodegenerative diseases are characterized by the accumulation of misfolded proteins. Thus, α-synuclein aggregates in Parkinson's disease and other synucleinopathies, TDP-43 (TAR DNA-binding protein 43) in TDP-43 proteinopathies, huntingtin in Huntington's disease and both β-amyloid and tau in Alzheimer's disease (Goedert *et al.*, 2010). Filaments made of hyperphosphorylated tau protein are a good predictor of the cognitive state in Alzheimer's disease, because a negative correlation has been described between the number of neurofibrillary tangles, and the Mini-Mental score (Giannakopoulos *et al.*, 2003).

Received January 13, 2012. Revised March 19, 2012. Accepted April 20, 2012. Advance Access publication June 10, 2012

Tau deposits also constitute the defining pathological hallmark of several other diseases, including progressive supranuclear palsy, corticobasal degeneration, Pick's disease and frontotemporal dementia and parkinsonism linked to chromosome 17 (Goedert and Jakes, 2005; Goedert and Spillantini, 2011). Since filament assembly is a concentration-dependent process, a reduction in the production and/or increased clearance of tau are potential targets.

In eukaryotic cells, there are two major systems responsible for the degradation of cytoplasmic proteins: the ubiquitin–proteasome system and the autophagy–lysosome pathway (Goldberg, 2003). The accumulation of ubiquitinated tau in intracellular filamentous inclusions suggests a possible impairment of tau degradation by the ubiquitin–proteasome system and/or the autophagy–lysosome pathway. Indeed, inactivation of the ubiquitin–proteasome system or the autophagy–lysosome pathway has been reported to lead to neurodegeneration associated with the presence of ubiquitinated aggregates (Hara *et al.*, 2006; Komatsu *et al.*, 2006; Bedford *et al.*, 2008; Riley *et al.*, 2010). Particularly, ubiquitin–proteasome system or autophagy–lysosome pathway inhibition induces the accumulation of tau (Blard *et al.*, 2006; Ramesh Babu *et al.*, 2008; Liu *et al.*, 2009; Lee *et al.*, 2010). Moreover, accumulation of autophagic vacuoles has been observed in Alzheimer's disease brain and in a mouse model of tauopathy (Lin *et al.*, 2003; Nixon *et al.*, 2005), suggesting a possible disturbance of lysosomal proteolysis in tauopathy. Macroautophagy (hereafter referred to as autophagy) is the major form of autophagy. Although it is known that the suppression of autophagy causes neurodegeneration (Hara *et al.*, 2006), relatively little is known about the role of autophagy in animal models of human tauopathy. In the triple transgenic mouse model of Alzheimer's disease and in a mouse model expressing human mutant tau on a null background for the E3 ubiquitin ligase parkin, stimulation of autophagy promoted the degradation of insoluble tau (Caccamo *et al.*, 2011; Majumder *et al.*, 2011; Rodriguez-Navarro *et al.*, 2011). However, these studies did not allow one to determine whether the effects of autophagy stimulation were due to a direct interaction between the autophagic machinery and tau or whether they were indirect. To date, there has been no report of the effect of increased autophagy in a mouse model of human tauopathy. We therefore administered trehalose, a mammalian target of rapamycin (mTOR)-independent activator of autophagy (Noda and Ohsumi, 1998; Sarkar *et al.*, 2007*a*), to mice transgenic for human mutant P301S tau.

Materials and methods

Antibodies

We used phosphorylation-independent anti-tau antibodies BR133 and BR134 which recognize both murine and human tau isoforms. Phosphorylation-dependent anti-tau antibodies AT8 and AT100 (Innogenetics) were also used. AT8 recognizes tau protein phosphorylated at S202 and T205 (Goedert *et al.*, 1995), whereas AT100 detects tau phosphorylated at T212, S214 and T217 (Yoshida and Goedert, 2006). Autophagy was assessed using an antibody against microtubule-associated protein light chain 3 (LC3) (Novus Biologicals). We also used an antibody against p62/SQSTM1 (Santa Cruz Biotechnology). To normalize protein levels, an anti-GAPDH (Millipore, Ltd.) antibody was used.

Animals and treatment

Homozygous human P301S tau transgenic mice (Allen *et al.*, 2002) and age-matched wild-type C57BL/6 mice were used ($n = 6$ per group for western blot analysis; $n = 3$ per group for immunohistochemistry and stereology experiments). From weaning onwards, the animals were treated with 2% trehalose or 2% sucrose, which were used as the control. A separate group received normal drinking water (no treatment). The water solutions were changed twice weekly. Animals were checked daily and the quantity of water drunk and the animals' weights were assessed twice a week. P301S tau transgenic mice develop motor deficits at ~3–4 months of age, as shown using Rotarod (Scattoni *et al.*, 2010). We routinely evaluated these deficits by visual inspection, as they form in a stereotypical manner consisting of an unstable gait followed by general stiffness and hindlimb paralysis. Furthermore, at 3–4 months of age, the human P301S tau mice are unable to extend their hindlimbs when lifted by the tail (Allen *et al.*, 2002). In this study, we assessed the motor deficits by visual inspection and used the time when all the animals had developed hindleg stiffness and were unable to extend their hindlimbs when suspended by the tail as the endpoint (20 weeks of age).

Tissue extraction

To extract sarkosyl-insoluble proteins from brain and spinal cord, frozen tissues were weighed and homogenized in cold extraction buffer [10 mM Tris–HCl, pH 7.4, 800 mM NaCl, 1 mM EGTA, 0.1 M phenylmethylsulphonyl fluoride, 10% sucrose and one tablet of complete protease inhibitor cocktail (Roche)]. The homogenates were spun at 6000*g* for 20 min and the supernatants incubated with 1% sarkosyl for 1 h at room temperature. After a 1 h centrifugation at 80 000 *g*, the supernatants were discarded and the pellets resuspended in 50 mM Tris–HCl, pH 7.4 (300 µl/*g* tissue). For investigation of soluble tau, brains and spinal cords were homogenized in 25 mM Tris–HCl, pH 7.4, 150 mM NaCl, 1 mM EDTA, 1 mM EGTA, 1 mM phenylmethylsulphonyl fluoride and one tablet of complete protease inhibitor cocktail. Samples were centrifuged at 80 000 *g* for 15 min. The resulting supernatant constituted the soluble fraction. The samples were analysed by SDS-PAGE.

Immunoblot analysis

After SDS-PAGE, the gels were blotted for 1 h at room temperature onto polyvinylidene difluoride membranes (Millipore). The membranes were blocked for 1 h at room temperature in 0.1 M phosphate buffer, pH 7.4, 0.2% Tween 20 and 5% milk, followed by an overnight incubation with the primary antibody in blocking buffer. Membranes were then washed in 0.1 M phosphate buffer, pH 7.4, 0.2% Tween 20 and incubated for 1 h at room temperature with peroxidase-conjugated secondary antibody (Pierce) in blocking solution. After washing, the blots were developed using enhanced chemiluminescence (Amersham Biosciences).

Quantification of proteins

Band intensities were quantified (Chemidoc™ XRS and Quantity One® software, Bio-Rad) and the amounts of soluble proteins normalized with respect to GAPDH. Insoluble tau was normalized relative to the tissue weight. Data were expressed as means ± SEM. Statistical analysis was performed using a one-way ANOVA test followed by Tukey's *post hoc* comparisons (Prism, GraphPad Software, Inc.).

Immunohistochemistry

Mice were perfused transcardially with 4% paraformaldehyde in 0.1 M phosphate buffer, pH 7.4. Brains and spinal cords were dissected and post-fixed overnight at 4°C, followed by cryoprotection in PBS containing 30% sucrose for at least 24 h. Serial sagittal brain sections (30 μm) were cut on a Leica SM2400 microtome (Leica Microsystems) and stored at 4°C in PBS containing 0.1% sodium azide. For fluorescence labelling, sections were permeabilized for 5 min with cold PBS containing 0.5% Triton X-100 and washed three times with PBS, 0.1% Triton X-100 (PBST). After 2 h blocking at room temperature with PBST containing 3% bovine serum albumin, sections were incubated with the primary antibodies in blocking solution for 24 h at 4°C. This was followed by three washes and a 2 h incubation at room temperature with Alexa Fluor® 488 (Molecular Probes) or Cy5 (Abcam) secondary antibodies in blocking solution. After washing and DAPI (4,6-diamidino-2-phenylindole) staining, the sections were mounted using Vectashield mounting medium (Vector Laboratories). They were analysed using a Leica DMRB fluorescence microscope (Leica) or a Radiance 2100 confocal microscope (Bio-Rad). Images were taken using a Sharp 2000 laser (Zeiss Bio-Rad) and were typically 512 × 512 pixels. Staining for neuronal nuclei (NeuN; Chemicon) (Mullen *et al.*, 1992; Wolf *et al.*, 1996; Lind *et al.*, 2005) and tau phosphorylated at the AT100 epitope were carried out in brains of wild-type and transgenic mice using immunoperoxidase (Vectastain ABC kit, Vector Laboratories). Endogenous peroxidase was quenched for 15 min with 3% H_2O_2 in distilled water. After washing, sections were blocked for 1 h with normal horse serum in PBST and incubated overnight with the anti-NeuN antibody (1:500) in blocking solution at 4°C. After three rinses with PBST, sections were incubated with a biotin-conjugated anti-mouse antibody for 2 h at room temperature. Next, the avidin–biotin-conjugated complex was applied for a further 2 h. Finally, the antigen was visualized using the Vector® VIP substrate kit (Vector Laboratories). Sections were mounted on SuperFrost® glass slides (VWR international) and dehydrated using a series of ascending ethanol solutions (70, 95 and 100%) and xylene.

Stereology

The Stereo Investigator 9 (MBF Bioscience) was used to quantify the number of NeuN-positive cells. Sections through the brain were sampled in a systematic random manner using 1:12 series for quantification of NeuN-positive and AT100-positive neurons. The thickness of each section was determined using the Stereo Investigator 9 software. For a given section, the outline of the region of interest was traced under a ×10 objective and the enclosed area calculated by the software. Sections within the highlighted area were then sampled at random and cells counted under the ×40 objective to determine the total number of immunoreactive cells. Statistical analyses were performed using a one-way ANOVA test followed by Tukey's *post hoc* comparisons (Prism, GraphPad Software, Inc.).

Results

Animal health

Water consumption of the three groups (no treatment, sucrose-treated and trehalose-treated) was similar. Sucrose and trehalose had no impact on the animals' weights or coat aspects, suggesting that the health of the mice was similar among the three groups. The human P301S tau mice were sacrificed at 20 weeks of age, when they developed an unstable gait and motor abnormalities, which is typical of homozygous transgenic mice (Allen *et al.*, 2002). The development of motor deficits was not significantly different between treated and non-treated human P301S tau transgenic mice. Thus, untreated mice developed the first motor deficits at 19 ± 0.19 weeks of age, which was not significantly different from the ages at which they appeared in sucrose-treated (18.8 ± 0.31 weeks) and trehalose-treated (19.25 ± 0.23 weeks) mice (Supplementary Fig. 1).

Effects of trehalose on autophagy activation

To investigate autophagy activation, we measured the conversion of LC3-I into LC3-II, a marker of autophagic vacuole formation (Kabeya *et al.*, 2000; Mizushima *et al.*, 2004; Tanida *et al.*, 2004). We observed the conversion of 17.5 ± 2.3% LC3-I into LC3-II in the brains of trehalose-treated mice, while no detectable LC3-I conversion was seen in untreated or sucrose-treated mice (Fig. 1A). Unexpectedly, trehalose had no effect on LC3-I conversion in the spinal cord (Fig. 1B). We therefore focused our study on the brain. Immunohistochemistry of brain sections from mice transgenic for human mutant P301S tau showed the presence of LC3 puncta in trehalose-treated mice (Fig. 1E). The punctate distribution of LC3 was absent from control groups (Fig. 1C and D). In trehalose-treated transgenic mice, AT100-positive tau aggregates were also immunoreactive for LC3, indicating the co-localization of autophagic vacuoles and tau aggregates (arrows, Fig. 1F–H).

Effects of trehalose on tau pathology and neuronal survival

Total soluble tau and soluble tau phosphorylated at the AT8 epitope were not affected by trehalose treatment (Supplementary Fig. 2). In contrast, quantification of sarkosyl-insoluble tau in the brain indicated that trehalose decreased the amount of insoluble tau compared with untreated controls (−53%, $P < 0.01$) or to controls treated with sucrose (−46%, $P < 0.05$) (Fig. 2A). Trehalose treatment had no effect on the amount of sarkosyl-insoluble tau in the spinal cord (Fig. 2B). Immunofluorescence staining for anti-tau antibody AT100 showed a drastic reduction in the number of positive cells in layers I–III of the cerebral cortex (−66.5% compared with untreated animals, $P < 0.01$; −80.1% compared with sucrose-treated mice, $P < 0.001$) (Fig. 2C–F) and in the brainstem, particularly the pontine nucleus

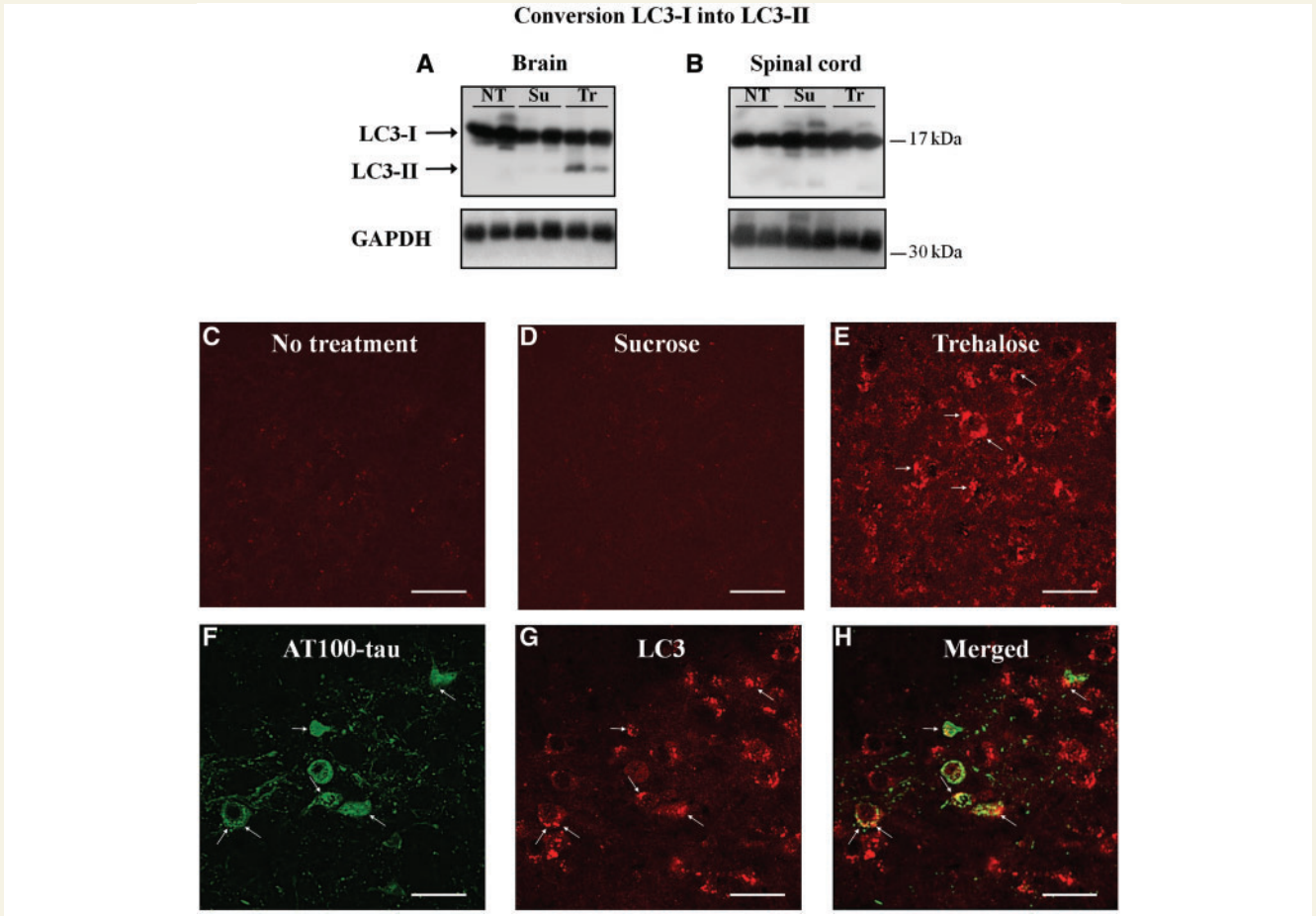

Figure 1 Conversion of LC3-I into LC3-II was assessed by western blotting in the spinal cord (**A**) and the brain (**B**) of mice transgenic for human P301S tau. LC3-II staining was only present in brain where autophagic vacuoles were observed in trehalose-treated mice (arrow in **E**). Autophagic vacuoles were not present in the brains of non-treated (**C**) or sucrose-treated (**D**) mice. (**F–H**) Confocal analysis indicated that AT100-positive tau inclusions (**F**) were also immunoreactive for LC3-II (**G**), suggesting the presence of tau inclusions in autophagic vacuoles in trehalose-treated transgenic mice (**H**). NT = no treatment; Su = sucrose-treated; Tr = trehalose-treated. Scale bar = 20 μm.

(−75% compared with untreated animals, $P < 0.001$; −58.6% compared with sucrose-treated mice, $P < 0.01$) (Fig. 2G–J). Nerve cell numbers were counted in layers I–III of the cerebral cortex and in the pontine nucleus. The number of neurons in layers I–III was higher in trehalose-treated P301S tau mice than in animals that received either no treatment (+55.5%, $P < 0.05$) or were treated with sucrose (+59.6%, $P < 0.05$) (Fig. 3A). The number of neurons in trehalose-treated mice and in untreated wild-type animals was not significantly different (Fig. 3A). In the pontine nucleus, the number of neurons increased in trehalose-treated animals compared with untreated (+79.2%, $P < 0.01$) and sucrose-treated controls (+61.6%, $P < 0.05$) (Fig. 3B). The number of NeuN-positive cells in the pontine nucleus was similar in trehalose-treated P301S tau mice and in wild-type controls (Fig. 3B).

Effects of trehalose on p62/SQSTM1

Immunohistochemistry revealed the co-localization of p62/SQSTM1 and AT100-positive tau aggregates in P301S tau transgenic mice (Fig. 4D–F), while no co-staining was observed in wild-type controls (Fig. 4A–C). We assessed the levels of p62/SQSTM1 in the brains of wild-type and transgenic P301S tau mice subjected to the different treatments. We observed a reduction in p62/SQSTM1 levels in mice treated with trehalose compared with mice that received either no treatment (−52.1%, $P < 0.05$) or sucrose (−46.7%, $P < 0.05$) (Fig. 4G). No significant difference was detected between wild-type controls and P301S tau transgenic mice (Fig. 4G).

Discussion

The assembly of normally soluble proteins into amyloid-like fibrils is a pathological hallmark of several neurodegenerative disorders, with tauopathies being the most common (Goedert *et al.*, 2010). Herein, we report on the effects of stimulation of autophagy on tau inclusions and nerve cell survival in a mouse line transgenic for human mutant P301S tau. Trehalose activated autophagy in the brain, as shown by the increased formation of LC3-II, and reduced

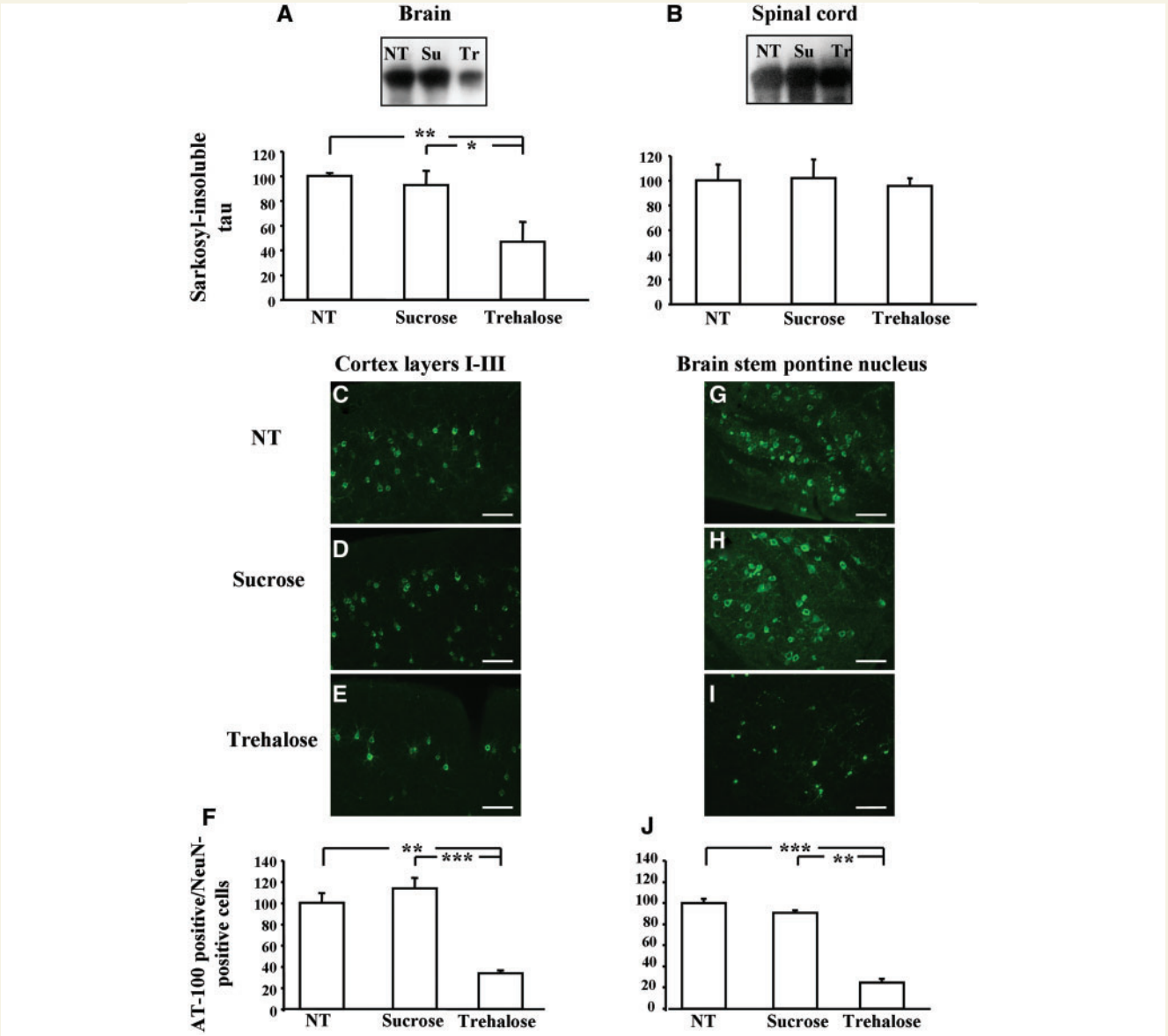

Figure 2 Sarkosyl-insoluble tau was decreased in the brain of trehalose-treated mice compared with non-treated or sucrose-treated animals (**A**), while trehalose treatment had no effect on sarkosyl-insoluble tau in the spinal cord (**B**). In trehalose-treated mice, the number of nerve cells with AT100-positive inclusions was drastically reduced in layers I–III of the cerebral cortex (**C–F**) and in the pontine nucleus of the brainstem (**G–J**). NT = no treatment; Su = sucrose-treated; Tr = trehalose-treated. $*P < 0.05$, $**P < 0.01$ and $***P < 0.001$.

the level of sarkosyl-insoluble tau. However, it did not stimulate autophagy in the spinal cord and consequently had no effect on the level of insoluble tau. The mechanism of action of trehalose is not completely understood, but it is believed to activate autophagy in an mTOR-independent manner (Sarkar *et al.*, 2007*a*). These findings suggest that autophagic pathways may differ between brain and spinal cord. The absence of a detectable effect of trehalose in the spinal cord probably accounted for the persistence of a pathological motor phenotype in treated P301S tau transgenic mice. We cannot exclude that a detailed behavioural assessment could have revealed subtle differences between treated and non-treated mice. However, the motor deficit characteristic of the human P301S tau transgenic mice probably results from the degeneration of spinal cord motor neurons, consequent to the development of a toxic filamentous tau pathology (Allen *et al.*, 2002; Delobel *et al.*, 2008), and possibly the sequestration of proteins important for motor behaviour. As tau pathology in the spinal cord was unchanged after trehalose administration, an improvement in motor function was unlikely. The reasons underlying our inability to activate autophagy in the spinal cord remain to be determined. They could be related to a less efficient delivery of trehalose to the spinal cord, although it has been shown that the blood–spinal cord barrier is more permeable to tracers and cytokines than the blood–brain barrier (Prockop *et al.*, 1995; Pan *et al.*, 1997). We hope that future experiments will allow us to overcome this limitation.

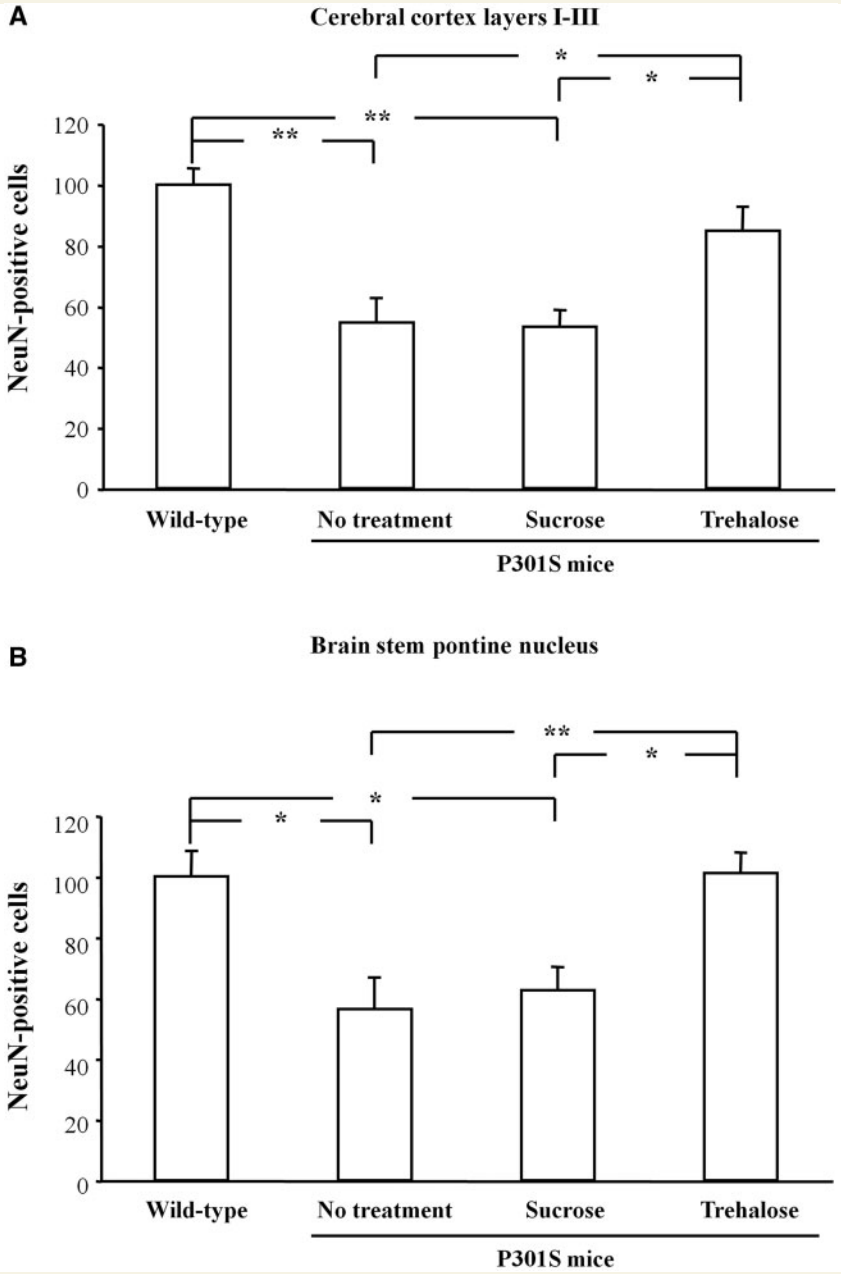

Figure 3 Nerve cell numbers were assessed using stereology. Trehalose treatment increased the number of neurons in layers I–III of the cerebral cortex (**A**) and in the pontine nucleus of the brainstem (**B**). $*P < 0.05$ and $**P < 0.01$.

In the brains of trehalose-treated mice, we observed a decrease in sarkosyl-insoluble tau and the number of nerve cells with tau inclusions. Besides its ability to activate autophagy, trehalose has also been reported to act as a protective chaperone in a murine model of Huntington's disease (Tanaka *et al.*, 2004). However, the reduction in tau inclusions in our mouse line was probably due to the degradation of tau aggregates by trehalose-induced autophagy. Indeed, we observed a decrease in tau inclusions only in regions where autophagy was activated. Moreover, we showed co-localization between autophagic vacuoles and tau inclusions, suggesting that tau aggregates were engulfed by autophagosomes before degradation. Sucrose, a chemical chaperone, which has been shown to reduce the conversion of the cellular prion protein to its protease-resistant form (DebBurman *et al.*, 1997), failed to reduce tau aggregates in the human mutant P301S tau transgenic mice, confirming that the effect of trehalose on tau aggregates was mediated through an increase in autophagy.

Altogether, our results indicate that the *in vivo* stimulation of autophagy reduced the amount of tau aggregates and improved nerve cell survival. A role for autophagy in the clearance of protein aggregates has been suggested for a number of proteins, including β-amyloid, α-synuclein, ataxin-3, prion protein and huntingtin (Webb *et al.*, 2003; Sarkar *et al.*, 2007*b*; Pickford *et al.*, 2008;

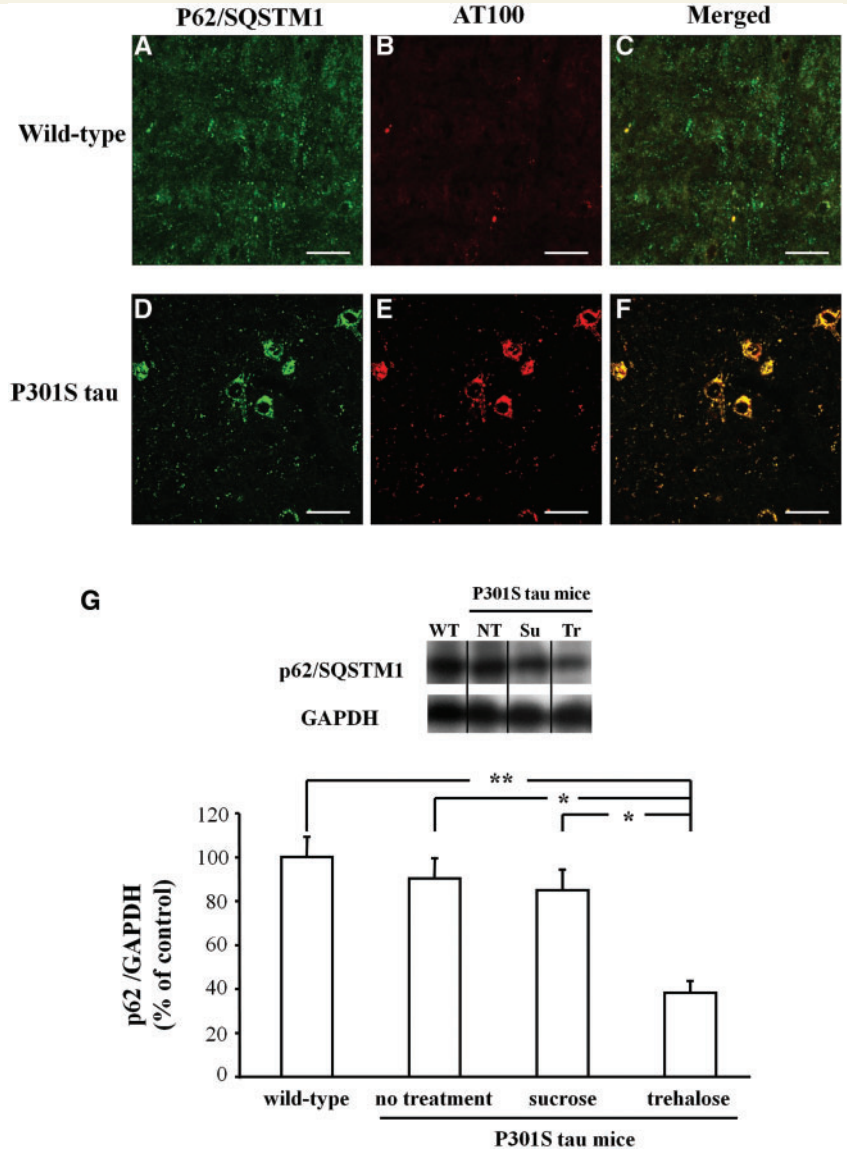

Figure 4 Immunohistochemistry for p62/SQSTM1 (**A** and **D**) and assembled tau (AT100; **B** and **E**) showed co-localization in P301S tau transgenic mice (**F**) but not in wild-type animals (**C**). Scale bar = 20 μm. (**G**) Western blot of p62/SQSTM1 levels in the brains of wild-type controls and mice transgenic for human mutant P301S tau that received either no treatment or were given sucrose or trehalose. The amount of p62/SQSTM1 signal is shown normalized with respect to GAPDH. $*P < 0.05$ and $**P < 0.01$.

Heiseke *et al.*, 2009; Casarejos *et al.*, 2011; Majumder *et al.*, 2011; Riedel *et al.*, 2011; Spilman *et al.*, 2011). Activation of autophagy has also shown protective effects in mouse and fly models of tauopathy (Berger *et al.*, 2006; Caccamo *et al.*, 2011; Majumder *et al.*, 2011; Rodriguez-Navarro *et al.*, 2011). However, in mice, tau was not the only engineered protein. In one study, the mice overexpressed human mutant tau and carried a deletion of the gene encoding parkin (Rodriguez-Navarro *et al.*, 2011), a potential mediator of autophagy (Olzmann *et al.*, 2007; Chin *et al.*, 2011). Therefore, not surprisingly, restoration of autophagic activity decreased the number of tau aggregates and improved cell survival. In separate studies, autophagy was activated in triple transgenic mice exhibiting tau and β-amyloid pathologies (Caccamo *et al.*, 2011; Majumder *et al.*, 2011). It is well established that β-amyloid can promote tau pathology in some brain regions (Götz *et al.*, 2001; Lewis *et al.*, 2001; Oddo *et al.*, 2003, 2004). However, direct evidence for the relevance of autophagy in modulating tau pathology was missing. We now show that the activation of autophagy markedly reduced the number of tau aggregates and nerve cell loss in a mouse model of human tauopathy.

We also investigated p62/SQSTM1 expression in wild-type and P301S tau transgenic mice. p62/SQSTM1 is a protein that acts as a receptor for selective autophagy, mainly because of its ability to bind both ubiquitin and LC3 (Pankiv *et al.*, 2007; Lamark *et al.*, 2009). It has previously been implicated in the degradation of protein inclusions (Bjorkoy *et al.*, 2006; Watanabe and Tanaka, 2011) and has been found in tau inclusions in human

neurodegenerative diseases (Kuusisto *et al.*, 2001, 2002; Zatloukal *et al.*, 2002). We now show co-localization of p62/SQSTM1 with tau inclusions in P301S tau transgenic mice, consistent with the human pathology. In addition, we observed a decrease in p62/SQSTM1 levels in trehalose-treated mice, suggesting that p62/SQSTM1 may be an adaptor molecule for tau inclusions before their degradation by autophagy. Although the majority of tau filaments in P301S tau transgenic are not ubiquitinated (Allen *et al.*, 2002), p62/SQSTM1 may nonetheless be involved, as it has been shown to play a role in the autophagic degradation of non-ubiquitinated protein aggregates (Watanabe and Tanaka, 2011). The levels of p62/SQSTM1 were similar between P301S tau transgenic mice and wild-type controls, indicating that p62/SQSTM1 synthesis and basal autophagy were not affected in the transgenic mice. In conclusion, we show that activation of autophagy in mice transgenic for human mutant P301S tau decreased the number of tau inclusions and increased nerve cell survival in cerebral cortex and brainstem.

Acknowledgements

We thank Angela Middleton and Claire Knox for their help with mice and the Biomedical Services (MRC Laboratory of Molecular Biology) for assistance.

Funding

This work was supported by the UK Medical Research Council (MRC file reference number U105184291) and, in part, by Alzheimer's Research UK. M.T. and D.T.W. are supported by the Swiss National Science Foundation (310030_135214 to M.T. and 32323B_123812 to D.W.T.).

Supplementary material

Supplementary material is available at *Brain* online.

References

Allen B, Ingram E, Takao M, Smith MJ, Jakes R, Virdee K, et al. Abundant tau filaments and nonapoptotic neurodegeneration in transgenic mice expressing human P301S tau protein. J Neurosci 2002; 22: 9340–51.

Bedford L, Hay D, Devoy A, Paine S, Powe DG, Seth R, et al. Depletion of 26S proteasomes in mouse brain neurons causes neurodegeneration and Lewy-like inclusions resembling human pale bodies. J Neurosci 2008; 28: 8189–98.

Berger Z, Ravikumar B, Menzies FM, Oroz LG, Underwood BR, Pangalos MN, et al. Rapamycin alleviates toxicity of different aggregate-prone proteins. Hum Mol Genet 2006; 15: 433—42.

Bjorkoy G, Lamark T, Johansen T. p62/SQSTM1: a missing link between protein aggregates and the autophagy machinery. Autophagy 2006; 2: 138–9.

Blard O, Frebourg T, Campion D, Lecourtois M. Inhibition of proteasome and Shaggy/Glycogen synthase kinase-3β kinase prevents clearance of phosphorylated tau in *Drosophila*. J Neurosci Res 2006; 84: 1107–15.

Caccamo A, Majumder S, Richardson A, Strong R, Oddo S. Molecular interplay between mammalian target of rapamycin (mTOR), amyloid-β, and Tau: effects on cognitive impairments. J Biol Chem 2011; 285: 13107–20.

Casarejos MJ, Solano RM, Gomez A, Perucho J, de Yebenes JG, Mena MA. The accumulation of neurotoxic proteins, induced by proteasome inhibition, is reverted by trehalose, an enhancer of autophagy, in human neuroblastoma cells. Neurochem Int 2011; 58: 512–20.

Chin LS, Olzmann JA, Li L. Parkin-mediated ubiquitin signalling in aggresome formation and autophagy. Biochem Soc Trans 2011; 38: 144–9.

DebBurman SK, Raymond GJ, Caughey B, Lindquist S. Chaperone-supervised conversion of prion protein to its protease-resistant form. Proc Natl Acad Sci USA 1997; 94: 13938–43.

Delobel P, Lavenir I, Fraser G, Ingram E, Holzer M, Ghetti B, et al. Analysis of tau phosphorylation and truncation in a mouse model of human tauopathy. Am J Pathol 2008; 172: 123–31.

Giannakopoulos P, Herrmann FR, Bussiere T, Bouras C, Kovari E, Perl DP, et al. Tangle and neuron numbers, but not amyloid load, predict cognitive status in Alzheimer's disease. Neurology 2003; 60: 1495–500.

Goedert M, Clavaguera F, Tolnay M. The propagation of prion-like protein inclusions in neurodegenerative diseases. Trends Neurosci 2010; 33: 317–25.

Goedert M, Jakes R. Mutations causing neurodegenerative tauopathies. Biochim Biophys Acta 2005; 1739: 240–50.

Goedert M, Jakes R, Vanmechelen E. Monoclonal antibody AT8 recognises tau protein phosphorylated at both serine 202 and threonine 205. Neurosci Lett 1995; 189: 167–9.

Goedert M, Spillantini MG. Pathogenesis of the Tauopathies. J Mol Neurosci 2011; 45: 7.

Goldberg AL. Protein degradation and protection against misfolded or damaged proteins. Nature 2003; 426: 895–9.

Götz J, Chen F, van Dorpe J, Nitsch RM. Formation of neurofibrillary tangles in P301L tau transgenic mice induced by Abeta 42 fibrils. Science 2001; 293: 1491–5.

Hara T, Nakamura K, Matsui M, Yamamoto A, Nakahara Y, Suzuki-Migishima R, et al. Suppression of basal autophagy in neural cells causes neurodegenerative disease in mice. Nature 2006; 441: 885–9.

Heiseke A, Aguib Y, Riemer C, Baier M, Schatzl HM. Lithium induces clearance of protease resistant prion protein in prion-infected cells by induction of autophagy. J Neurochem 2009; 109: 25–34.

Kabeya Y, Mizushima N, Ueno T, Yamamoto A, Kirisako T, Noda T, et al. LC3, a mammalian homologue of yeast Apg8p, is localized in autophagosome membranes after processing. EMBO J 2000; 19: 5720–8.

Komatsu M, Waguri S, Chiba T, Murata S, Iwata J, Tanida I, et al. Loss of autophagy in the central nervous system causes neurodegeneration in mice. Nature 2006; 441: 880–4.

Kuusisto E, Salminen A, Alafuzoff I. Ubiquitin-binding protein p62 is present in neuronal and glial inclusions in human tauopathies and synucleinopathies. Neuroreport 2001; 12: 2085–90.

Kuusisto E, Salminen A, Alafuzoff I. Early accumulation of p62 in neurofibrillary tangles in Alzheimer's disease: possible role in tangle formation. Neuropathol Appl Neurobiol 2002; 28: 228–37.

Lamark T, Kirkin V, Dikic I, Johansen T. NBR1 and p62 as cargo receptors for selective autophagy of ubiquitinated targets. Cell Cycle 2009; 8: 1986–90.

Lee BH, Lee MJ, Park S, Oh DC, Elsasser S, Chen PC, et al. Enhancement of proteasome activity by a small-molecule inhibitor of USP14. Nature 2010; 467: 179–84.

Lewis J, Dickson DW, Lin WL, Chisholm L, Corral A, Jones G, et al. Enhanced neurofibrillary degeneration in transgenic mice expressing mutant tau and APP. Science 2001; 293: 1487–91.

Lin WL, Lewis J, Yen SH, Hutton M, Dickson DW. Ultrastructural neuronal pathology in transgenic mice expressing mutant (P301L) human tau. J Neurocytol 2003; 32: 1091–105.

Lind D, Franken S, Kappler J, Jankowski J, Schilling K. Characterization of the neuronal marker NeuN as a multiply phosphorylated antigen with discrete subcellular localization. J Neurosci Res 2005; 79: 295–302.

Liu YH, Wei W, Yin J, Liu GP, Wang Q, Cao FY, et al. Proteasome inhibition increases tau accumulation independent of phosphorylation. Neurobiol Aging 2009; 30: 1949–61.

Majumder S, Richardson A, Strong R, Oddo S. Inducing autophagy by rapamycin before, but not after, the formation of plaques and tangles ameliorates cognitive deficits. PLoS One 2011; 6: e25416.

Mizushima N, Yamamoto A, Matsui M, Yoshimori T, Ohsumi Y. *In vivo* analysis of autophagy in response to nutrient starvation using transgenic mice expressing a fluorescent autophagosome marker. Mol Biol Cell 2004; 15: 1101–11.

Mullen RJ, Buck CR, Smith AM. NeuN, a neuronal specific nuclear protein in vertebrates. Development 1992; 116: 201–11.

Nixon RA, Wegiel J, Kumar A, Yu WH, Peterhoff C, Cataldo A, et al. Extensive involvement of autophagy in Alzheimer disease: an immuno-electron microscopy study. J Neuropathol Exp Neurol 2005; 64: 113–22.

Noda T, Ohsumi Y. Tor, a phosphatidylinositol kinase homologue, controls autophagy in yeast. J Biol Chem 1998; 273: 3963–6.

Oddo S, Billings L, Kesslak JP, Cribbs DH, LaFerla FM. Aβ immunotherapy leads to clearance of early, but not late, hyperphosphorylated tau aggregates via the proteasome. Neuron 2004; 43: 321–32.

Oddo S, Caccamo A, Kitazawa M, Tseng BP, LaFerla FM. Amyloid deposition precedes tangle formation in a triple transgenic model of Alzheimer's disease. Neurobiol Aging 2003; 24: 1063–70.

Olzmann JA, Li L, Chudaev MV, Chen J, Perez FA, Palmiter RD, et al. Parkin-mediated K63-linked polyubiquitination targets misfolded DJ-1 to aggresomes via binding to HDAC6. J Cell Biol 2007; 178: 1025–38.

Pan W, Banks WA, Kastin AJ. Permeability of the blood-brain and blood-spinal cord barriers to interferons. J Neuroimmunol 1997; 76: 105–11.

Pankiv S, Clausen TH, Lamark T, Brech A, Bruun JA, Outzen H, et al. p62/SQSTM1 binds directly to Atg8/LC3 to facilitate degradation of ubiquitinated protein aggregates by autophagy. J Biol Chem 2007; 282: 24131–45.

Pickford F, Masliah E, Britschgi M, Lucin K, Narasimhan R, Jaeger PA, et al. The autophagy-related protein beclin 1 shows reduced expression in early Alzheimer disease and regulates amyloid beta accumulation in mice. J Clin Invest 2008; 118: 2190–9.

Prockop LD, Naidu KA, Binard JE, Ransohoff J. Selective permeability of [^{3}H]-D-mannitol and [^{14}C]-carboxyl-inulin across the blood-brain barrier and blood-spinal cord barrier in the rabbit. J Spinal Cord Med 1995; 18: 221–6.

Ramesh Babu J, Lamar Seibenhener M, Peng J, Strom AL, Kemppainen R, Cox N, et al. Genetic inactivation of p62 leads to accumulation of hyperphosphorylated tau and neurodegeneration. J Neurochem 2008; 106: 107–20.

Riedel M, Goldbaum O, Schwarz L, Schmitt S, Richter-Landsberg C. 17-AAG induces cytoplasmic α-synuclein aggregate clearance by induction of autophagy. PLoS One 2011; 5: e8753.

Riley BE, Kaiser SE, Shaler TA, Ng AC, Hara T, Hipp MS, et al. Ubiquitin accumulation in autophagy-deficient mice is dependent on the Nrf2-mediated stress response pathway: a potential role for protein aggregation in autophagic substrate selection. J Cell Biol 2010; 191: 537–52.

Rodriguez-Navarro JA, Rodriguez L, Casarejos MJ, Solano RM, Gomez A, Perucho J, et al. Trehalose ameliorates dopaminergic and tau pathology in parkin deleted/tau overexpressing mice through autophagy activation. Neurobiol Dis 2011; 39: 423–38.

Sarkar S, Davies JE, Huang Z, Tunnacliffe A, Rubinsztein DC. Trehalose, a novel mTOR-independent autophagy enhancer, accelerates the clearance of mutant huntingtin and α-synuclein. J Biol Chem 2007a; 282: 5641–52.

Sarkar S, Perlstein EO, Imarisio S, Pineau S, Cordenier A, Maglathlin RL, et al. Small molecules enhance autophagy and reduce toxicity in Huntington's disease models. Nat Chem Biol 2007b; 3: 331–8.

Scattoni ML, Gasparini L, Alleva E, Goedert M, Calamandrei G, Spillantini MG. Early behavioural markers of disease in P301S tau transgenic mice. Behav Brain Res 2010; 208: 250–7.

Spilman P, Podlutskaya N, Hart MJ, Debnath J, Gorostiza O, Bredesen D, et al. Inhibition of mTOR by rapamycin abolishes cognitive deficits and reduces amyloid-beta levels in a mouse model of Alzheimer's disease. PLoS One 2011; 5: e9979.

Tanaka M, Machida Y, Niu S, Ikeda T, Jana NR, Doi H, et al. Trehalose alleviates polyglutamine-mediated pathology in a mouse model of Huntington disease. Nat Med 2004; 10: 148–54.

Tanida I, Ueno T, Kominami E. LC3 conjugation system in mammalian autophagy. Int J Biochem Cell Biol 2004; 36: 2503–18.

Watanabe Y, Tanaka M. p62/SQSTM1 in autophagic clearance of a non-ubiquitylated substrate. J Cell Sci 2011; 124: 2692–701.

Webb JL, Ravikumar B, Atkins J, Skepper JN, Rubinsztein DC. α-Synuclein is degraded by both autophagy and the proteasome. J Biol Chem 2003; 278: 25009–13.

Wolf HK, Buslei R, Schmidt-Kastner R, Schmidt-Kastner PK, Pietsch T, Wiestler OD, et al. NeuN: a useful neuronal marker for diagnostic histopathology. J Histochem Cytochem 1996; 44: 1167–71.

Yoshida H, Goedert M. Sequential phosphorylation of tau protein by cAMP-dependent protein kinase and SAPK4/p38δ or JNK2 in the presence of heparin generates the AT100 epitope. J Neurochem 2006; 99: 154–64.

Zatloukal K, Stumptner C, Fuchsbichler A, Heid H, Schnoelzer M, Kenner L, et al. p62 is a common component of cytoplasmic inclusions in protein aggregation diseases. Am J Pathol 2002; 160: 255–63.

DISCUSSION *and* PERSPECTIVES

In 2011, about 107'500 people living in Switzerland were suffering of dementia including Alzheimer's disease (AD) [6]. Unfortunately, this number will increase to approximately 200'000 by 2030 and 300'000 by 2050, according to the Swiss Alzheimer Association [6]. Nowadays, there is no curative treatment available for AD or other tauopathies, as pharmacological therapies are limited to symptomatic approaches. Although numerous research projects are currently trying to unravel the pathomechanisms leading to dementia, the exact molecular and cellular events associated to their onset and progression are still only partly understood. While the attention had been focused for a long time on the amyloid-ß peptide, tau is now recognized as an equal key element of the pathogenesis and progression of AD.

During my thesis, the development of novel mouse models allowed to better understand the pathomechanisms at play in tauopathies. These studies established that tau fragmentation, which likely happens at the pretangle stage and aggravates the propensity of tau protein to aggregate, might constitute a major, early event in neuronal dysfunction. This toxicity and the associated alterations of the nervous system were reversed when the expression of the tau fragment was halted, hence shedding light on new, promising therapeutic strategies to counter the progression of the disease. As described for other neurodegenerative pathologies, pharmacological treatments promoting the induction of autophagy also showed their efficiency to improve tauopathies in transgenic mouse models.

These data open novel avenues regarding the pathogenesis and potential therapeutic approaches for dementia, but also underline important questions that remain to be answered in follow up studies.

From mouse models to the identification of the early molecular mechanisms involved in the onset and progression of tauopathies

What is toxic in tau protein? What do we learn from a novel mouse model for tauopathies?

One of the hallmarks of AD is the presence of extracellular accumulation of amyloid-ß (Aß) peptide, a cleavage product of the APP protein, which constitutes the major component of the amyloid fibrils forming senile plaques. Aß activates multiple deleterious events leading to altered neuronal homeostasis, such as mitochondria dysfunction, increased oxidative stress and hyperphosphorylation of tau protein [232, 233]. The hypothesis of the "amyloid cascade" as the central, determining event of AD pathogenesis was originaly based on *in vitro* and *in vivo* studies showing the toxicity of Aß peptide, on findings in trisomie 21 patients and then

supported by the discovery of genetic mutations in the *APP, PS1 and PS2* genes in familial AD [129]. Recent reports further indicate that this amyloid cascade would be triggered by the oligomeric and fibrillary forms of Aß, which constitute the most toxic forms of the peptide [234].

The exact role of tau protein in the onset and progression of AD is still unknown. Its involvement in neuronal dysfunction is underlined by its accumulation, in the absence of extracellular Aß deposition, in the brain of patients suffering from neurodegenerative diseases other than AD [235]. Furthermore, diverse mutations in the *MAPT* gene, encoding tau protein, were associated with FTDP-17 [163, 236, 237]. Reproduction of these mutations lead to the generation of different transgenic animal models, which mimic various aspects of tauopathies, including age-related accumulation of filamentous tau, neuron loss and axonal transport defects [238].

In tauopathies, tau accumulates in different forms associated with post-translational modifications such as phosphorylation, glycosylation, ubiquitination as well as truncation. Tau aggregation and its abnormally high phosphorylation had been widely recognized as the toxic elements involved in neuron dysfunction. Recent reports furthermore suggested that tau truncation, a characteristic feature observed in human, sporadic AD, would constitute an upstream event in the proteolytic cascade occurring in the disease and would precede tau tangles formation [239-242]. *In vitro* studies further established that fragmentation of tau favours its polymerization compared to the full-length forms of the protein, hence paving the way for new mechanisms implicated in the onset of neurodegenerative diseases [85, 100].

During my thesis, I analyzed a novel inducible, transgenic mouse model to study the impact of a short, wild-type Δtau fragment *in vivo*. TAU62 mice express the 3R repeat domain-containing $\Delta tau_{151\text{-}421}$ fragment and developed a mild to moderate motor deficiency with a slowly progressive axonopathy. This phenotype was similar to that observed in aged transgenic ALZ17 mice expressing the human, full-length tau (2N4R) [243]. Interestingly, tau fragment expression in TAU62 mice was sufficient to cause a pretangle tau pathology, characterized by tau hyperphosphorylation in cerebral and spinal cord neurons, its cellular redistribution and impaired neuron function, in the absence of tangles formation and insoluble tau accumulation. Similarly, McMillan group generated a mouse model expressing 1N4R tau fragment cleaved at E391 in the C-terminal insert, which did not develop tau tangles [99]. Notwithstanding, this contrasts with previous reports linking the overexpression of tau fragments in rats with the development of neurofibrillary degeneration [172, 173]. Based on

the mild phenotype of our TAU62 mice, we concluded that in the absence of the full-length human form of tau, $\Delta tau_{151-421}$ has only minor toxic effects similar to that of full-length forms of wild-type tau.

What are the early events in the molecular cascade leading to tauophathies? What is the propensity of different forms of tau to aggregate?

Previous studies have suggested that tau mutant fragments are highly toxic, which was related to their important propensity to aggregate [244, 245]. Indeed, truncation increases the ability of tau to form filaments in both *in vivo* and *in vitro* models. Caspase-3 induces cleavage of tau at D421 and the truncated (Δtau) form was shown to exacerbate the toxicity of mutant full-length tau [89]. In order to mimic better the pathological situation of AD where truncated and full-length forms are co-existing, we next co-expressed the wild type $\Delta tau_{151-421}$ fragment with the full-length, mutant (P301S) human form of tau, by breeding TAU62 mice with the P301S transgenic mice. Missense mutations in the *MAPT* gene had been shown to cause FTDP-17 disease, which is characterized by neuronal loss, astrocystic gliosis, filamentous accumulation of hyperphosphorylation of tau, as well as motor and cognitive impairment [161]. Accordingly, P301S transgenic mice display motor deficit and accumulation of tau filaments in brainstem and spinal cord [165]. Importantly, our double transgenic $P62^{on}$ mice developed an unexpected early, severe motor impairment. Complete hind limb palsy was observed as soon as at 3 weeks of age and this severe phenotype was associated with neuronal dysfunctions, such as mild tau hyperphosphorylation, intraneuronal accumulation of neurofilaments, formation of axonal spheroids and reactive gliosis. Notwithstanding, breeding of TAU62 mice with the ALZ17 animals expressing the wild type, full-length tau (2N4R) lead to a less pronounced neurodegenerative phenotype, although some of these mice develop a severe paralysis around 1 month of age. The main between 2N4R tau isoform and the mutant P301S form of tau (0N4R), resides in their aggregation propensity. Further investigations remain to be done to understand and confirm these observations and to characterize the influence of the aggregation propensity of the co-expressed full-length tau form. It should be noted that cross-breeding of P301S animals with ALZ31 mice expressing the wild-type, human full-length 0N3R form of tau, did not lead to the same aggravation of the motor phenotype.

Hence, our data reveal that Δtau, when associated with full-length forms of tau, strikingly exacerbates the toxicity of tau protein and its propensity to cause neuron dysfunction. By contrast, these tau forms alone (i.e. full-length or truncated) exert a less

detrimental effect on neuronal homeostasis. In both mouse models with co-expression of Δtau and a full-length form of the protein, we observed severe neuronal impairment while tangle formation and insoluble forms of tau were not detected. Similarly, drosophila models for tauopathies displayed severe neuron degeneration, associated with behavioural phenotypes, without developing any tau filaments [240, 241, 246-248]. Our results confirmed these previous reports suggesting that tau tangles formation constitutes a secondary event in the pathology and that tangles are not the decisive toxic agent in tauopathies.

Is abnormal oligomerization of the full-length and truncated forms of tau involved in the onset of the pathology?

Tau oligomers can contain hyperphosphorylated and non-phosphorylated tau proteins and can form both soluble and insoluble products. They have been identified in AD and FTDP-17 brains [239, 249, 250] and are considered to intermediate events between soluble tau monomers and insoluble tau filaments. According to these observations, tau oligomers might play a crucial role in the onset and progression of tauopathies. Notably, previous studies revealed that tau oligomers have a toxic effect on axonal transport [251-253]. Moreover, tau oligomerization may be promoted by other oligomers such as Aß oligomers in AD or alpha-synuclein in PD and FTDP-17 [252, 254] and co-localization between tau oligomers and Aß has been observed in synaptosomal fractions of brain from AD patients [254].

P62 mice constitute an ideal tool to identify, which forms of tau are present in the pre-tangle stage and associated with the severe form of the phenotype. Our preliminary data suggest that tau-containing complexes of higher molecular weight (55-250kDa) are present in the brain of these mice, which likely correspond to soluble oligomers [255]. Although the exact role of tau oligomers is not clear, some studies showed that formation of aggregates has beneficial effect [256, 257], whereas others observed that these forms are toxic [258]. Here, we establish that Δtau exerts a toxic effect on neurons *in vivo*. Since a co-aggregation between full-length tau and Δtau was observed in brain homogenates from mutant mice, it would be interesting to determine the exact role of Δtau in the formation of tau oligomers. In this light, it is planned to investigate the levels of the different isoforms (3R/4R) of tau as well as of the murine endogeneous tau in P62, ALZ17xTAU62 and P301SxALZ31 mice. Formation of tau oligomers may also derive from an imperfect clearance of misfolded tau protein by the ubiquitin-proteasome or the chaperone systems [251, 256]. Hence, futher studies may test whether increasing their activity in P62 mice would limit the accumulation of toxic tau and thereby ameliorate the phenotype of the mice.

Outlook: what are the consequences of endogenous murine tau protein expression on the phenotypes of transgenic mouse models?

This general question underlines the potential importance of murine tau protein in transgenic mice expressing wild type or mutant, human forms of tau. A previous study, analyzing the consequences of the breeding of the AD mouse model Tg30 with mice depleted for Tau (TauKO), suggested that the murine tau protein has an anti-aggregation role and thus limits the phenotype of transgenic mouse models for tauopathies [259]. Based on this observation, it would be interesting to determine the role of the endogenous murine tau for the evolution of tau pathology and the severe phenotype of P62 mice. Breeding of TAU62 mice with TauKO mutant animals may be conducted, before crossing the resulting mice with P301S animals. The new mice obtained would allow to determine the impact of Δtau without endogenous tau and see whether its toxicity is aggravated. So far, the mechanism by which endogenous tau limits tau aggregation is unknown, and it remains essential to elucidate the question. It is known that the N-terminal region of the murine and human tau proteins only share 75% of homology, while C-terminal domains show an almost perfect homology [260]. One can thus hypothesize that the protective effect of mouse tau may reside on its N-terminal region, which may limit the aggregation of tau protein. Depletion of this form in our mouse models may therefore reveal futher neuronal alteration, which may mimic more efficiently the pathomechanisms at play in human diseases.

Identifying the cellular events underlying neuronal dysfunction in tauopathies by using a novel, severe mouse model for tauopathies

The development of a novel, severe model for tauopathies allowed us to elucidate the mechanisms associated with tau toxicity *in vivo*. Future challenges will aim to dissect the molecular pathways and cellular processes by which Δtau causes the massive, widespread, neurological changes observed in mutant mice.

Microtubule destabilization and impaired axonal transport as primary events in tauopathies

Tau associates with microtubules and participates in their stability and dynamics [261]. Through this tight association, tau proteins also play an important role in microtubule-dependent trafficking of organelles in cells and are determinant for the efficient axonal

transport of intracellular components, such as mitochondria, ER and lysosomes [262]. Destabilization of the microtubules is a consequence of tau hyperphosphorylation, which provokes a lost of its affinity for binding and leads to traffic impairments. However, recent works suggested that increased affinity and binding to microtubules would rather be the cause for the altered kinesin-dependent traffic in cells [263]. It remains unclear what corresponds to these 'hyperbound' forms of tau [264] and how they form; in this hypothesis, hyperphosphorylation of tau may constitute an adaptative, protective process to limit the binding of tau to the microtubules. Another gain of pathological function hypothesis proposes that increase in the ability of tau to bind to kinesin would block the interaction of the motor protein with cargoes and/or microtubules, and thus impair axonal transport [36, 265, 266]. Altered axonal transport has been implicated in the pathogenesis of different neurodegenerative disorders [267, 268] and was related to the abnormal accumulation of neurofilaments in axons of motor neurons in AD, PD and ALS [269-271].

Interestingly, P62^{on} mice displayed signs of microtubule destabilization and axonal transport disruption, which are likely caused by Δtau toxicity. Further investigations remain to be conducted to determine the mechanisms leading to these defects in detail. To this end, it would be interesting to assess the effect of microtubule stabilizers, such as Paclitaxel and Epothilone D [272-275], as microtubule stabilizing agents were recently shown to partly rescue tau induced axonal transport deficits in other models [272-274]. The affinity of Δtau and tau oligomers for tubulin and kinesin may also be studied in order to better understand the origin of the defects. Immunoprecipitation and co-immunohistochemistry may also give an idea of the interaction between tau, microtubules and motor proteins in the brain of P62 mice. Moreover, deregulation of the interaction between kinesin and cargoes has been related to tau-mediated mislocalisation of the c-Jun N-terminal kinase interacting protein 1 (JIP1) in the soma, which may constitute another event at play in axonal transport deficits in tauopathies [276]. Therefore, one might test the localisation of JIP1 in these mice to see whether it is implicated in the defects observed. It could be also interesting to test the interaction between phospho-tau and JIP1 in order to determine how hyperphosphorylated tau impair axonal transport by its implication with kinesin. Lastly, it has been suggested that JNK pathway is involved in the regulation of microtubule stability in neurons and promotes kinesin-mediated fast axonal transport, thereby contributing to neuron function and synaptic plasticity [277]. JNK protein belongs to MAPK family and seems to play a role in the pathogenesis of AD by targeting neurofilaments [278]. Its phosphorylation induces tau pathology in PS1/APP

transgenic AD model [279], and it has been observed that phospho-tau colocalizes with activated form of JNK [280, 281]. Since the mechanism behind the hyperphosphorylation of tau is still unclear, an imbalance between kinases such as JNK and phosphatases has been suggested to play a role in tau pathology. For these reasons, analysis of JNK pathway and its involvement in neuronal dysfunction in $P62^{on}$ mice would be relevant.

Neuronal alteration relies on impaired axonal transport: mitochondrial dysfunction, synaptic disorganisation and Golgi fragmentation

Several reports established that transport deficits are responsible for mitochondria mislocation, identified as an early, key component in the neurodegenerative cascades [282-284]. Mitochondrial homeostasis is essential in neurons, which have high-energy requests and prolonged processes, hence requiring organized, efficient organelle traffic [285, 286]. Mitochondria dysfunction may be responsible for synaptic impairment and synapse loss, early observed in AD [287, 288], and seems to be targeted by toxic truncated forms of tau [289]. In parallel, there is evidence that fragmentation of Golgi apparatus (GA) also occurs at early stage in many neurodegenerative diseases [290]. GA is involved in transport, processing and targeting of proteins to the dendrites and axon in order to maintain cell polarity [291]. Thus, dysfunction of the GA machinery impairs a regulated system involved in protein sorting in neuronal compartments. Several studies using *in vitro* and *in vivo* models suggested that accumulation and hyperphosphorylation of tau induce GA fragmentation in hippocampus and that this process is not caused by apoptosis. Moreover, these morphological changes of GA were shown to develop before the formation of tangles [290].

Interestingly, in P62 mice, histological features e.g. swollen and fragmented GA as well as accumulation of mitochondria in the hippocampus of the mice, were observed in the absence of tangles. Additional experiments, focusing on the fission/fusion processes of mitochondria, the expression of specific components involved in the tricarboxylic acid (TCA) cycle and oxidative phosphorylation (OXPHOS) systems, as well as the production of ROS, might help to better characterize the mitochondrial dysfunction in P62 mice, and their consequences on cell homeostasis. Regarding GA alteration, it could be of interest to confirm that GA fragmentation is not related to neuron apoptosis in this model. Lastlty, synaptophysin proteins, which play a role in synaptic function, also accumulated in the hippocampus of paralyzed P62 mice and sorting of VAMP2 (or synaptobrevin II), one of synaptophysin binding partners, was altered. These preliminary data suggested that missorting of synaptic

proteins in the GA could affect synapse function by depleting newly synthetized vesicular proteins. Quantification of functional synapses and identification of the binding partners of synaptophysin in P62 mice may help to understand the molecular mechanisms at play in the control of vesicle recycling and their alterations in AD. Such changes occurring early during the progression of the pathology could reveal new therapeutic targets.

What is causing muscle atrophy in tauopathy mouse models?

$P62^{on}$ mice developed a rapidly progressive hind limb palsy associated with severe muscle wasting. Histology revealed marked muscle fibre atrophy where both fibre types were severely affected and display angulated profiles. These findings were consistent with a neurogenic atrophy. Several reports have already described that muscle disuse causes severe muscle atrophy, which was related to an important activation of the catabolic pathways, the ubiquitin-proteasome (UPS) and the lysosome-autophagy process, in muscle tissue. Among the molecular mechanisms shown to mediate these changes, activation of FoxO signalling and inhibition of the mTORC1 pathway were of central importance [292].

FoxO (Forkhead box O) factors constitute positive regulators of the two proteolytic pathways by promoting the transcriptional expression of atrogenes (encoding the E3 ubiquitin ligase, MurF1 and Atrogin1) and autophagy-related genes (such as LC3 and Bnip3) [293, 294]. Inversely, mTORC1 increases protein synthesis and inhibits autophagy induction in muscles [295]. While induction of the proteasome system leads to muscle wasting, both increased and reduced autophagy flux were shown to impair muscle homeostasis and cause muscle atrophy [296-298]. Excessive induction of autophagy leads to the elimination of fraction of cytoplasm and to muscle degeneration, as observed, for instance, in merosin-deficient congenital myopathies (MDC1A) [299]. In contrast, inhibition of autophagy conducts to the detrimental accumulation of vacuoles and abnormal organelles as observed in collagen VI-related myopathies [298, 300, 301]. Functional defects of axonal transport seem to be responsible for muscle wasting in a variety of neurodegenerative diseases such as ALS [302], AD [303] and HD [207]. In these pathologies, FoxO/mTORC1 signalling, as well as the UPS and autophagy processes have been implicated in the appearance of muscle atrophy [304].

Here, it would be interesting to investigate whether the UPS activity and the autophagy flux are modified in muscles from $P62^{on}$, compared to control mice. In this line, analysis of autophagy markers, such as LC3 or p62 proteins, as well as quantification of the transcriptional expression of atrogenes could be performed. Furthermore, the mTORC1/FoxO

signalling, as well as other signalling, including HDAC5/Myostatin [305] or TWEAK/Fn14 [306] related to denervation-induced proteolysis, could be studied in muscles from $P62^{on}$ to determine the upstream events causing muscle atrophy. Lastly, since muscle atrophy was widely restored following extinction of Δtau expression, it will be of major interest to identify the processes involved in this gain of muscle mass. In particular, re-activation of mTORC1 may participate in this hypertrophy but the up-stream events leading to its activation remain to be fixed. Observation of centronuclear fibers in muscles from $P62^{on\text{-}off}$ mice also suggested that activation of satellite cells may be important in the hypertrophy process, by forming new fibers or enlarging pre-existant, atrophic fibers. Immunohistochemistry against myogenic markers, such as Pax7, MyoD, Myogenin or embryonic myosin heavy chain, may help to better understand the mechanisms at play in the restoration of muscle fibers [307-310].

Outlook: The role of autophagy in neuronal dysfunction

Impairment of autophagy in AD has been widely described [203] and considered to be responsible for the accumulation of misfolded and aggregated proteins. Reduced autophagy flux was related in AD to decreased expression of Beclin1, an essential protein for autophagy processing [206] and abnormal activation of the JNK signalling, which would cause inhibition of FoxO factors and repression of autophagy-related genes [311]. Altered lysosome-mediated clearance of autophagosomes may also be responsible for the accumulation of autophagy-related vesicles in AD and may be caused by the inefficient traffic of lysosomes within neurons. Moreover, macroautophagy and chaperone-mediated autophagy are involved in the degradation of different forms of tau and fragmented tau may also derive from imperfect autophagy processing [312]. Importantly, while autophagy blockade would promote the accumulation of tau aggregates, increased levels of tau protein may further alter axonal transport and thereby the autophagy flux.

In P62 mice, it is of major importance to test whether Δtau expression or the early formation of soluble oligomers of tau is sufficient to impact on the autophagy flux. In complement to experiments testing the axonal transport in P62 mice, western blot and immunohistochemistry against autophagy markers, including LC3 and p62, will allow to identify potential dysfunction in the flux. In this light, we have treated P301S mice with either rapamycin or trehalose and we showed that these treatments have beneficial effects [313, 314]. Treating P62 mice with drugs inducing (e.g. rapamycin) autophagy will also bring insight on the process at play in the specific degradation of Δtau and oligomers.

Rationale for the development of therapeutic strategies for tauopathies: *what we learnt from our mouse models?*

Up to now, the current therapies for AD addressed only symptomatic aspects and notably tried to delay the cognitive decline of affected patients. Since Aß accumulation was considered as the central upstream event leading to neurodegeneration in AD, most of the strategies were developed either to reduce Aß formation or to promote its clearance. But these clinical trials so far mainly failed to ameliorate the neuropathology and the degeneration of the neurons [315]. Most importantly, these therapies could not prevent the progression of concomitant tau pathology, once initiated. Design of new therapies targeting tau pathology now constitutes another interesting approach for AD and other tauopathies.

A promising observation: the phenotype of tau transgenic mice is reversible

As observed in other models [316], the severe phenotype and the histopathological features observed in $P62^{on}$ mice are largely reversible when the expression of Δtau is suppressed. In particular, the accumulation of AT8 phosphorylated tau and tau oligomers are reversed in $P62^{on\text{-}off}$ mice. Moreover, the defects in GA, mitochondria mislocation and the altered sorting of synapse-associated proteins are not longer present in these mice, although more detailed, quantitative experiments remain to be done to confirm these observations. Hence, these data revealed that the toxic effect of Δtau in association with mutated full-length tau can be reversed even after the onset and progression of the pathological changes.

Rationale for the development of therapeutic strategies targeting the inhibition of tau fragmentation

Based on our results, it appears obvious that Δtau elements, when combined with different tau isoforms, are more toxic than full-length tau and exacerbate tau aggregation. Proteins inducing neurodegeneration are the substrates for many proteases such as caspases, calpains or cathepsins: in HD brain, caspase-3 cleaves huntingtin fragments before the clinical onset [317, 318], and in AD brain, the cleavage of tau proteins is initiated by caspase-3 or -6 in both early and late NFT stages as well as during cognitive decline [74, 75, 319]. One might consider the use of inhibitors of caspase-3 or calpains, such as minocycline, a second generation of tetracycline, in AD pathology [320]. Recent studies described the beneficial effect of minocycline in primary cortical neurons: the cleavage of tau by caspase-3 is reduced as well as Aß-mediated activation of caspases. Similar observations have been made in mice

expressing human tau, where tau phosphorylation and cleavage were reduced upon treatment with minocycline [321, 322]. These data hence suggest that targeting the proteolytic activity involved in tau truncation may constitute a relevant therapeutic approach for tau pathology.

Rationale for the pursuit of therapeutics countering tau aggregation

In proteinopathies, such as AD, PD and HD, abnormal accumulation, aggregation and removal of proteins, constitute a specific, detrimental event associated with the pathogenesis and the cognitive deficits. Preventing tau aggregation or oligomerization may therefore constitute a promising option to limit tau toxicity and neuronal dysfunction associated with tauopathies.

The efficiency of different inhibitors of amyloid and tau aggregation has already been assessed in *in vitro* or *in vivo* AD models. For instance, the epigallocatechin gallate, a green tea derived polyphenol, efficiently limits amyloid-β aggregation *in vitro* and neutralizes amyloid-β oligomers [323-326]. The substance is also sufficient to restrict tau aggregation and particularly its oligomerization *in vitro* [326]. Other plant derived substances with *in vitro* proven anti-amyloid aggregation capacity include cinnamon extracts [327] and Tannic acid [328]. The phenylthiazolyl-hydrazide BSc3094 [329], Methylene blue [330] and Curcumin [331] also had positive effect on amyloid-β and/or tau accumulation, as well as on memory deficits in transgenic tau mouse model.

Based on these previous reports and on the severe phenotype observed in $P62^{on}$ mice, the ability of different inhibitors of tau aggregation to prevent or limit the toxicity of Δtau and the associated neuronal alteration in mutant mice could be tested. Treating these mice with different pharmacological drugs may help to determine whether inhibiting the aggregation of tau would prevent the onset of the pathology and, more specifically, which pathological cellular events can be restored.

Inducing autophagy as a promising therapeutical option for tauopathies

In parallel of therapeutic options targeting the formation of tau and amyloid-β aggregates, promoting the clearance of tau protein represents another effective and realistic strategy for dementia treatment. As described before, a downward cycle between formation of tau aggregates and impairment in autophagy is likely at play in a majority of neurodegenerative diseases. For these reasons, drug-induced up-regulation of autophagy has been widely tested in animal models for tauopathies and envisioned for AD, PD or HD.

One part of my thesis aimed to determine if autophagy stimulation would promote tau clearance in tau transgenic mice and could ameliorate their neurodegenerative phenotype. To this end, P301S mutant mice were treated with two distinct autophagy-inducing agents: i) rapamycin, a well-known inhibitor of the mTORC1 pathway and FDA-accepted pharmacological drug [313] and ii) trehalose, a mTORC1-independent activator of autophagy. Rapamycin treatment significantly delayed the progression of tau pathology and the associated histopathological and biochemical changes in P301S mice [313]. While aged mutant mice treated with saline sham solution developed robust tau tangle disease, tangle formation and accumulation of sarcosyl-insoluble tau were largely prevented in rapamycin treated mice. Comparably, trehalose also improved neuronal survival in the brain of P301S mice and reduced the number of AT100 positive neurons as well as the amount of insoluble tau protein. [332].

Although these results open promising avenues regarding potential, efficient therapeutic strategies toward AD and other tauopathies, further complementary investigations remain to be conducted. For instance, we have not assessed in details whether rapamycin also ameliorated behavioural and functional parameters. Furthermore, one limitation of these treatments was the absence of effect in the brainstem and most probably in spinal cords as seen with trehalose. Additional experiments might be done to determine why the induction of autophagy had no effect on the spinal cord and why the motor deficit was not reversed in threhalose-treated mice. One possible explanation may come from the strong expression of mutated tau and the associated formation of tangles, which may be resistant to autophagy-mediated clearance. It could be also interesting to investigate the efficiency of axonal transport in P301S mice, treated or not with rapamycin/trehalose drugs, to determine whether autophagy induction restores the process.

Lastly, our results may be even more instructive on the protective effect of autophagy induction by treating, as mentioned above, the severely affected P62 mice. Analysis of the molecular and cellular consequences of pharmacological drug promoting autophagy in these mice will help to determine the benefits of such treatment and their limits.

Together, the insights gained by our current observations and the proposed perspectives shall contribute to a better understanding of the pathomechanisms leading to tauopathies and the development of novel therapeutic approaches. In long term, other therapeutic strategies, such as immunotherapy targeting tau oligomers [333] may be tested in the P62 model. Hence, our novel P62 mouse model offers a unique configuration to test new

therapeutic strategies and unravel the different molecular events conducting to the onset and the progression of tauopathies and AD.

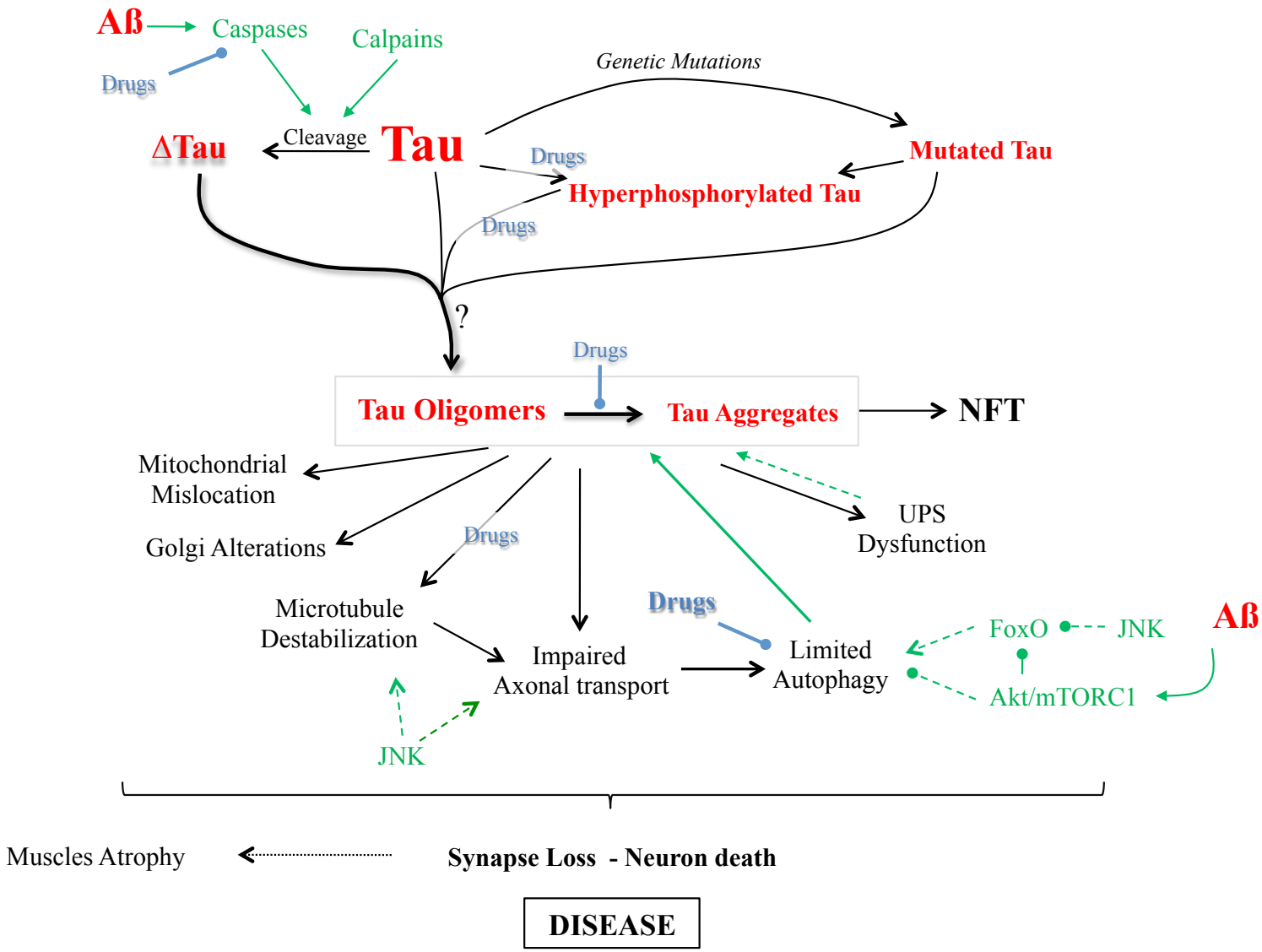

Figure 11: Schematic overview on the pathology of tau protein in neurodegeneration and on the treatment strategies to reduce tau pathology

MATERIALS *and* METHODS

Animal model

Inducible Δtau expressing TAU62 transgenic mice have been generated by co-injection of two Thy 1.2 minigenes based constructs into C57BL/6J oocytes. The Thy 1.2-tTS construct was obtained by replacing exon 2 of the murine Thy 1.2 promoter by a tetracycline controlled transcriptional silencer element (tTS). The Thy 1.2-TRE-Δtau construct contained a tetracycline responsive element (TRE) upstream of the human wild-type Δtau cDNA encoding amino acids 151 to 421 of a 3-repeat domain spanning human wild-type tau fragment (3R0N $tau_{151-421}$). A total of 6 positive transgenic founder TAU62 mice (C57BL/6J-TgN(tTS-Thy1-$\Delta tau_{151-421}$) were identified and the inducible expression of human Δtau was assessed by western blot and immunohistochemistry. Lines 62-2 and 62-48 exhibited comparable and robust Δtau expression without leakage upon doxycycline withdrawal. All quantitative experiments were performed with mice of the TAU62-48 line, abbreviated TAU62 mice (C57BL/6J-TgN(tTS-Thy1-Tau) 62). TAU62-2 mice were used in order to rule out an insertion side effect causing the drastic motor phenotype observed in P301Sx TAU62/48 double transgenic mice.

For the generation of ALZ31 wild-type human 3R0N tau transgenic mice (C57BL/6J-TgN(Thy1-ALZ) 31), 0N3R human cDNA was cloned into a standard neuron-specific Thy 1.2 promoter element and injected into C57BL/6J oocytes.

ALZ17 wild-type human 2N4R tau transgenic mice (C57BL/6J-TgN(Thy1-ALZ) 17) generation has been described previously [243]. Briefly, cDNA encoding the longest human tau isoform has been subcloned into a murine Thy 1.2 gene. Subcloning htau40 cDNA by using XhoI restriction site produced the tau expression construct, ALZ17 transgene. After microinjection into pronuclei of B6D2F1 x B6D2F1 embryos, the founders were analysed by PCR and then intercrossed with C57BL/6J mice to obtain strains

Generation of P301S mutant 0N4R tau transgenic mice (C57BL/6J-TgN(Thy1-$hTau_{P301S}$)) has been described previously [165]. Shortly, cDNA encoding the shortest human four-repeat tau isoform (383 amino acids isoforms of human tau) was used to obtain the P301S mutation. After subcloning the mutated cDNA into a murine Thy 1.2 genomic expression vector, this tau construct was produced by subcloning P301S htau43 cDNA using XhoI restriction site. Transgenic mice were generated by microinjection into pronuclei of (C57BL/6J x CBA/ca) F1 generation. PCR analysis was performed done to identify the founders and these were interbred with C57BL/6J mice to obtain strains.

P301SxTAU62 double transgenic mice have been obtained by crossing P301S mice with Δtau transgenic mouse lines. All double transgenic mice were heterozygous for the transgenes of interest. Chow containing 500mg/kg doxycycline was provided *ad libitum* to induce Δtau expression. All animal experiments were approved by the local Ethics and Animal Care and Use Committees.

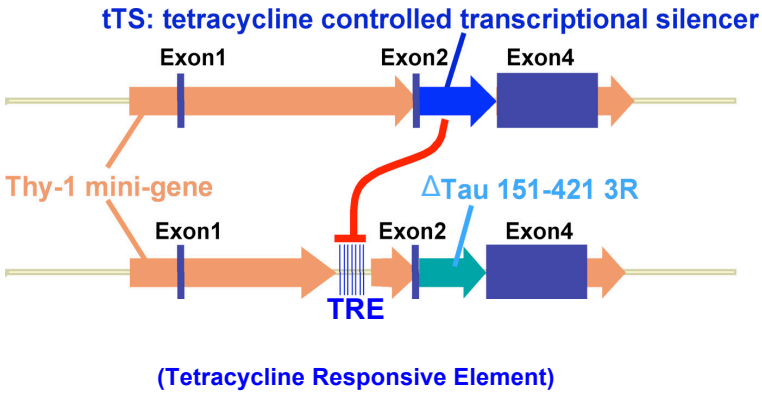

Figure 12: Generation of TAU62 mice

In Tau62 mice, neuronal ΔTau expression was driven by an inducible Thy1.2 promoter element under a tetracycline controlled transcriptional silencer element (tTS).

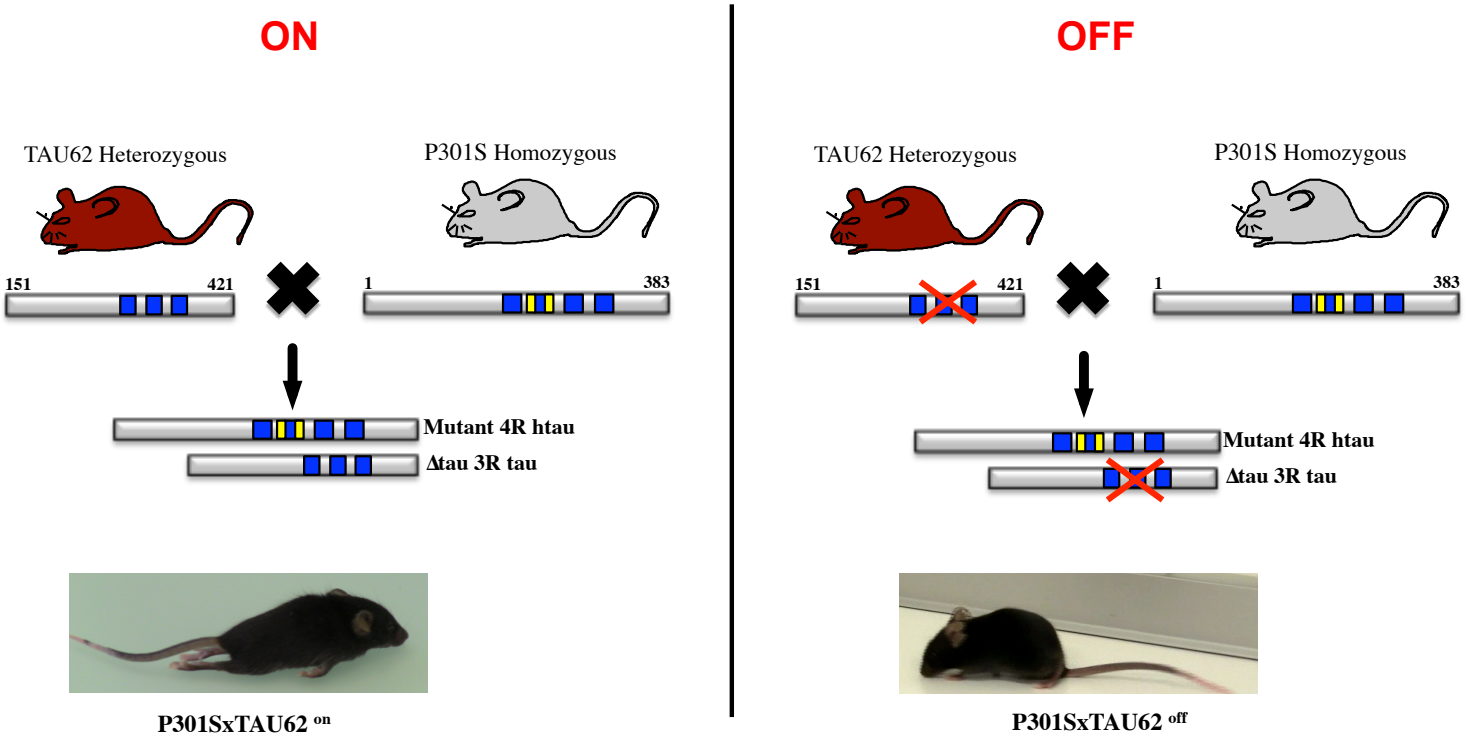

Cross breeding P301SxTAU62 transgenic mice

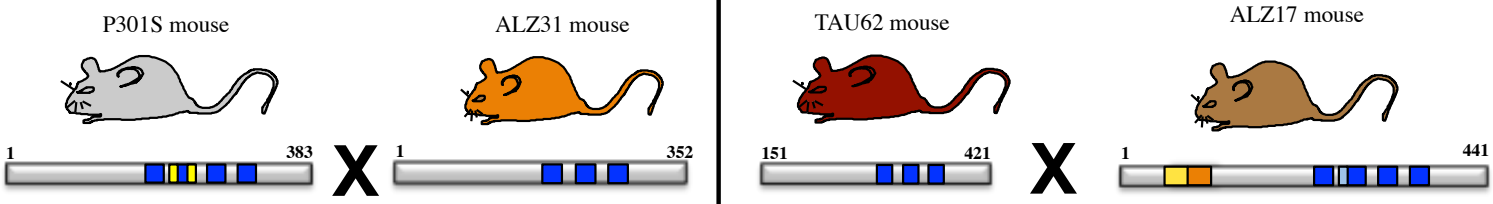

Cross breeding ALZ31xP301S transgenic mice

Cross breeding ALZ17xTAU62 transgenic mice

<u>Figure 13:</u> Mice used to study the effect of Δtau and the corresponding breeding (P62, ALZ31xP301S and ALZ17xTAU62)

Genotyping

Lysis buffer

	Concentration	Supplier
Tris	100 mM (pH 8.5)	Biomol # 08003
EDTA	5 mM	Fluka BioChemika # 03690
NaCl	200 mM	Merck # 1.06404.10 000
SDS	0.20%	Bio Rad # 161 0301

Pieces of mouse ears were incubated in lysis buffer containing 0.1 mg/ml Proteinase K (Macherey-Nagel # 740506.75) in Eppendorf Thermomixer comfort shaker (650 rpm, 55°C over night (O/N)). The solution was centrifuged (13000rpm, 5 min) and 550µl of the supernatant was transferred into 500µl isopropanol. The solution was mixed by inverting and centrifuged (13000 rpm, 10 min). The pellet was washed with 75% ethanol and centrifuged again (13000 rpm, 10 min). DNA was consequently dried on Eppendorf Thermomixer comfort shaker (55°C, 5-10 min) and resuspended with 250µl dH_2O. DNA was dissolved by agitation at 50°C 1h before performing the PCR.

PCR Master Mix for 25µl reaction volume:

	Concentration	Supplier
Master Mix	2X TaqDNA polymerase	QIAGEN # 200403
	QIAGEN PCR buffer	
	3 mM MgCl2	
	400 µM dNTP (each)	
Forward primer	10 pmol	Eurofins MWG/opreon
Reverse Primer	10 pmol	Eurofins MWG/opreon
DNA	2 µl	

Primer pair TauF151 detect the Δtau allele (383 bp length) and primer pair P301S detected 4R tau allele (600 bp length).

PCR amplification protocol for genotyping

TauF151 program:

Step 1: 95°C for 2 min

Step 2: 95°C for 1 min

Step 3: 60°C for 1 min

Step 4: 72°C for 2 min

Step 5: 72°C for 10 min (final extension)

Steps 2-4 were repeated for 30 cycles.

P301S program:

Step 1: 95°C for 4 min

Step 2: 95°C for 1 min

Step 3: 60°C for 1 min

Step 4: 72°C for 3 min

Step 5: 72°C for 10 min (final extension)

Steps 2-4 were repeated for 30 cycles.

PCR products were loaded on 1.5 % agarose gels and run at 150 Volt.

Primers for genotyping (all sequences are written 5' → 3')

	Forward primer	Reverse primer
TauF151	GTG GAT CTC AAG CCC TCA AG	GGC GAC TTG GGT GGA GTA
P301S	GGT TTT TGC TGG AAT CCT GG	GGA GTT CGA AGT GAT GGA AG

Behavioural assessment

Phenotypic characterisation included the observation of motor behaviour (gait ataxia and tremor) by testing hind limb reflexes at ages of 21 days and after switching off the expression of Δtau. Quantitative motor testing was performed on the grid test.

For grid testing, mice were placed on a vertical mesh grid and the latency to fall of the grid was measured. Non-paralyzed mice attached to the grid climb towards the upper end of the grid and explored the whole grid, while paralyzed mice fall of the grid within the observation period of 180 seconds.

Figure 14: Picture of grid-test used to analyse motor phenotype.

Histology and immunohistochemistry

Mice were anaesthetized with a mixture of 100mg/kg ketamine (Ketalar®, Pfizer) and 10mg/kg xylazine (Rompun® 2%, Bayer #79762704) by intraperitoneally and after deep sleeping, mice were injected by sodium pentobarbital (Pentothal® 0.5g, Ospedalia AG #6900) (100mg/kg) and transcardially perfused with 0.01M cold phosphate-buffered saline (PBS, Bichsel #1000326).

Theses sections describe the principles for staining paraffin embedded samples.

Brain, Spinal cord and nerve preparation

After perfusion, the spinal cord, sciatic nerve and the brain were quickly removed and one half of the brain was immersion fixed in 4% paraformaldehyde O/N and embedded in

paraffin. Paraffin sections were deparaffinised in Xylol (Biosystems #253-VI53TE) for 20 min, rehydrated in 100% EtOH for 3 min, then two times for 3 min in 96% EtOH and two times for 3 min in 70% EtOH. After rehydration in histological grade ethanol, sections were washed in PBS. In order to mask antigenic sites, antigen retrieval were performed in Citric acid buffer pH 6.0 (Pro Taps® # 400300692) according to the primary antibody manufacturer's recommendation. After blocking in normal horse serum for anti-rabbit (Vector Laboratories #S-1000) or in 2.5% normal horse serum (Vector Laboratories #S-2012) for 30 min at room temperature (RT), sections were incubated O/N at 4°C with primary antibody. The next day, the sections were washed in Tris/PBS solution three times for 5 min and then incubated with ImmPRES™ Reagent peroxidase for anti-mouse antibody (Vector Laboratories #MP-7402) or Biotinylated anti-rabbit IgG (H+L) (Vector Laboratories # BA-1000) for 30 min at RT. After the end of incubation time, the sections were washed with Tris/PBS three times for 5 min and developed by using chromogen ImmPACT™ NovaRED™ Peroxidase substrate kit (Vector Laboratories #SK-4805). After application of chromogen, the sections were washed with PBS to stop the reaction and then the slides were counterstained with hematoxyline (J.T. Baker #3873). Finally, sections were rehydrated in 70% ethanol for 1 min, both two times in 96% and 100% EtOH and finally in xylol, before to apply Pertex mounting medium (Biosystems #41-4012-00)

Gallyas silver staining

After deparaffinisation and rehydration the sections were incubated in 3% Periodic Acid (Sigma #P7875) for 30 min at RT. Then, the slides were washed in dH2O, one time for 2 min and followed by incubation in 1% Alkaline Silver solution composed of 1M sodium hydroxide (Merck #106498); 0.6M potassium iodide (Merck # 105043); 1% silver nitrate solution (Merck #101512), for 10 min at RT. During this meantime, solution ABC were prepared as followed:

	Concentration	Supplier
Solution A		
Sodium Carbonate Anhydride	0.5 M	Merck #106392
Solution B		
Ammonium nitrate	24 mM	Fluka #09890
Silver Nitrate	0.01 M	Merck #101512
Tungstosilicic Acid Hydrate	3.5 mM	Aldrich #95395
Solution C		
Ammonium nitrate	24 mM	Fluka #09890
Silver Nitrate	0.01 M	Merck #101512
Tungstosilicic Acid Hydrate	3.5 mM	Aldrich #95395
Formalin Solution	0,26%	Merck #104003

After incubation in ABC solution, the sections were treated with 0.5% Acetic Acid (Merck #100063) to block the reaction during 30 min in RT. After that, during 2 min (not too long), the slides were washed in dH2O and incubated in 5 % Sodium thiosulfate (Merck #106516) for 2 min in RT. They were then washed in cold tap water for 2 min at RT and nuclei were stained with hematoxyline for 5-15 sec. The sections were washed again in cold tap water for few minutes and in HCl for 5-15 sec, followed by washing in hot tap water for few minutes. Finally, the sections were dehydrated in EtOH (70%, 96% and 100%) and xylol (Biosystems #253-VI53TE) before to apply Pertex mounting medium (Biosystems #41-4012-00).

Improved Thioflavin-S staining (adapted from A. Sun et al., JHC 2002)

Before to start the staining, paraffin sections were deparaffinised and rehydrated as described before. First of all, it is important to quench the auto-fluorescence, the slides were incubated in 0.3% $KMnO_4$ (Riedel-deHaën # 31404) for 4 min at RT and washed in water. After that, the sections were treated with a solution of bleaching solution, composed of both 1% $K_2S_2O_5$ (Merck # 105057) and Oxalic acid (Merck #100495), until the brown colour was removed from the tissue (20-40 sec), followed by a washing step with water. The sections were incubated in 1% sodium Borohydride ($NaBH_4$, Sigma #452882) (which is prepared 2h before use) for 5 min at RT. After reducing background auto-fluorescence, the slides were washed three times with dH_2O and were stained with 0.01% Thioflavin-S solution (Sigma # T1892), 50% ethanol (Pharmacy USB) in the dark for 8 min. Again, the sections were washed two times in 80% EtOH for 10 sec and three times in large volumes of dH_2O. Following the washing step, the sections were incubated in a high concentrated phosphate buffer, containing 411mM NaCl (Merck # 106404), 8.1mM KCl (Merck # 104936), 30mM Na2HPO4 (Merck #106580), 5.2mM KH2PO4 (Merck #104873), pH 7.2, at 4°C for 30 min or more and after

the end of the incubation time, the slides were rinsed with dH2O and finally, mounted using glycerine and kept in dark.

Hematoxylin and Eosin Staining

After deparaffinisation and rehydratation two times in 100% EtOH, two times in 96% and then one time in 70% EtOH for 3 min respectively, the sections were rinsed in cold tap water and stained in hematoxylin for 5-8 min. After washing in cold tap water and decolorizing shortly in alcohol-HCl (Pharmacy USB), the slides were washed again in cold tap water and blueing for 10 min in warm water and immersed in 1% erythrosine B solution (RAL diagnosis #361990) for 2-3 min. After this incubation time, the sections were washed shortly in cold tap water, dehydrated in gradient EtOH (one time in 70%, two times in 96% and two times in 100%) and finally cleared in xylol before to apply Pertex mounting medium.

Holmes Silver Nitrate-Luxol Fast Blue staining

	Concentration	Supplier
Impregnation solution		
Boric acid	1,24%	Merck #165
Dinatriumtetraborat (Borax)	1,90%	Merck #
Silver nitrate	1%	Merck #1.01512
Pyridin solution	10%	J.T.Baker #8073
Reduction solution		
Sodium sulfite	0.8M	Merck #1.06657
Hydrochinon	90mM	Merck #8.22333
Gold chloride	0,25%	Sigma-Aldrich #HT1004
Acid oxalic	2%	Merck #1.00495
Sodium thiosulfate	5%	Merck #1.06516
Luxol Fast Blue solution		
Luxol fast blue	0,1%	Medite #1B-389
Ethanol	96%	Pharmacy USB
Acetic acid	10%	Merck #100063

The sections were deparaffinised and rehydrated as describe before and placed in 20% Silver nitrate solution (Merck #1.01512), for 90 min in the dark at RT. The slides were washed in dH_2O three times and incubated in impregnation solution at 37°C O/N. Next day, sections were placed onto filter paper to remove superfluous fluid and transferred directly in reduction solution for 10 min. Afterwards, the sections were washed in tap water for 5 min and rinsed

slides were placed in dH_2O. During 5 min, the sections were moved in 0.25 % Gold chloride solution and then rinsed in dH_2O for 10 min. The wash slides were incubated in 2% Acid oxalic for 10 min and when the axons were thoroughly blue-grey, the reaction were stopped by rinsing the sections in dH_2O. After that, the slides were placed in 5 % sodium thiosulfate solution for 5 min and again rinsed in tap water before placing the slides briefly one time in 70% and two times in 96% EtOH. Next the sections were incubated for 2 hours at 60°C in Luxol fast blue solution and briefly washed two times in 96% EtOH to remove excess stain, then placed in running cold tap water for 5 min and transferred into dH_2O. For the differentiation, the slides were placed in 0.1% Lithium carbonate for few seconds and distained in 70% EtOH before to be washed in dH_2O. Finally, the slides were immersed in Cresyl violet solution for 10 min at RT and washed first two times in 96% EtOH for few seconds to remove excess stain and then in two times in 100% EtOH before to place in xylol and apply Pertex mounting medium.

Masson Trichrome staining (Nerve)

	Concentration	Supplier
Weigert's Iron Hematoxylin solution I		
Solution I		
Hematoxyline	33 mM	Merck #1.04302
Ethanol	96%	Pharmacy USB
Ferric chloride solution		
Solution II		
Iron (III) chloride	32 mM	Merck #1.05512
Acid-HCl	25%	Merck #1.00316
Acid fuchsin Ponceau		
Solution I		
Fuchsin acid	17 mM	Merck #7629
Acetic acid	1%	Merck #1.00063
Solution II		
Ponceau	23 mM	Chroma #1B 205
Acetic acid	1%	Merck #1.00063
Aniline blue solution		
Aniline blue	34 mM	Chroma #1B 501
Acetic acid	2,5%	Merck #100063

The sections were deparaffinised and incubated in Weigert's Iron Hematoxylin solution for 1 min and washed in running cold water followed by warm water for 5-10 min. After that, slides were placed in Acid fuchsin Ponceau solution for 5 min, followed by washing in tap water. Then, the sections were incubated in 1% Acid Phosphomolibdic (Merck #1.00532) for

5 min and Aniline blue solution was added directly on the slides for 3 min (without discarding the 1% Acid Phosphomolibdic) under shaking. Afterwards, the sections were rinsed three-five times in dH_2O and briefly (5 sec) transferred in 1% acetic acid. Finally, the rinsed slides were dehydrated two times in absolute EtOH, then in xylol, and coverslipped.

Muscles preparation

After perfusion, whole gastrocnemius (GC), soleus (Sol), tibialis anterior (TA) and extensor digitorum longus (EDL) were removed and embedded on a small mound of O.C.T™ compound (Tissue-Tek® Sakura #4583) that is placed on a cork disc and snap frozen in liquid nitrogen cooled isopentane, and stored at -80°C. Coronal sections were cut into 10-12µm thick cryosections with a cryostat (HydraxC, Histocom AG) maintained at - 20°C.

Myosin-ATPase (Adenosintriphosphatase) staining (pH4.2)

This section describes the procedure for staining frozen sections of O.C.T embedded samples.

	Concentration	Supplier
Veronalacetate buffer (stock solution)		
Sodium acetate	0.1M	Merck # 6265
Sodium barbiturate (Veronal)	0.1M	Sigma # 32001
ATP pH 4.2 solution		
Veronalacetate buffer pH 4.2	0.1M	Sigma # 32001
HCl	0.1M	
Veronal Ca buffer (stock solution)		
Sodium barbiturate (Veronal)	0.1M	Sigma # 32001
CaCl2	0.03M	Merck #1.02378
Veronal Ca ATP pH 9.4 solution		
Adenosin-5-triphosphate disodium (ATP)	4.5mM	Fluka # 02060
Cobalt chloride	2%	Merck # 2539
HCl	0.1M	
NaOH	1M	Merck 1.06498
Ammonium sulfide solution	21%	Sigma # 09981

Before cryosectioning, the samples were equilibrated O/N at -20°C, and then placed into the cryostat for minimum 20 minutes. The samples were mounted on the round metallic mount of the cryostat with O.C.T and the sections were cut at 10µm and then collected on warm slides at RT. Before to proceed the staining, the sections must be dry at least 1h at RT. The slides

were directly transferred in ATP pH 4.2 solution for 10 min at RT and placed shortly for washing in Veronal-Ca pH 9.4 buffer. After what, the sections were incubated in Veronal-Ca-ATP pH 9.4 solution for 45 min at RT. Then, the slides were washed two times in tap water and directly moved in dH_2O before transferring in 2% Cobalt Chloride for 5 min. After three washing in tap water, the sections were placed in Ammoniumsulfide solution for 14 sec and finally the slides were rinsed before to be rehydrated in ascending EtOH (one time in 70%, two times in 96% and two times in 100%) and transferred in xylol and apply Pertex mounting medium.

Semithin sections for Sciatic nerve

This procedure is for staining semithin sections of resin embedded samples.

Sciatic nerves were dissected at the upper thigh and nerves were fixed for at least 2-3h in 2.5 % of Glutaraldehyde (Fisher Scientific # BP 2548-1) in RT and washed in 0.01M PBS overnight. After incubation in PBS, 1 % Osmium tetroxide (Oxkem Limited 10x1g) was added and incubated for 2h in RT. Tissue were washed in histological grade ethanol (70%, 80%, 90% and two times in 100%) for 20 min each and two times in Acetone (Merck # 1.00014) for 30 min. After this washing step, tissue were incubated in Acetone-Durcupan (1:1) solution for 60 min and after in Acetone-Durcupan (1:3) O/N at 4°C. Later, the tissue were mounted in Durcupan resin, containing 150ml of Durcupan A (Fluka #44611), 150 ml of Durcupan B (Fluka #44612), 3.1 ml of Durcupan C (Fluka #44613), 4 ml of Durcupan D (Fluka #44614), and cooked at 60°C for 2-3 days and processed for light microscopy. Semi-thin section of the nerve was performed and ultrathin section (1.5 µm) was cut using a glass trip, which was equipped with a Reichert-Jung apparatus.

Para-Phenylendiamin staining (p-phenylendiamine)

After collecting the ultrathin cryosections on the slides and dried on warm plate, the sections were incubated in 1% p-Phenylendiamine (Sigma #P-6001) solution for 2-3 hours. Later, the slides were rinsed six-ten times in dH_2O and dried at RT.

Electron microscopy protocol (Spinal Cords)

After deep anaesthesia with a mixture of 100mg/kg ketamine (Ketalar®, Pfizer) and 10mg/kg xylazine (Rompun® 2%, Bayer #79762704) intraperitoneally and sodium pentobarbital (Pentothal® 0.5g, Ospedalia AG #6900) (100mg/kg) injection, mice were transcardially

perfused with 0.01M cold phosphate-buffered saline (PBS, Bichsel #1000326) for 2-4min under hood and proceeded without pause with fixative solution composed of 2% PFA (Pharmacy USB); 2% Glutaraldehyde (Fisher Scientific #BP 2548-1); 0.1M PBS pH 7.4 (Bichsel # 1000326); for 1h. After perfusion, the brain and spinal cords were removed and postfixed in the same fixative for 1h in RT and the tissue were rinsed in 0.01M of PBS. Then the tissue were reduced in 1% Osmiumtetroxid and 1.5% Potassium Ferrocyanide for 40 min and after the tissue were transferred in 1% Osmiumtetroxid for 40 min. Following washing step, the tissue were dehydrated in an ascending series of EtOH and aceton, then embedded in Epon. During dehydration, the sections were treated with 1% uranyl acetate in 70% ethanol for 60 min. Sections were cut with a microtom Ultracut E from Leica and collected on single-slot grids, stained 6% Uranyl acetate for 60 min and with lead acetat for 2 min, and examined with a Morgagni FEI 80kV electron microscope.

Sarkosyl extraction

Extraction buffer

	Concentration	Supplier
Tris	25 mM (pH 7.4)	Biomol # 08003
NaCl	150 mM	Merck # 1.06404.10 000
EDTA	1 mM	Fluka BioChemika # 03690
EGTA	1 mM	Sigma # E3889
Sodium pyrophosphate	5 mM	Sigma # P8010
PhosSTOP®, Phosphatase inhibito cocktail tablets	1 tablet	Roche # 04906837001
Sodium fluoride	30 mM	Merck Suprapur # 1.06450.0025
Complete Mini, Protease inhibitor cocktail tablets	1 tablet	Roche # 04693124001
Phenylmethyl sulfonyl fluoride (PMSF)	1 mM	Sigma # P-7626
Leupeptine	10 µg/ml	Sigma # L-2884
Aprotinine	10 µg/ml	Sigma # A-1153
Pepstatine	10 µg/ml	Sigma # P-5318

A68 Buffer

	Concentration	Supplier
Tris	10 mM (pH 7.4)	Biomol # 08003
NaCl	800 mM	Merck # 1.06404.10 000
Sucrose	10%	Fluka BioChemika # 03690
EGTA	1 mM	Sigma # E3889
Phenylmethyl sulfonyl fluoride (PMSF)	1 mM	Sigma # P-7626
Leupeptine	10 µg/ml	Sigma # L-2884
Aprotinine	10 µg/ml	Sigma # A-1153
Pepstatine	10 µg/ml	Sigma # P-5318

Phosphatase and protease inhibitors were freshly added to the extraction and A68 buffer.

Following PBS (Bichsel #1000326) perfusion, one half of the mouse brain was dissected into forebrain and brain stem and immediately frozen in liquid nitrogen. Sarkosyl extraction was performed as described previously [95]. The brain tissue was homogenized in 3X volume of cold Extraction buffer (w/v) by using ultraturrax T8 (IKA labortechnik) and briefly sonicated (Bandelin *SONOPLUS*, 90% power, 10 % cycle, 10 sec pulses) Then the samples were centrifuged at 80 000g (28 000rpm) for 15 min by using ultracentrifuge (Beckman Coulter, Optima^{TM} L-70K Ultracentrifuge) by using SW55Ti rotor (Beckman Coulter #99E3241). The supernatant was collected to use for the analysis of soluble tau and the remaining pellets are homogenized in A68 buffer (w/v). Samples were centrifuges at 5 000 rpm for 20 min and 1% of sarkosyl (N-laurylsarcosine, Sigma #L74414) added for 1h30 at 37 °C in thermoshaker (Eppendorf Thermomixer comfort shaker) under shaking (max rpm). Samples were then centrifuged at 80 000g (28 000rpm) for 30 min and the pellet is resuspended in 150µl/g of tissue 50mM Tris HCl pH 7.4, considered as sarkosyl insoluble tau.

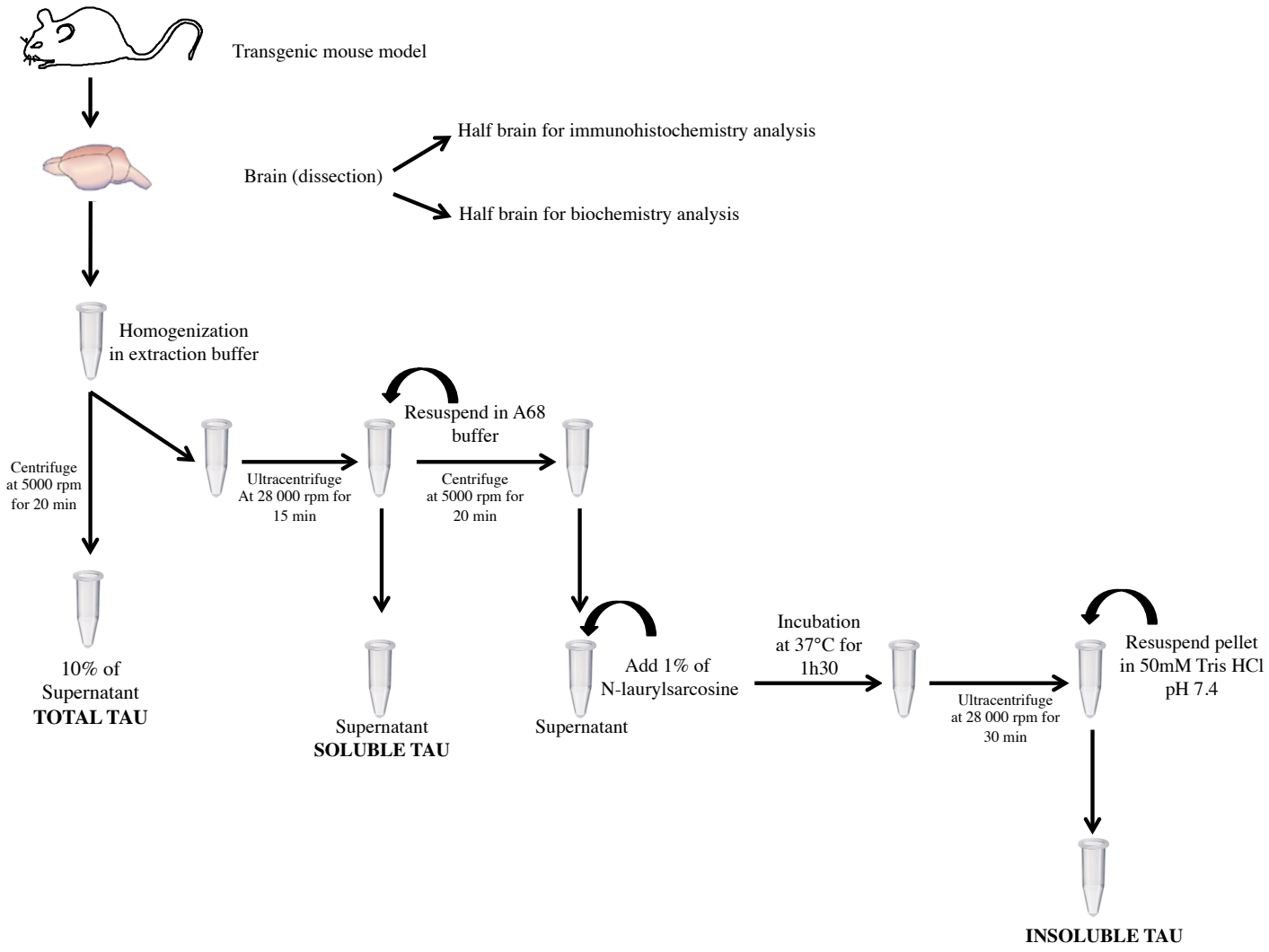

<u>Figure 15:</u> Schematic representation of sarkosyl extraction procedure

Western Blot analysis

Following PBS (Bichsel #1000326) perfusion, one half of the mouse brain was dissected into forebrain and brain stem and immediately frozen in liquid nitrogen. The brain tissue was homogenized in 1:10 volume of TBS-Complete buffer, containing 20mM Tris pH 7.5 (Biomol #08003); 137mM NaCl (Merck #1.06404); 1 tablet of complete mini, protease inhibitor cocktail tablets (Roche # 04693124001); by using Ultraturrax T8 (IKA labortechnik) and then sonicated (Bandelin *Sonopuls*) at 90% power, 10% cycle and 10 pulses. The samples were centrifuged at 5000 rpm for 30 min and the supernatant was collected and aliquoted.

Western blot was performed with the NuPAGE® System from Invitrogen, all materials and reagents were purchased from Invitrogen, BioRad and Amersham.

Gels were loaded with 10µl molecular weight marker and an appropriate amount of protein diluted in TBS-Complete buffer and incubated with 5 µl NuPAGE LDS sample buffer (# NP0007), 2 µl NuPAGE reducing agent (# NP0004) was used to work under reducing or non-reducing conditions.

Reagent	Reduced Sample	Non-reduced Sample
Sample	x μl	x μl
NuPAGE® LDS Sample Buffer (4X)	5 μl	5 μl
NuPAGE® Reducing Agent (10X)	2 μl	--
Deionized Water	x μl	x μl
Total Volume	20 μl	20 μl

Samples were heated for 5 min at 95°C and quickly spin down and then loaded onto a gel. The proteins were separated on 7% Tris-acetate gels at 125V for 90 min. NuPage gels were carefully removed from the cassette and after activation of PVDF membrane (# RPN303F, Amersham Biosciences) in methanol for 30 seconds and 5 min in transfer buffer, NuPage gels were transferred onto PVDF membranes at 30V for 2h at RT by using the XCell II™ Blot Module. Unspecific binding epitopes were blocked with 5% non-fat milk in PBS-T (0.01M PBS pH 7.4; 0.05 % Tween-20 (Calbiochem # 655205)) for 1h at RT and incubated with appropriate dilution of primary antibody O/N at 4°C on a shaker. After washing three times with PBS-T for 5 min at RT, membranes were incubated with horseradish peroxidase (HRP)-conjugated anti-mouse or -rabbit secondary antibody for 1h at RT. Then, membranes were washed three times with PBS-T for 5 min at RT and detected by electrochemiluminescence (ECL) (GE Healthcare, Amersham™ ECL™ #RPN2209).

The following antibodies were used for immunohistochemistry and western blot.

Antibody	Species	Specificity	dilution	Source
Tau-C3	Mouse	Detection of caspase-cleaved Tau (truncated at Asp421)	WB 1:1000; IHC 1:1000	Santa Cruz Biotechnology, Inc, Dallas, Texas #sc-32240
AT8	Mouse	Detection of PHF-tau (Ser202/Thr205)	WB 1:1000; IHC 1:800	Pierce, Rockford, IL #MN1020
AT100	Mouse	Detection of PHF-tau (Ser212/Thr214)	WB 1:1000; IHC 1:500	Pierce, Rockford, IL #MN1060
PHF-1	Mouse	Phosphoserine 396/404	WB 1:2000; IHC 1:1000	Peter Davies, Albert Einstein College of Medecine, Bronx, NY
MC1	Mouse	Detection of aa's 5-15, 312-322	IHC 1:100	Peter Davies, Albert Einstein College of Medecine, Bronx, NY
RD3, clone 8E6/C11	Mouse	Human tau, recognize 3R, residue 209-224	WB 1:4000; IHC 1:3000	Millipore Corporation, Billerica, MA #05-803
RD4, clone1E1/A6	Mouse	Human tau and mouse, recognize 4R, aa 275-291	WB 1:4000; IHC 1:100	Millipore Corporation, Billerica, MA #05-804
HT7	Mouse	Human tau, PHF-tau, residue 159-163	WB 1:4000; IHC 1:800	Pierce, Rockford, IL #MN1000
2F11	Mouse	Axons of CNS, PNS, react with NF-L(70KDa)	IHC 800	Dako, Glostrup, DK #M0762
NF200	Mouse	Neurofilament heavy protein	IHC 1:100	Probst et al., 2000, *Acta Neuropathol*
GFAP	Mouse	Mature astrocytes	IHC 1:500	LabVision (Thermo Fisher Scientific Inc. Kalamazoo, MI #MS-1407-R7
Synaptophysin	Mouse	Specific for presynaptic vesicles	IHC 1:1000	Millipore Corporation, Billerica, MA #MAB5258
MG160	Rabbit	Golgi apparatus	IHC 1:1000	Nicholas Gonatas, Pathology and Laboratory Medicine, University of Pennsylvania, PA
VAMP2/Synaptobrevin 2	Rabbit	Detection of fusion of transport vesicles	IHC 1:1000	Synaptic system, Goettingen, Germany # 104 202
ß-actin	Mouse	Specific for actin	WB 1:5000	Sigma-Aldrich, Saint Louis, MO #A5316
T49	Mouse	Specific for rodent tau	WB 1:10 000	Virginia Lee, CNDR, University of Pennsylvania School of Medicine, Philadelphia, PA
Cox subunit 1a	Mouse	Mitochondrial staining	IHC 1:200	Abcam plc, Cambridge, UK #ab14705

Statistical analysis was performed using IBM® SPSS® Statistics Version 19 for t-tests and ANOVA.

REFERENCES

Scientific papers

1. Hippocrates, *On the sacred disease, Hippocrates, 400 B.C.E*, 1923-1995, London: Heinemann; New York: Putnam.
2. Finger, S., *Origins of Neuroscience: A History of Explorations into Brain Function*. 2001 ed, Oxford and New York: Oxford University Press 1994.
3. Dale Purves, et al., *Neuroscience*. 2nd Edition ed2001, Sunderland (MA): Sinauer Associates Inc.
4. Kandel, R., J.H. Schwartz, and T.M. Jessell, *Principle of neuroscience*. 4th Edition ed2000, New York: McGraw-Hill Medical.
5. Lodish, H., et al., *Molecular Cell Biology*. 4th Edition ed2000, New York: W.H. Freeman.
6. Blankman, K., et al., *World Alzheimer Report 2012*, September 2012, Alzheimer's Disease International (ADI): London.
7. Weingarten, M.D., et al., *A protein factor essential for microtubule assembly.* Proc Natl Acad Sci U S A, 1975. **72**(5): p. 1858-62.
8. Grundke-Iqbal, I., et al., *Microtubule-associated protein tau. A component of Alzheimer paired helical filaments.* J Biol Chem, 1986. **261**(13): p. 6084-9.
9. Kosik, K.S., C.L. Joachim, and D.J. Selkoe, *Microtubule-associated protein tau (tau) is a major antigenic component of paired helical filaments in Alzheimer disease.* Proc Natl Acad Sci U S A, 1986. **83**(11): p. 4044-8.
10. Nukina, N. and Y. Ihara, *One of the Antigenic Determinants of Paired Helical Filaments Is Related to Tau Protein.* Journal of Biochemistry, 1986. **99**(5): p. 1541-1544.
11. Wood, J.G., et al., *Neurofibrillary Tangles of Alzheimer-Disease Share Antigenic Determinants with the Axonal Microtubule-Associated Protein Tau (Tau).* Proceedings of the National Academy of Sciences of the United States of America, 1986. **83**(11): p. 4040-4043.
12. Andreadis, A., W.M. Brown, and K.S. Kosik, *Structure and novel exons of the human tau gene.* Biochemistry, 1992. **31**(43): p. 10626-33.
13. Goedert, M., et al., *Multiple isoforms of human microtubule-associated protein tau: sequences and localization in neurofibrillary tangles of Alzheimer's disease.* Neuron, 1989. **3**(4): p. 519-26.
14. Kosik, K.S., et al., *Developmentally regulated expression of specific tau sequences.* Neuron, 1989. **2**(4): p. 1389-97.
15. De Jesus, J.B., et al., *Iron modulates ecto-phosphohydrolase activities in pathogenic trichomonads.* Parasitol Int, 2006. **55**(4): p. 285-90.
16. Lee, G., R.L. Neve, and K.S. Kosik, *The microtubule binding domain of tau protein.* Neuron, 1989. **2**(6): p. 1615-24.
17. Brandt, R. and G. Lee, *Functional organization of microtubule-associated protein tau. Identification of regions which affect microtubule growth, nucleation, and bundle formation in vitro.* J Biol Chem, 1993. **268**(5): p. 3414-9.
18. Goedert, M., et al., *Cloning and sequencing of the cDNA encoding an isoform of microtubule-associated protein tau containing four tandem repeats: differential expression of tau protein mRNAs in human brain.* EMBO J, 1989. **8**(2): p. 393-9.
19. Himmler, A., et al., *Tau consists of a set of proteins with repeated C-terminal microtubule-binding domains and variable N-terminal domains.* Mol Cell Biol, 1989. **9**(4): p. 1381-8.
20. Lee, G., N. Cowan, and M. Kirschner, *The primary structure and heterogeneity of tau protein from mouse brain.* Science, 1988. **239**(4837): p. 285-8.

21. Bohm, K.J., et al., *Effect of MAP 1, MAP 2, and tau-proteins on structural parameters of tubulin assemblies.* Acta Histochem Suppl, 1990. **39**: p. 357-64.
22. Brandt, R. and G. Lee, *The balance between tau protein's microtubule growth and nucleation activities: implications for the formation of axonal microtubules.* J Neurochem, 1993. **61**(3): p. 997-1005.
23. Cleveland, D.W., S.Y. Hwo, and M.W. Kirschner, *Physical and chemical properties of purified tau factor and the role of tau in microtubule assembly.* J Mol Biol, 1977. **116**(2): p. 227-47.
24. Cleveland, D.W., S.Y. Hwo, and M.W. Kirschner, *Purification of tau, a microtubule-associated protein that induces assembly of microtubules from purified tubulin.* J Mol Biol, 1977. **116**(2): p. 207-25.
25. Nixon, R.A. and R.K. Sihag, *Neurofilament phosphorylation: a new look at regulation and function.* Trends Neurosci, 1991. **14**(11): p. 501-6.
26. Drubin, D.G. and W.J. Nelson, *Origins of cell polarity.* Cell, 1996. **84**(3): p. 335-44.
27. Goodson, H.V., C. Valetti, and T.E. Kreis, *Motors and membrane traffic.* Curr Opin Cell Biol, 1997. **9**(1): p. 18-28.
28. Waterman-Storer, C.M. and E.D. Salmon, *Microtubule dynamics: treadmilling comes around again.* Curr Biol, 1997. **7**(6): p. R369-72.
29. Brady, S.T. and A.O. Sperry, *Biochemical and functional diversity of microtubule motors in the nervous system.* Curr Opin Neurobiol, 1995. **5**(5): p. 551-8.
30. Lippincott-Schwartz, J., et al., *Kinesin is the motor for microtubule-mediated Golgi-to-ER membrane traffic.* J Cell Biol, 1995. **128**(3): p. 293-306.
31. Morris, R.L. and P.J. Hollenbeck, *The regulation of bidirectional mitochondrial transport is coordinated with axonal outgrowth.* J Cell Sci, 1993. **104 (Pt 3)**: p. 917-27.
32. Tanaka, Y., et al., *Targeted disruption of mouse conventional kinesin heavy chain, kif5B, results in abnormal perinuclear clustering of mitochondria.* Cell, 1998. **93**(7): p. 1147-58.
33. Hollenbeck, P.J. and J.A. Swanson, *Radial extension of macrophage tubular lysosomes supported by kinesin.* Nature, 1990. **346**(6287): p. 864-6.
34. Wiemer, E.A., et al., *Visualization of the peroxisomal compartment in living mammalian cells: dynamic behavior and association with microtubules.* J Cell Biol, 1997. **136**(1): p. 71-80.
35. Scales, S.J., R. Pepperkok, and T.E. Kreis, *Visualization of ER-to-Golgi transport in living cells reveals a sequential mode of action for COPII and COPI.* Cell, 1997. **90**(6): p. 1137-48.
36. Trinczek, B., et al., *Tau regulates the attachment/detachment but not the speed of motors in microtubule-dependent transport of single vesicles and organelles.* J Cell Sci, 1999. **112 (Pt 14)**: p. 2355-67.
37. Baudier, J., S.H. Lee, and R.D. Cole, *Separation of the different microtubule-associated tau protein species from bovine brain and their mode II phosphorylation by Ca2+/phospholipid-dependent protein kinase C.* J Biol Chem, 1987. **262**(36): p. 17584-90.
38. Grundke-Iqbal, I., et al., *Abnormal phosphorylation of the microtubule-associated protein tau (tau) in Alzheimer cytoskeletal pathology.* Proc Natl Acad Sci U S A, 1986. **83**(13): p. 4913-7.
39. Ihara, Y., et al., *Phosphorylated tau protein is integrated into paired helical filaments in Alzheimer's disease.* J Biochem, 1986. **99**(6): p. 1807-10.

40. Correas, I., J. Diaz-Nido, and J. Avila, *Microtubule-associated protein tau is phosphorylated by protein kinase C on its tubulin binding domain.* J Biol Chem, 1992. **267**(22): p. 15721-8.
41. Woodgett, J.R., *Molecular cloning and expression of glycogen synthase kinase-3/factor A.* EMBO J, 1990. **9**(8): p. 2431-8.
42. Leroy, K. and J.P. Brion, *Developmental expression and localization of glycogen synthase kinase-3beta in rat brain.* J Chem Neuroanat, 1999. **16**(4): p. 279-93.
43. Cho, J.H. and G.V. Johnson, *Glycogen synthase kinase 3beta phosphorylates tau at both primed and unprimed sites. Differential impact on microtubule binding.* J Biol Chem, 2003. **278**(1): p. 187-93.
44. Lovestone, S., et al., *Phosphorylation of tau by glycogen synthase kinase-3 beta in intact mammalian cells: the effects on the organization and stability of microtubules.* Neuroscience, 1996. **73**(4): p. 1145-57.
45. Wagner, U., et al., *Cellular phosphorylation of tau by GSK-3 beta influences tau binding to microtubules and microtubule organisation.* J Cell Sci, 1996. **109 (Pt 6)**: p. 1537-43.
46. Lucas, J.J., et al., *Decreased nuclear beta-catenin, tau hyperphosphorylation and neurodegeneration in GSK-3beta conditional transgenic mice.* EMBO J, 2001. **20**(1-2): p. 27-39.
47. Spittaels, K., et al., *Glycogen synthase kinase-3beta phosphorylates protein tau and rescues the axonopathy in the central nervous system of human four-repeat tau transgenic mice.* J Biol Chem, 2000. **275**(52): p. 41340-9.
48. Hong, M., et al., *Lithium reduces tau phosphorylation by inhibition of glycogen synthase kinase-3.* J Biol Chem, 1997. **272**(40): p. 25326-32.
49. Lovestone, S., et al., *Lithium reduces tau phosphorylation: effects in living cells and in neurons at therapeutic concentrations.* Biol Psychiatry, 1999. **45**(8): p. 995-1003.
50. Stambolic, V., L. Ruel, and J.R. Woodgett, *Lithium inhibits glycogen synthase kinase-3 activity and mimics wingless signalling in intact cells.* Curr Biol, 1996. **6**(12): p. 1664-8.
51. Sergeant, N., A. Delacourte, and L. Buee, *Tau protein as a differential biomarker of tauopathies.* Biochim Biophys Acta, 2005. **1739**(2-3): p. 179-97.
52. Lau, L.F., et al., *Tau protein phosphorylation as a therapeutic target in Alzheimer's disease.* Curr Top Med Chem, 2002. **2**(4): p. 395-415.
53. Avila, J., et al., *Tau in neurodegenerative diseases: tau phosphorylation and assembly.* Neurotox Res, 2004. **6**(6): p. 477-82.
54. Yamamoto, H., et al., *Dephosphorylation of microtubule proteins by brain protein phosphatases 1 and 2A, and its effect on microtubule assembly.* J Neurochem, 1988. **50**(5): p. 1614-23.
55. Wang, J.Z., et al., *Dephosphorylation of Alzheimer paired helical filaments by protein phosphatase-2A and -2B.* J Biol Chem, 1995. **270**(9): p. 4854-60.
56. Gong, C.X., et al., *Phosphorylation of microtubule-associated protein tau is regulated by protein phosphatase 2A in mammalian brain. Implications for neurofibrillary degeneration in Alzheimer's disease.* J Biol Chem, 2000. **275**(8): p. 5535-44.
57. Goedert, M., et al., *Protein phosphatase 2A is the major enzyme in brain that dephosphorylates tau protein phosphorylated by proline-directed protein kinases or cyclic AMP-dependent protein kinase.* J Neurochem, 1995. **65**(6): p. 2804-7.
58. Liu, F., et al., *Dephosphorylation of tau by protein phosphatase 5: impairment in Alzheimer's disease.* J Biol Chem, 2005. **280**(3): p. 1790-6.
59. Gong, C.X., et al., *Dephosphorylation of microtubule-associated protein tau by protein phosphatase 5.* J Neurochem, 2004. **88**(2): p. 298-310.

60. Gong, C.X., et al., *Post-translational modifications of tau protein in Alzheimer's disease.* J Neural Transm, 2005. **112**(6): p. 813-38.
61. Arnaud, L.T., N. Myeku, and M.E. Figueiredo-Pereira, *Proteasome-caspase-cathepsin sequence leading to tau pathology induced by prostaglandin J2 in neuronal cells.* J Neurochem, 2009. **110**(1): p. 328-42.
62. David, D.C., et al., *Proteasomal degradation of tau protein.* J Neurochem, 2002. **83**(1): p. 176-85.
63. Liu, Y.H., et al., *Proteasome inhibition increases tau accumulation independent of phosphorylation.* Neurobiol Aging, 2009. **30**(12): p. 1949-61.
64. Zhang, J.Y., et al., *Microtubule-associated protein tau is a substrate of ATP/Mg(2+)-dependent proteasome protease system.* J Neural Transm, 2005. **112**(4): p. 547-55.
65. Keller, J.N., K.B. Hanni, and W.R. Markesbery, *Impaired proteasome function in Alzheimer's disease.* J Neurochem, 2000. **75**(1): p. 436-9.
66. Nixon, R.A., *Autophagy, amyloidogenesis and Alzheimer disease.* J Cell Sci, 2007. **120**(Pt 23): p. 4081-91.
67. Oddo, S., *The ubiquitin-proteasome system in Alzheimer's disease.* J Cell Mol Med, 2008. **12**(2): p. 363-73.
68. von Bergen, M., et al., *Tau aggregation is driven by a transition from random coil to beta sheet structure.* Biochim Biophys Acta, 2005. **1739**(2-3): p. 158-66.
69. Perez, M., et al., *In vitro assembly of tau protein: mapping the regions involved in filament formation.* Biochemistry, 2001. **40**(20): p. 5983-91.
70. Morishima, M. and Y. Ihara, *Posttranslational modifications of tau in paired helical filaments.* Dementia, 1994. **5**(5): p. 282-8.
71. Iqbal, K. and I. Grundke-Iqbal, *Ubiquitination and abnormal phosphorylation of paired helical filaments in Alzheimer's disease.* Mol Neurobiol, 1991. **5**(2-4): p. 399-410.
72. Kidd, M., *Paired helical filaments in electron microscopy of Alzheimer's disease.* Nature, 1963. **197**: p. 192-3.
73. Mena, R., et al., *Staging the pathological assembly of truncated tau protein into paired helical filaments in Alzheimer's disease.* Acta Neuropathol, 1996. **91**(6): p. 633-41.
74. Rissman, R.A., et al., *Caspase-cleavage of tau is an early event in Alzheimer disease tangle pathology.* J Clin Invest, 2004. **114**(1): p. 121-30.
75. Gamblin, T.C., et al., *Caspase cleavage of tau: linking amyloid and neurofibrillary tangles in Alzheimer's disease.* Proc Natl Acad Sci U S A, 2003. **100**(17): p. 10032-7.
76. Gendron, T.F. and L. Petrucelli, *The role of tau in neurodegeneration.* Mol Neurodegener, 2009. **4**: p. 13.
77. Guillozet-Bongaarts, A.L., et al., *Tau truncation during neurofibrillary tangle evolution in Alzheimer's disease.* Neurobiol Aging, 2005. **26**(7): p. 1015-22.
78. Mondragon-Rodriguez, S., et al., *Cleavage and conformational changes of tau protein follow phosphorylation during Alzheimer's disease.* Int J Exp Pathol, 2008. **89**(2): p. 81-90.
79. Saito, M., et al., *Tau phosphorylation and cleavage in ethanol-induced neurodegeneration in the developing mouse brain.* Neurochem Res, 2010. **35**(4): p. 651-9.
80. Rohn, T.T., et al., *Caspase Activation in the Alzheimer's Disease Brain: Tortuous and Torturous.* Drug News Perspect, 2002. **15**(9): p. 549-557.
81. de la Monte, S.M., Y.K. Sohn, and J.R. Wands, *Correlates of p53- and Fas (CD95)-mediated apoptosis in Alzheimer's disease.* J Neurol Sci, 1997. **152**(1): p. 73-83.

82. Fasulo, L., et al., *The neuronal microtubule-associated protein tau is a substrate for caspase-3 and an effector of apoptosis.* J Neurochem, 2000. **75**(2): p. 624-33.
83. Wai, M.S., et al., *Co-localization of hyperphosphorylated tau and caspases in the brainstem of Alzheimer's disease patients.* Biogerontology, 2009. **10**(4): p. 457-69.
84. Canu, N., et al., *Tau cleavage and dephosphorylation in cerebellar granule neurons undergoing apoptosis.* J Neurosci, 1998. **18**(18): p. 7061-74.
85. Abraha, A., et al., *C-terminal inhibition of tau assembly in vitro and in Alzheimer's disease.* J Cell Sci, 2000. **113 Pt 21**: p. 3737-45.
86. Basurto-Islas, G., et al., *Accumulation of aspartic acid421- and glutamic acid391-cleaved tau in neurofibrillary tangles correlates with progression in Alzheimer disease.* J Neuropathol Exp Neurol, 2008. **67**(5): p. 470-83.
87. Horowitz, P.M., et al., *Early N-terminal changes and caspase-6 cleavage of tau in Alzheimer's disease.* J Neurosci, 2004. **24**(36): p. 7895-902.
88. Bandyopadhyay, B., et al., *Tau aggregation and toxicity in a cell culture model of tauopathy.* J Biol Chem, 2007. **282**(22): p. 16454-64.
89. Fasulo, L., G. Ugolini, and A. Cattaneo, *Apoptotic effect of caspase-3 cleaved tau in hippocampal neurons and its potentiation by tau FTDP-mutation N279K.* J Alzheimers Dis, 2005. **7**(1): p. 3-13.
90. Chun, W. and G.V. Johnson, *The role of tau phosphorylation and cleavage in neuronal cell death.* Front Biosci, 2007. **12**: p. 733-56.
91. Quintanilla, R.A., et al., *Truncated tau and Abeta cooperatively impair mitochondria in primary neurons.* Neurobiol Aging, 2012. **33**(3): p. 619 e25-35.
92. Matthews-Roberson, T.A., et al., *Immortalized cortical neurons expressing caspase-cleaved tau are sensitized to endoplasmic reticulum stress induced cell death.* Brain Res, 2008. **1234**: p. 206-12.
93. Zhang, Q., X. Zhang, and A. Sun, *Truncated tau at D421 is associated with neurodegeneration and tangle formation in the brain of Alzheimer transgenic models.* Acta Neuropathol, 2009. **117**(6): p. 687-97.
94. Filipcik, P., et al., *Cortical and hippocampal neurons from truncated tau transgenic rat express multiple markers of neurodegeneration.* Cell Mol Neurobiol, 2009. **29**(6-7): p. 895-900.
95. Delobel, P., et al., *Analysis of tau phosphorylation and truncation in a mouse model of human tauopathy.* Am J Pathol, 2008. **172**(1): p. 123-31.
96. de Calignon, A., et al., *Caspase activation precedes and leads to tangles.* Nature, 2010. **464**(7292): p. 1201-4.
97. Koson, P., et al., *Truncated tau expression levels determine life span of a rat model of tauopathy without causing neuronal loss or correlating with terminal neurofibrillary tangle load.* Eur J Neurosci, 2008. **28**(2): p. 239-46.
98. Cente, M., et al., *Expression of a truncated tau protein induces oxidative stress in a rodent model of tauopathy.* Eur J Neurosci, 2006. **24**(4): p. 1085-90.
99. McMillan, P.J., et al., *Truncation of tau at E391 promotes early pathologic changes in transgenic mice.* J Neuropathol Exp Neurol, 2011. **70**(11): p. 1006-19.
100. Garcia-Sierra, F., et al., *Accumulation of C-terminally truncated tau protein associated with vulnerability of the perforant pathway in early stages of neurofibrillary pathology in Alzheimer's disease.* J Chem Neuroanat, 2001. **22**(1-2): p. 65-77.
101. Garcia-Sierra, F., S. Mondragon-Rodriguez, and G. Basurto-Islas, *Truncation of tau protein and its pathological significance in Alzheimer's disease.* J Alzheimers Dis, 2008. **14**(4): p. 401-9.
102. Alzheimer, A., et al., *An English translation of Alzheimer's 1907 paper, "Uber eine eigenartige Erkankung der Hirnrinde".* Clin Anat, 1995. **8**(6): p. 429-31.

103. Alzheimer, A., *Über eine eigenartige Erkrankung der Hirnrinde.* Allg Z Psychiat Psych-Gerichtl Med, 1907. **64**(1): p. 146-148.
104. Alzheimer, A., *Über einen eigenartigen schweren Erkrankungsprozess der Hirnrinde.* Neurologisches Centralblatt, 1906. **25**(23): p. 1134.
105. Alzheimer, A., *Über eigenartige Krankheitsfälle des späteren Alters. Z ges.* Neurol Psychiat, 1911. **4**: p. p. 356-385.
106. Mouton, P.R., et al., *Cognitive decline strongly correlates with cortical atrophy in Alzheimer's dementia.* Neurobiol Aging, 1998. **19**(5): p. 371-7.
107. Terry, R.D., et al., *Physical basis of cognitive alterations in Alzheimer's disease: synapse loss is the major correlate of cognitive impairment.* Ann Neurol, 1991. **30**(4): p. 572-80.
108. West, M.J., et al., *Differences in the pattern of hippocampal neuronal loss in normal ageing and Alzheimer's disease.* Lancet, 1994. **344**(8925): p. 769-72.
109. Gomez-Isla, T., et al., *Profound loss of layer II entorhinal cortex neurons occurs in very mild Alzheimer's disease.* J Neurosci, 1996. **16**(14): p. 4491-500.
110. Castellani, R.J., et al., *Alzheimer disease pathology as a host response.* J Neuropathol Exp Neurol, 2008. **67**(6): p. 523-31.
111. Blocq, P. and G. Marinesco, *Sur les lésions et la pathogénie de l'épilepsie dite essentielle.* La Semaine Médicale 1892: p. 12: p. 445-446.
112. Castellani, R.J., R.K. Rolston, and M.A. Smith, *Alzheimer disease.* Dis Mon, 2010. **56**(9): p. 484-546.
113. Itagaki, S., et al., *Relationship of microglia and astrocytes to amyloid deposits of Alzheimer disease.* J Neuroimmunol, 1989. **24**(3): p. 173-82.
114. Wisniewski, H.M., et al., *Spectrum of morphological appearance of amyloid deposits in Alzheimer's disease.* Acta Neuropathol, 1989. **78**(4): p. 337-47.
115. Tagliavini, F., et al., *Preamyloid deposits in the cerebral cortex of patients with Alzheimer's disease and nondemented individuals.* Neurosci Lett, 1988. **93**(2-3): p. 191-6.
116. Yamaguchi, H., et al., *Electron micrograph of diffuse plaques. Initial stage of senile plaque formation in the Alzheimer brain.* Am J Pathol, 1989. **135**(4): p. 593-7.
117. Mandybur, T.I., *The incidence of cerebral amyloid angiopathy in Alzheimer's disease.* Neurology, 1975. **25**(2): p. 120-6.
118. Vinters, H.V., et al., *Immunohistochemical study of cerebral amyloid angiopathy. II. Enhancement of immunostaining using formic acid pretreatment of tissue sections.* Am J Pathol, 1988. **133**(1): p. 150-62.
119. Glenner, G.G. and C.W. Wong, *Alzheimer's disease and Down's syndrome: sharing of a unique cerebrovascular amyloid fibril protein.* Biochem Biophys Res Commun, 1984. **122**(3): p. 1131-5.
120. Masters, C.L., et al., *Amyloid plaque core protein in Alzheimer disease and Down syndrome.* Proc Natl Acad Sci U S A, 1985. **82**(12): p. 4245-9.
121. Selkoe, D.J., et al., *Isolation of low-molecular-weight proteins from amyloid plaque fibers in Alzheimer's disease.* J Neurochem, 1986. **46**(6): p. 1820-34.
122. Cappai, R. and A.R. White, *Amyloid beta.* Int J Biochem Cell Biol, 1999. **31**(9): p. 885-9.
123. Selkoe, D.J., *Alzheimer's disease: genes, proteins, and therapy.* Physiol Rev, 2001. **81**(2): p. 741-66.
124. Wong, C.W., V. Quaranta, and G.G. Glenner, *Neuritic plaques and cerebrovascular amyloid in Alzheimer disease are antigenically related.* Proc Natl Acad Sci U S A, 1985. **82**(24): p. 8729-32.

125. Kang, J., et al., *The precursor of Alzheimer's disease amyloid A4 protein resembles a cell-surface receptor.* Nature, 1987. **325**(6106): p. 733-6.
126. Edbauer, D., et al., *Reconstitution of gamma-secretase activity.* Nat Cell Biol, 2003. **5**(5): p. 486-8.
127. Vassar, R., et al., *Beta-secretase cleavage of Alzheimer's amyloid precursor protein by the transmembrane aspartic protease BACE.* Science, 1999. **286**(5440): p. 735-41.
128. Hardy, J. and D. Allsop, *Amyloid deposition as the central event in the aetiology of Alzheimer's disease.* Trends Pharmacol Sci, 1991. **12**(10): p. 383-8.
129. Hardy, J. and D.J. Selkoe, *The amyloid hypothesis of Alzheimer's disease: progress and problems on the road to therapeutics.* Science, 2002. **297**(5580): p. 353-6.
130. Dickson, D.W., et al., *Identification of normal and pathological aging in prospectively studied nondemented elderly humans.* Neurobiol Aging, 1992. **13**(1): p. 179-89.
131. Arriagada, P.V., K. Marzloff, and B.T. Hyman, *Distribution of Alzheimer-type pathologic changes in nondemented elderly individuals matches the pattern in Alzheimer's disease.* Neurology, 1992. **42**(9): p. 1681-8.
132. Klein, W.L., G.A. Krafft, and C.E. Finch, *Targeting small Abeta oligomers: the solution to an Alzheimer's disease conundrum?* Trends Neurosci, 2001. **24**(4): p. 219-24.
133. Kirkitadze, M.D., G. Bitan, and D.B. Teplow, *Paradigm shifts in Alzheimer's disease and other neurodegenerative disorders: the emerging role of oligomeric assemblies.* J Neurosci Res, 2002. **69**(5): p. 567-77.
134. Selkoe, D.J., *Alzheimer's disease is a synaptic failure.* Science, 2002. **298**(5594): p. 789-91.
135. Walsh, D.M., et al., *Amyloid-beta oligomers: their production, toxicity and therapeutic inhibition.* Biochem Soc Trans, 2002. **30**(4): p. 552-7.
136. Masters, C.L., et al., *Molecular mechanisms for Alzheimer's disease: implications for neuroimaging and therapeutics.* J Neurochem, 2006. **97**(6): p. 1700-25.
137. Roberson, E.D., et al., *Reducing endogenous tau ameliorates amyloid beta-induced deficits in an Alzheimer's disease mouse model.* Science, 2007. **316**(5825): p. 750-4.
138. Ittner, L.M., et al., *Dendritic function of tau mediates amyloid-beta toxicity in Alzheimer's disease mouse models.* Cell, 2010. **142**(3): p. 387-97.
139. Gotz, J., et al., *Formation of neurofibrillary tangles in P301l tau transgenic mice induced by Abeta 42 fibrils.* Science, 2001. **293**(5534): p. 1491-5.
140. Steele, J.C., J.C. Richardson, and J. Olszewski, *Progressive Supranuclear Palsy. A Heterogeneous Degeneration Involving the Brain Stem, Basal Ganglia and Cerebellum with Vertical Gaze and Pseudobulbar Palsy, Nuchal Dystonia and Dementia.* Arch Neurol, 1964. **10**: p. 333-59.
141. Albert, M.L., R.G. Feldman, and A.L. Willis, *The 'subcortical dementia' of progressive supranuclear palsy.* J Neurol Neurosurg Psychiatry, 1974. **37**(2): p. 121-30.
142. Cummings, J.L. and D.F. Benson, *Subcortical dementia. Review of an emerging concept.* Arch Neurol, 1984. **41**(8): p. 874-9.
143. Probst, A., et al., *Progressive supranuclear palsy: extensive neuropil threads in addition to neurofibrillary tangles. Very similar antigenicity of subcortical neuronal pathology in progressive supranuclear palsy and Alzheimer's disease.* Acta Neuropathol, 1988. **77**(1): p. 61-8.
144. Litvan, I., et al., *Clinical research criteria for the diagnosis of progressive supranuclear palsy (Steele-Richardson-Olszewski syndrome): report of the NINDS-SPSP international workshop.* Neurology, 1996. **47**(1): p. 1-9.

145. Hauw, J.J., et al., *Constant neurofibrillary changes in the neocortex in progressive supranuclear palsy. Basic differences with Alzheimer's disease and aging.* Neurosci Lett, 1990. **119**(2): p. 182-6.
146. Sha, S., et al., *Are frontotemporal lobar degeneration, progressive supranuclear palsy and corticobasal degeneration distinct diseases?* Nat Clin Pract Neurol, 2006. **2**(12): p. 658-65.
147. Rebeiz, J.J., E.H. Kolodny, and E.P. Richardson, Jr., *Corticodentatonigral degeneration with neuronal achromasia.* Arch Neurol, 1968. **18**(1): p. 20-33.
148. Grimes, D.A., A.E. Lang, and C.B. Bergeron, *Dementia as the most common presentation of cortical-basal ganglionic degeneration.* Neurology, 1999. **53**(9): p. 1969-74.
149. Mathuranath, P.S., et al., *Corticobasal ganglionic degeneration and/or frontotemporal dementia? A report of two overlap cases and review of literature.* J Neurol Neurosurg Psychiatry, 2000. **68**(3): p. 304-12.
150. Constantinidis, J., J. Richard, and R. Tissot, *Pick's disease. Histological and clinical correlations.* Eur Neurol, 1974. **11**(4): p. 208-17.
151. Brion, S., J. Plas, and A. Jeanneau, *[Pick's disease. Anatomo-clinical point of view].* Rev Neurol (Paris), 1991. **147**(11): p. 693-704.
152. Uchihara, T., K. Ikeda, and K. Tsuchiya, *Pick body disease and Pick syndrome.* Neuropathology, 2003. **23**(4): p. 318-26.
153. Ikeda, K., et al., *Pick-body-like inclusions in corticobasal degeneration differ from Pick bodies in Pick's disease.* Acta Neuropathol, 2002. **103**(2): p. 115-8.
154. Oda, T., et al., *Pick's disease with Pick bodies: an unusual autopsy case showing degeneration of the pontine nucleus, dentate nucleus, Clarke's column, and lower motor neuron.* Neuropathology, 2007. **27**(1): p. 81-9.
155. Braak, H. and E. Braak, *Argyrophilic grain disease: frequency of occurrence in different age categories and neuropathological diagnostic criteria.* J Neural Transm, 1998. **105**(8-9): p. 801-19.
156. Tolnay, M., A.U. Monsch, and A. Probst, *Argyrophilic grain disease. A frequent dementing disorder in aged patients.* Adv Exp Med Biol, 2001. **487**: p. 39-58.
157. Braak, H. and E. Braak, *Argyrophilic grains: characteristic pathology of cerebral cortex in cases of adult onset dementia without Alzheimer changes.* Neurosci Lett, 1987. **76**(1): p. 124-7.
158. Braak, H. and E. Braak, *Cortical and subcortical argyrophilic grains characterize a disease associated with adult onset dementia.* Neuropathol Appl Neurobiol, 1989. **15**(1): p. 13-26.
159. Saito, Y., et al., *Severe involvement of the ambient gyrus in a case of dementia with argyrophilic grain disease.* J Neurol Sci, 2002. **196**(1-2): p. 71-5.
160. Wilhelmsen, K.C., et al., *Localization of disinhibition-dementia-parkinsonism-amyotrophy complex to 17q21-22.* Am J Hum Genet, 1994. **55**(6): p. 1159-65.
161. Foster, N.L., et al., *Frontotemporal dementia and parkinsonism linked to chromosome 17: a consensus conference. Conference Participants.* Ann Neurol, 1997. **41**(6): p. 706-15.
162. Heutink, P., et al., *Hereditary frontotemporal dementia is linked to chromosome 17q21-q22: a genetic and clinicopathological study of three Dutch families.* Ann Neurol, 1997. **41**(2): p. 150-9.
163. Hutton, M., et al., *Association of missense and 5'-splice-site mutations in tau with the inherited dementia FTDP-17.* Nature, 1998. **393**(6686): p. 702-5.

164. Lewis, J., et al., *Neurofibrillary tangles, amyotrophy and progressive motor disturbance in mice expressing mutant (P301L) tau protein.* Nat Genet, 2000. **25**(4): p. 402-5.
165. Allen, B., et al., *Abundant tau filaments and nonapoptotic neurodegeneration in transgenic mice expressing human P301S tau protein.* J Neurosci, 2002. **22**(21): p. 9340-51.
166. Bugiani, O., et al., *Frontotemporal dementia and corticobasal degeneration in a family with a P301S mutation in tau.* J Neuropathol Exp Neurol, 1999. **58**(6): p. 667-77.
167. D'Souza, I. and G.D. Schellenberg, *Regulation of tau isoform expression and dementia.* Biochim Biophys Acta, 2005. **1739**(2-3): p. 104-15.
168. Stanford, P.M., et al., *Mutations in the tau gene that cause an increase in three repeat tau and frontotemporal dementia.* Brain, 2003. **126**(Pt 4): p. 814-26.
169. Liu, F. and C.X. Gong, *Tau exon 10 alternative splicing and tauopathies.* Mol Neurodegener, 2008. **3**: p. 8.
170. Brion, J.P., G. Tremp, and J.N. Octave, *Transgenic expression of the shortest human tau affects its compartmentalization and its phosphorylation as in the pretangle stage of Alzheimer's disease.* Am J Pathol, 1999. **154**(1): p. 255-70.
171. Cuervo, A.M., *Autophagy in neurons: it is not all about food.* Trends Mol Med, 2006. **12**(10): p. 461-4.
172. Filipcik, P., et al., *First transgenic rat model developing progressive cortical neurofibrillary tangles.* Neurobiol Aging, 2012. **33**(7): p. 1448-56.
173. Zilka, N., et al., *Truncated tau from sporadic Alzheimer's disease suffices to drive neurofibrillary degeneration in vivo.* FEBS Lett, 2006. **580**(15): p. 3582-8.
174. Rao, R.V. and D.E. Bredesen, *Misfolded proteins, endoplasmic reticulum stress and neurodegeneration.* Curr Opin Cell Biol, 2004. **16**(6): p. 653-62.
175. Kopito, R.R. and D. Ron, *Conformational disease.* Nat Cell Biol, 2000. **2**(11): p. E207-9.
176. Selkoe, D.J., *Folding proteins in fatal ways.* Nature, 2003. **426**(6968): p. 900-4.
177. Taylor, J.P., J. Hardy, and K.H. Fischbeck, *Toxic proteins in neurodegenerative disease.* Science, 2002. **296**(5575): p. 1991-5.
178. Mizushima, N. and M. Komatsu, *Autophagy: renovation of cells and tissues.* Cell, 2011. **147**(4): p. 728-41.
179. Klionsky, D.J., et al., *A unified nomenclature for yeast autophagy-related genes.* Dev Cell, 2003. **5**(4): p. 539-45.
180. Xie, Z. and D.J. Klionsky, *Autophagosome formation: core machinery and adaptations.* Nat Cell Biol, 2007. **9**(10): p. 1102-9.
181. Ohsumi, Y. and N. Mizushima, *Two ubiquitin-like conjugation systems essential for autophagy.* Semin Cell Dev Biol, 2004. **15**(2): p. 231-6.
182. Kabeya, Y., et al., *LC3, a mammalian homologue of yeast Apg8p, is localized in autophagosome membranes after processing.* EMBO J, 2000. **19**(21): p. 5720-8.
183. Tanida, I., T. Ueno, and E. Kominami, *Human light chain 3/MAP1LC3B is cleaved at its carboxyl-terminal Met121 to expose Gly120 for lipidation and targeting to autophagosomal membranes.* J Biol Chem, 2004. **279**(46): p. 47704-10.
184. Noda, T. and Y. Ohsumi, *Tor, a phosphatidylinositol kinase homologue, controls autophagy in yeast.* J Biol Chem, 1998. **273**(7): p. 3963-6.
185. Ravikumar, B., et al., *Inhibition of mTOR induces autophagy and reduces toxicity of polyglutamine expansions in fly and mouse models of Huntington disease.* Nat Genet, 2004. **36**(6): p. 585-95.

186. Mordier, S., et al., *Leucine limitation induces autophagy and activation of lysosome-dependent proteolysis in C2C12 myotubes through a mammalian target of rapamycin-independent signaling pathway.* J Biol Chem, 2000. **275**(38): p. 29900-6.
187. Kanazawa, T., et al., *Amino acids and insulin control autophagic proteolysis through different signaling pathways in relation to mTOR in isolated rat hepatocytes.* J Biol Chem, 2004. **279**(9): p. 8452-9.
188. Sarkar, S., et al., *Small molecules enhance autophagy and reduce toxicity in Huntington's disease models.* Nat Chem Biol, 2007. **3**(6): p. 331-8.
189. Grune, T., et al., *Decreased proteolysis caused by protein aggregates, inclusion bodies, plaques, lipofuscin, ceroid, and 'aggresomes' during oxidative stress, aging, and disease.* Int J Biochem Cell Biol, 2004. **36**(12): p. 2519-30.
190. Qin, Z.H., et al., *Autophagy regulates the processing of amino terminal huntingtin fragments.* Hum Mol Genet, 2003. **12**(24): p. 3231-44.
191. Anglade, P., et al., *Apoptosis and autophagy in nigral neurons of patients with Parkinson's disease.* Histol Histopathol, 1997. **12**(1): p. 25-31.
192. Yu, W.H., et al., *Autophagic vacuoles are enriched in amyloid precursor protein-secretase activities: implications for beta-amyloid peptide over-production and localization in Alzheimer's disease.* Int J Biochem Cell Biol, 2004. **36**(12): p. 2531-40.
193. Shintani, T. and D.J. Klionsky, *Autophagy in health and disease: a double-edged sword.* Science, 2004. **306**(5698): p. 990-5.
194. Yue, Z., et al., *A novel protein complex linking the delta 2 glutamate receptor and autophagy: implications for neurodegeneration in lurcher mice.* Neuron, 2002. **35**(5): p. 921-33.
195. Dauer, W. and S. Przedborski, *Parkinson's disease: mechanisms and models.* Neuron, 2003. **39**(6): p. 889-909.
196. Ravikumar, B., R. Duden, and D.C. Rubinsztein, *Aggregate-prone proteins with polyglutamine and polyalanine expansions are degraded by autophagy.* Hum Mol Genet, 2002. **11**(9): p. 1107-17.
197. Webb, J.L., et al., *Alpha-Synuclein is degraded by both autophagy and the proteasome.* J Biol Chem, 2003. **278**(27): p. 25009-13.
198. Malagelada, C., et al., *Rapamycin protects against neuron death in in vitro and in vivo models of Parkinson's disease.* J Neurosci, 2010. **30**(3): p. 1166-75.
199. Dehay, B., et al., *Pathogenic lysosomal depletion in Parkinson's disease.* J Neurosci, 2010. **30**(37): p. 12535-44.
200. Ross, C.A. and S.J. Tabrizi, *Huntington's disease: from molecular pathogenesis to clinical treatment.* Lancet Neurol, 2011. **10**(1): p. 83-98.
201. Wang, T., U. Lao, and B.A. Edgar, *TOR-mediated autophagy regulates cell death in Drosophila neurodegenerative disease.* J Cell Biol, 2009. **186**(5): p. 703-11.
202. Ittner, L.M. and J. Gotz, *Amyloid-beta and tau--a toxic pas de deux in Alzheimer's disease.* Nat Rev Neurosci, 2011. **12**(2): p. 65-72.
203. Nixon, R.A., et al., *Extensive involvement of autophagy in Alzheimer disease: an immuno-electron microscopy study.* J Neuropathol Exp Neurol, 2005. **64**(2): p. 113-22.
204. Khurana, V., et al., *TOR-mediated cell-cycle activation causes neurodegeneration in a Drosophila tauopathy model.* Curr Biol, 2006. **16**(3): p. 230-41.
205. Berger, Z., et al., *Rapamycin alleviates toxicity of different aggregate-prone proteins.* Hum Mol Genet, 2006. **15**(3): p. 433-42.
206. Pickford, F., et al., *The autophagy-related protein beclin 1 shows reduced expression in early Alzheimer disease and regulates amyloid beta accumulation in mice.* J Clin Invest, 2008. **118**(6): p. 2190-9.

207. Yang, D.S., et al., *Reversal of autophagy dysfunction in the TgCRND8 mouse model of Alzheimer's disease ameliorates amyloid pathologies and memory deficits.* Brain, 2011. **134**(Pt 1): p. 258-77.
208. Hung, S.Y., et al., *Autophagy protects neuron from Abeta-induced cytotoxicity.* Autophagy, 2009. **5**(4): p. 502-10.
209. Caccamo, A., et al., *Molecular interplay between mammalian target of rapamycin (mTOR), amyloid-beta, and Tau: effects on cognitive impairments.* J Biol Chem, 2010. **285**(17): p. 13107-20.
210. Spilman, P., et al., *Inhibition of mTOR by rapamycin abolishes cognitive deficits and reduces amyloid-beta levels in a mouse model of Alzheimer's disease.* PLoS One, 2010. **5**(4): p. e9979.
211. Li, X., et al., *Levels of mTOR and its downstream targets 4E-BP1, eEF2, and eEF2 kinase in relationships with tau in Alzheimer's disease brain.* FEBS J, 2005. **272**(16): p. 4211-20.
212. Harrison, D.E., et al., *Rapamycin fed late in life extends lifespan in genetically heterogeneous mice.* Nature, 2009. **460**(7253): p. 392-5.
213. Zhang, S., et al., *Rapamycin promotes beta-amyloid production via ADAM-10 inhibition.* Biochem Biophys Res Commun, 2010. **398**(3): p. 337-41.
214. Cully, M. and J. Downward, *Translational responses to growth factors and stress.* Biochem Soc Trans, 2009. **37**(Pt 1): p. 284-8.
215. Nemoto, T., et al., *Homologous posttranscriptional regulation of insulin-like growth factor-I receptor level via glycogen synthase kinase-3beta and mammalian target of rapamycin in adrenal chromaffin cells: effect on tau phosphorylation.* Neuropharmacology, 2010. **58**(7): p. 1097-108.
216. Mendelsohn, A.R. and J.W. Larrick, *Rapamycin as an antiaging therapeutic?: targeting mammalian target of rapamycin to treat Hutchinson-Gilford progeria and neurodegenerative diseases.* Rejuvenation Res, 2011. **14**(4): p. 437-41.
217. Watanabe, R., L. Wei, and J. Huang, *mTOR signaling, function, novel inhibitors, and therapeutic targets.* J Nucl Med, 2011. **52**(4): p. 497-500.
218. Feldman, M.E., et al., *Active-site inhibitors of mTOR target rapamycin-resistant outputs of mTORC1 and mTORC2.* PLoS Biol, 2009. **7**(2): p. e38.
219. Pous, C. and P. Codogno, *Lysosome positioning coordinates mTORC1 activity and autophagy.* Nat Cell Biol, 2011. **13**(4): p. 342-4.
220. Pei, J.J. and J. Hugon, *mTOR-dependent signalling in Alzheimer's disease.* J Cell Mol Med, 2008. **12**(6B): p. 2525-32.
221. Rosner, M., et al., *The mTOR pathway and its role in human genetic diseases.* Mutat Res, 2008. **659**(3): p. 284-92.
222. Meske, V., F. Albert, and T.G. Ohm, *Coupling of mammalian target of rapamycin with phosphoinositide 3-kinase signaling pathway regulates protein phosphatase 2A- and glycogen synthase kinase-3 -dependent phosphorylation of Tau.* J Biol Chem, 2008. **283**(1): p. 100-9.
223. Powers, R.W., 3rd, et al., *Extension of chronological life span in yeast by decreased TOR pathway signaling.* Genes Dev, 2006. **20**(2): p. 174-84.
224. Bjedov, I., et al., *Mechanisms of life span extension by rapamycin in the fruit fly Drosophila melanogaster.* Cell Metab, 2010. **11**(1): p. 35-46.
225. Hall, M.N., *mTOR-what does it do?* Transplant Proc, 2008. **40**(10 Suppl): p. S5-8.
226. Medvedik, O., et al., *MSN2 and MSN4 link calorie restriction and TOR to sirtuin-mediated lifespan extension in Saccharomyces cerevisiae.* PLoS Biol, 2007. **5**(10): p. e261.

227. Martel, R.R., J. Klicius, and S. Galet, *Inhibition of the immune response by rapamycin, a new antifungal antibiotic.* Can J Physiol Pharmacol, 1977. **55**(1): p. 48-51.
228. Janes, M.R. and D.A. Fruman, *Immune regulation by rapamycin: moving beyond T cells.* Sci Signal, 2009. **2**(67): p. pe25.
229. Caccamo, A., et al., *Rapamycin rescues TDP-43 mislocalization and the associated low molecular mass neurofilament instability.* J Biol Chem, 2009. **284**(40): p. 27416-24.
230. Santos, R.X., et al., *Effects of rapamycin and TOR on aging and memory: implications for Alzheimer's disease.* J Neurochem, 2011. **117**(6): p. 927-36.
231. Wyttenbach, A., et al., *Amelioration of protein misfolding disease by rapamycin: translation or autophagy?* Autophagy, 2008. **4**(4): p. 542-5.
232. Selkoe, D.J., *Amyloid protein and Alzheimer's disease.* Sci Am, 1991. **265**(5): p. 68-71, 74-6, 78.
233. Buee, L., et al., *Tau protein isoforms, phosphorylation and role in neurodegenerative disorders.* Brain Res Brain Res Rev, 2000. **33**(1): p. 95-130.
234. Vieira, M.N., et al., *Soluble oligomers from a non-disease related protein mimic Abeta-induced tau hyperphosphorylation and neurodegeneration.* J Neurochem, 2007. **103**(2): p. 736-48.
235. Lee, V.M., M. Goedert, and J.Q. Trojanowski, *Neurodegenerative tauopathies.* Annu Rev Neurosci, 2001. **24**: p. 1121-59.
236. Poorkaj, P., et al., *Tau is a candidate gene for chromosome 17 frontotemporal dementia.* Ann Neurol, 1998. **43**(6): p. 815-25.
237. Spillantini, M.G., et al., *Mutation in the tau gene in familial multiple system tauopathy with presenile dementia.* Proc Natl Acad Sci U S A, 1998. **95**(13): p. 7737-41.
238. Gotz, J., et al., *Transgenic animal models of Alzheimer's disease and related disorders: histopathology, behavior and therapy.* Mol Psychiatry, 2004. **9**(7): p. 664-83.
239. Berger, Z., et al., *Accumulation of pathological tau species and memory loss in a conditional model of tauopathy.* J Neurosci, 2007. **27**(14): p. 3650-62.
240. Mudher, A., et al., *GSK-3beta inhibition reverses axonal transport defects and behavioural phenotypes in Drosophila.* Mol Psychiatry, 2004. **9**(5): p. 522-30.
241. Cowan, C.M., et al., *Soluble hyper-phosphorylated tau causes microtubule breakdown and functionally compromises normal tau in vivo.* Acta Neuropathol, 2010. **120**(5): p. 593-604.
242. Kimura, T., et al., *Hyperphosphorylated tau in parahippocampal cortex impairs place learning in aged mice expressing wild-type human tau.* EMBO J, 2007. **26**(24): p. 5143-52.
243. Probst, A., et al., *Axonopathy and amyotrophy in mice transgenic for human four-repeat tau protein.* Acta Neuropathol, 2000. **99**(5): p. 469-81.
244. Mocanu, M.M., et al., *The potential for beta-structure in the repeat domain of tau protein determines aggregation, synaptic decay, neuronal loss, and coassembly with endogenous Tau in inducible mouse models of tauopathy.* J Neurosci, 2008. **28**(3): p. 737-48.
245. Sydow, A., et al., *Tau-induced defects in synaptic plasticity, learning, and memory are reversible in transgenic mice after switching off the toxic Tau mutant.* J Neurosci, 2011. **31**(7): p. 2511-25.
246. Wittmann, C.W., et al., *Tauopathy in Drosophila: neurodegeneration without neurofibrillary tangles.* Science, 2001. **293**(5530): p. 711-4.

247. Williams, D.W., M. Tyrer, and D. Shepherd, *Tau and tau reporters disrupt central projections of sensory neurons in Drosophila.* J Comp Neurol, 2000. **428**(4): p. 630-40.
248. Chee, F.C., et al., *Over-expression of tau results in defective synaptic transmission in Drosophila neuromuscular junctions.* Neurobiol Dis, 2005. **20**(3): p. 918-28.
249. Maeda, S., et al., *Granular tau oligomers as intermediates of tau filaments.* Biochemistry, 2007. **46**(12): p. 3856-61.
250. Maeda, S., et al., *Increased levels of granular tau oligomers: an early sign of brain aging and Alzheimer's disease.* Neurosci Res, 2006. **54**(3): p. 197-201.
251. Patterson, K.R., et al., *Heat shock protein 70 prevents both tau aggregation and the inhibitory effects of preexisting tau aggregates on fast axonal transport.* Biochemistry, 2011. **50**(47): p. 10300-10.
252. Lasagna-Reeves, C.A., et al., *Preparation and characterization of neurotoxic tau oligomers.* Biochemistry, 2010. **49**(47): p. 10039-41.
253. Lasagna-Reeves, C.A., et al., *Tau oligomers impair memory and induce synaptic and mitochondrial dysfunction in wild-type mice.* Mol Neurodegener, 2011. **6**: p. 39.
254. Henkins, K.M., et al., *Extensive p-tau pathology and SDS-stable p-tau oligomers in Alzheimer's cortical synapses.* Brain Pathol, 2012. **22**(6): p. 826-33.
255. Lasagna-Reeves, C.A., et al., *Identification of oligomers at early stages of tau aggregation in Alzheimer's disease.* FASEB J, 2012. **26**(5): p. 1946-59.
256. Ali, Y.O., K. Ruan, and R.G. Zhai, *NMNAT suppresses tau-induced neurodegeneration by promoting clearance of hyperphosphorylated tau oligomers in a Drosophila model of tauopathy.* Hum Mol Genet, 2012. **21**(2): p. 237-50.
257. Spires-Jones, T.L., et al., *Are tangles as toxic as they look?* J Mol Neurosci, 2011. **45**(3): p. 438-44.
258. Van der Jeugd, A., et al., *Cognitive defects are reversible in inducible mice expressing pro-aggregant full-length human Tau.* Acta Neuropathol, 2012. **123**(6): p. 787-805.
259. Ando, K., et al., *Deletion of murine tau gene increases tau aggregation in a human mutant tau transgenic mouse model.* Biochem Soc Trans, 2010. **38**(4): p. 1001-5.
260. Kampers, T., et al., *Assembly of paired helical filaments from mouse tau: implications for the neurofibrillary pathology in transgenic mouse models for Alzheimer's disease.* FEBS Lett, 1999. **451**(1): p. 39-44.
261. Lindwall, G. and R.D. Cole, *Phosphorylation affects the ability of tau protein to promote microtubule assembly.* J Biol Chem, 1984. **259**(8): p. 5301-5.
262. Kosik, K.S., *The molecular and cellular biology of tau.* Brain Pathol, 1993. **3**(1): p. 39-43.
263. Ambegaokar, S.S. and G.R. Jackson, *Functional genomic screen and network analysis reveal novel modifiers of tauopathy dissociated from tau phosphorylation.* Hum Mol Genet, 2011. **20**(24): p. 4947-77.
264. Ambegaokar, S.S. and G.R. Jackson, *The downward spiral of tau and autolysosomes: a new hypothesis in neurodegeneration.* Autophagy, 2012. **8**(7): p. 1144-5.
265. Dubey, M., et al., *Tau inhibits anterograde axonal transport and perturbs stability in growing axonal neurites in part by displacing kinesin cargo: neurofilaments attenuate tau-mediated neurite instability.* Cell Motil Cytoskeleton, 2008. **65**(2): p. 89-99.
266. Cuchillo-Ibanez, I., et al., *Phosphorylation of tau regulates its axonal transport by controlling its binding to kinesin.* FASEB J, 2008. **22**(9): p. 3186-95.
267. Zala, D., et al., *Vesicular glycolysis provides on-board energy for fast axonal transport.* Cell, 2013. **152**(3): p. 479-91.

268. Hirokawa, N., S. Niwa, and Y. Tanaka, *Molecular motors in neurons: transport mechanisms and roles in brain function, development, and disease.* Neuron, 2010. **68**(4): p. 610-38.
269. Sternberger, N.H., L.A. Sternberger, and J. Ulrich, *Aberrant neurofilament phosphorylation in Alzheimer disease.* Proc Natl Acad Sci U S A, 1985. **82**(12): p. 4274-6.
270. Pollanen, M.S., C. Bergeron, and L. Weyer, *Characterization of a shared epitope in cortical Lewy body fibrils and Alzheimer paired helical filaments.* Acta Neuropathol, 1994. **88**(1): p. 1-6.
271. Manetto, V., et al., *Phosphorylation of neurofilaments is altered in amyotrophic lateral sclerosis.* J Neuropathol Exp Neurol, 1988. **47**(6): p. 642-53.
272. Ballatore, C., et al., *Microtubule stabilizing agents as potential treatment for Alzheimer's disease and related neurodegenerative tauopathies.* J Med Chem, 2012. **55**(21): p. 8979-96.
273. Barten, D.M., et al., *Hyperdynamic microtubules, cognitive deficits, and pathology are improved in tau transgenic mice with low doses of the microtubule-stabilizing agent BMS-241027.* J Neurosci, 2012. **32**(21): p. 7137-45.
274. Brunden, K.R., et al., *Brain-penetrant microtubule-stabilizing compounds as potential therapeutic agents for tauopathies.* Biochem Soc Trans, 2012. **40**(4): p. 661-6.
275. Das, V. and J.H. Miller, *Microtubule stabilization by peloruside A and paclitaxel rescues degenerating neurons from okadaic acid-induced tau phosphorylation.* Eur J Neurosci, 2012. **35**(11): p. 1705-17.
276. Ittner, L.M., Y.D. Ke, and J. Gotz, *Phosphorylated Tau interacts with c-Jun N-terminal kinase-interacting protein 1 (JIP1) in Alzheimer disease.* J Biol Chem, 2009. **284**(31): p. 20909-16.
277. Seo, J., et al., *c-Jun N-terminal phosphorylation is essential for hippocampal synaptic plasticity.* Neurosci Lett, 2012. **531**(1): p. 14-9.
278. Ploia, C., et al., *JNK plays a key role in tau hyperphosphorylation in Alzheimer's disease models.* J Alzheimers Dis, 2011. **26**(2): p. 315-29.
279. Wang, D., et al., *beta2 Adrenergic Receptor, Protein Kinase A (PKA) and c-Jun N-terminal Kinase (JNK) Signaling Pathways Mediate Tau Pathology in Alzheimer Disease Models.* J Biol Chem, 2013. **288**(15): p. 10298-307.
280. Mohit, A.A., J.H. Martin, and C.A. Miller, *p493F12 kinase: a novel MAP kinase expressed in a subset of neurons in the human nervous system.* Neuron, 1995. **14**(1): p. 67-78.
281. Zhu, X., et al., *Activation and redistribution of c-jun N-terminal kinase/stress activated protein kinase in degenerating neurons in Alzheimer's disease.* J Neurochem, 2001. **76**(2): p. 435-41.
282. Manczak, M., et al., *Differential expression of oxidative phosphorylation genes in patients with Alzheimer's disease: implications for early mitochondrial dysfunction and oxidative damage.* Neuromolecular Med, 2004. **5**(2): p. 147-62.
283. Mosconi, L., A. Pupi, and M.J. De Leon, *Brain glucose hypometabolism and oxidative stress in preclinical Alzheimer's disease.* Ann N Y Acad Sci, 2008. **1147**: p. 180-95.
284. Gibson, G.E., K.F. Sheu, and J.P. Blass, *Abnormalities of mitochondrial enzymes in Alzheimer disease.* J Neural Transm, 1998. **105**(8-9): p. 855-70.
285. Du, H., et al., *Early deficits in synaptic mitochondria in an Alzheimer's disease mouse model.* Proc Natl Acad Sci U S A, 2010. **107**(43): p. 18670-5.
286. Hollenbeck, P.J. and W.M. Saxton, *The axonal transport of mitochondria.* J Cell Sci, 2005. **118**(Pt 23): p. 5411-9.

287. Li, Z., et al., *The importance of dendritic mitochondria in the morphogenesis and plasticity of spines and synapses.* Cell, 2004. **119**(6): p. 873-87.
288. Moreira, P.I., et al., *Mitochondrial dysfunction is a trigger of Alzheimer's disease pathophysiology.* Biochim Biophys Acta, 2010. **1802**(1): p. 2-10.
289. Quintanilla, R.A., et al., *Caspase-cleaved tau expression induces mitochondrial dysfunction in immortalized cortical neurons: implications for the pathogenesis of Alzheimer disease.* J Biol Chem, 2009. **284**(28): p. 18754-66.
290. Liazoghli, D., et al., *Fragmentation of the Golgi apparatus induced by the overexpression of wild-type and mutant human tau forms in neurons.* Am J Pathol, 2005. **166**(5): p. 1499-514.
291. van Vliet, C., et al., *Intracellular sorting and transport of proteins.* Prog Biophys Mol Biol, 2003. **83**(1): p. 1-45.
292. Neri, C., *Role and Therapeutic Potential of the Pro-Longevity Factor FOXO and Its Regulators in Neurodegenerative Disease.* Front Pharmacol, 2012. **3**: p. 15.
293. Santiago, S., et al., *Perinatal and parental determinants of childhood overweight in 6-12 years old children.* Nutr Hosp, 2012. **27**(2): p. 599-605.
294. Sandri, M., et al., *Foxo transcription factors induce the atrophy-related ubiquitin ligase atrogin-1 and cause skeletal muscle atrophy.* Cell, 2004. **117**(3): p. 399-412.
295. Castets, P., et al., *Sustained Activation of mTORC1 in Skeletal Muscle Inhibits Constitutive and Starvation-Induced Autophagy and Causes a Severe, Late-Onset Myopathy.* Cell Metab, 2013.
296. Masiero, E., et al., *Autophagy is required to maintain muscle mass.* Cell Metab, 2009. **10**(6): p. 507-15.
297. Dobrowolny, G., et al., *Skeletal muscle is a primary target of SOD1G93A-mediated toxicity.* Cell Metab, 2008. **8**(5): p. 425-36.
298. Levine, B. and G. Kroemer, *Autophagy in the pathogenesis of disease.* Cell, 2008. **132**(1): p. 27-42.
299. Carmignac, V., et al., *Autophagy is increased in laminin alpha2 chain-deficient muscle and its inhibition improves muscle morphology in a mouse model of MDC1A.* Hum Mol Genet, 2011. **20**(24): p. 4891-902.
300. Temiz, P., C.C. Weihl, and A. Pestronk, *Inflammatory myopathies with mitochondrial pathology and protein aggregates.* J Neurol Sci, 2009. **278**(1-2): p. 25-9.
301. Mathew, R., et al., *Autophagy suppresses tumorigenesis through elimination of p62.* Cell, 2009. **137**(6): p. 1062-75.
302. Munoz, D.G., et al., *Accumulation of phosphorylated neurofilaments in anterior horn motoneurons of amyotrophic lateral sclerosis patients.* J Neuropathol Exp Neurol, 1988. **47**(1): p. 9-18.
303. Stokin, G.B., et al., *Axonopathy and transport deficits early in the pathogenesis of Alzheimer's disease.* Science, 2005. **307**(5713): p. 1282-8.
304. Mammucari, C., et al., *FoxO3 controls autophagy in skeletal muscle in vivo.* Cell Metab, 2007. **6**(6): p. 458-71.
305. Moresi, V., et al., *Myogenin and class II HDACs control neurogenic muscle atrophy by inducing E3 ubiquitin ligases.* Cell, 2010. **143**(1): p. 35-45.
306. Mittal, A., et al., *The TWEAK-Fn14 system is a critical regulator of denervation-induced skeletal muscle atrophy in mice.* J Cell Biol, 2010. **188**(6): p. 833-49.
307. Seale, P., et al., *Pax7 is required for the specification of myogenic satellite cells.* Cell, 2000. **102**(6): p. 777-86.
308. Sabourin, L.A. and M.A. Rudnicki, *The molecular regulation of myogenesis.* Clin Genet, 2000. **57**(1): p. 16-25.

309. Cao, Y., et al., *Global and gene-specific analyses show distinct roles for Myod and Myog at a common set of promoters.* EMBO J, 2006. **25**(3): p. 502-11.
310. Hall-Craggs, E.C. and H.S. Seyan, *Histochemical changes in innervated and denervated skeletal muscle fibers following treatment with bupivacaine (marcain).* Exp Neurol, 1975. **46**(2): p. 345-54.
311. Xu, P., et al., *JNK regulates FoxO-dependent autophagy in neurons.* Genes Dev, 2011. **25**(4): p. 310-22.
312. Rubinsztein, D.C., G. Marino, and G. Kroemer, *Autophagy and aging.* Cell, 2011. **146**(5): p. 682-95.
313. Ozcelik, S., et al., *Rapamycin Attenuates the Progression of Tau Pathology in P301S Tau Transgenic Mice.* PLoS One, 2013. **8**(5): p. e62459.
314. Schaeffer, V., et al., *Stimulation of autophagy reduces neurodegeneration in a mouse model of human tauopathy.* Brain, 2012. **135**(Pt 7): p. 2169-77.
315. Delrieu, J., et al., *'Clinical trials in Alzheimer's disease': immunotherapy approaches.* J Neurochem, 2012. **120 Suppl 1**: p. 186-93.
316. Hochgrafe, K., A. Sydow, and E.M. Mandelkow, *Regulatable transgenic mouse models of Alzheimer disease: onset, reversibility and spreading of Tau pathology.* FEBS J, 2013.
317. Wellington, C.L., et al., *Caspase cleavage of gene products associated with triplet expansion disorders generates truncated fragments containing the polyglutamine tract.* J Biol Chem, 1998. **273**(15): p. 9158-67.
318. Wellington, C.L., et al., *Caspase cleavage of mutant huntingtin precedes neurodegeneration in Huntington's disease.* J Neurosci, 2002. **22**(18): p. 7862-72.
319. Guo, H., et al., *Active caspase-6 and caspase-6-cleaved tau in neuropil threads, neuritic plaques, and neurofibrillary tangles of Alzheimer's disease.* Am J Pathol, 2004. **165**(2): p. 523-31.
320. Choi, Y., et al., *Minocycline attenuates neuronal cell death and improves cognitive impairment in Alzheimer's disease models.* Neuropsychopharmacology, 2007. **32**(11): p. 2393-404.
321. Rego, G., et al., *High prevalence and advanced silicosis in active granite workers: a dose-response analysis including FEV1.* J Occup Environ Med, 2008. **50**(7): p. 827-33.
322. Zhang, C. and A.M. Cuervo, *Restoration of chaperone-mediated autophagy in aging liver improves cellular maintenance and hepatic function.* Nat Med, 2008. **14**(9): p. 959-65.
323. Sinha, S., et al., *Comparison of Three Amyloid Assembly Inhibitors: The Sugar scyllo-Inositol, the Polyphenol Epigallocatechin Gallate, and the Molecular Tweezer CLR01.* ACS Chem Neurosci, 2012. **3**(6): p. 451-8.
324. Prabhudesai, S., et al., *A novel "molecular tweezer" inhibitor of alpha-synuclein neurotoxicity in vitro and in vivo.* Neurotherapeutics, 2012. **9**(2): p. 464-76.
325. Levites, Y., et al., *Neuroprotection and neurorescue against Abeta toxicity and PKC-dependent release of nonamyloidogenic soluble precursor protein by green tea polyphenol (-)-epigallocatechin-3-gallate.* FASEB J, 2003. **17**(8): p. 952-4.
326. Rushworth, J.V., et al., *Prion protein-mediated toxicity of amyloid-beta oligomers requires lipid rafts and the transmembrane LRP1.* J Biol Chem, 2013.
327. Peterson, D.W., et al., *Cinnamon extract inhibits tau aggregation associated with Alzheimer's disease in vitro.* J Alzheimers Dis, 2009. **17**(3): p. 585-97.
328. Yao, J., et al., *Molecular hairpin: a possible model for inhibition of tau aggregation by tannic acid.* Biochemistry, 2013.

329. Fatouros, C., et al., *Inhibition of tau aggregation in a novel Caenorhabditis elegans model of tauopathy mitigates proteotoxicity.* Hum Mol Genet, 2012. **21**(16): p. 3587-603.
330. Medina, D.X., A. Caccamo, and S. Oddo, *Methylene blue reduces abeta levels and rescues early cognitive deficit by increasing proteasome activity.* Brain Pathol, 2011. **21**(2): p. 140-9.
331. Ma, Q.L., et al., *Curcumin suppresses soluble tau dimers and corrects molecular chaperone, synaptic, and behavioral deficits in aged human tau transgenic mice.* J Biol Chem, 2013. **288**(6): p. 4056-65.
332. Tizon, B., et al., *Induction of autophagy by cystatin C: a mechanism that protects murine primary cortical neurons and neuronal cell lines.* PLoS One, 2010. **5**(3): p. e9819.
333. Kayed, R. and G.R. Jackson, *Prefilament tau species as potential targets for immunotherapy for Alzheimer disease and related disorders.* Curr Opin Immunol, 2009. **21**(3): p. 359-63.

Internet sites

www.alz.ch (*Vivre avec la maladie d'Alzheimer – Chiffres-clés 2)*

CURRICULUM VITAE

Sefika Ozcelik

Kannenfeldplatz 2

CH-4056 Basel

mobile: +41 78 891 12 42

email: s.oezcelik@unibas.ch

nationalities: French

date of birth: 15.07.1979

EDUCATION

2009-2013 **PhD in Neurobiology**
PhD at the Institute of Pathology, University of Basel
Laboratory of Dr. Winkler David, Department of Neuropathology
University Hospital Basel, Switzerland

2008-2009 **PhD Studentship in Molecular Biology**
University of Bern, Medical Faculty, Graduate School for Cellular and Biomedical Sciences
Bern University Hospital "Inselspital", Department of Clinical Research, Department of Nephrology and Hypertension
Bern Switzerland

2006-2008 **M.Sc. Pharmacology**
Louis Pasteur University
Strasbourg, France

2006 **B.Sc. degree in Cellular Biology and Physiology**
Louis Pasteur University
Strasbourg, France

2005 **Undergraduate degree (DEUG) in Biology**
Louis Pasteur University
Strasbourg, France

2003 **Undergraduate in medicine (PCEM1)**
Louis Pasteur University
Strasbourg, France

2001 **Certificate of Maturity** (Baccalauréat) in Science (Biology)
High School Fabert
Metz, France

PUBLICATIONS

2012 Stimulation of autophagy reduces neurodegeneration in a mouse model of human tauopathy. Schaeffer V, Lavenir I, **Ozcelik S**, Tolnay M, Winkler DT, Goedert M. **Brain. 2012 Jul**; 135 (Pt 7): 2169-77.

2013 Rapamycin attenuates the progression of tau pathology in P301S tau transgenic mice. **Sefika Ozcelik**, Graham Fraser, Perrine Castets, Véronique Schaeffer, Zhiva Skachokova, Karin Breu, Florence Clavaguera, Michael Sinnreich Ludwig Kappos, Michel Goedert Markus Tolnay, David T. Winkler. **PLoS One. 2013 May 7**;8(5):e62459.

PhD COURSES

2010-2012	Neuroscience, University of Basel
Fall 2012	Effective Scientific Communication, University of Basel
Fall 2011	Genetic Approaches in Biomedical research, University of Basel
Fall 2011	Writing an Effective Scientific article, University of Basel
Spring 2009	Molecular Biology of Inflammation (Prof. B. Engelhardt), University of Bern
Sept 2009	Animal Experimentation (Module 1 RESAL), University of Geneva
Fall 2009	Dynamics of cellular contacts: Cell-cell contacts and cell motility (Prof. B. Engelhardt), University of Bern
Oct 2009	Fluorescent staining and Confocal & Imaging analysis course (27/28 October)